NAVAL POSTGRADUATE SCHOOL

MONTEREY, CALIFORNIA

THESIS

BIO-OPTICAL AND HYDROGRAPHIC CHARACTERISTICS OF THE WESTERN PACIFIC OCEAN FOR UNDERSEA WARFARE USING SEAGLIDER DATA

by

Ramon P. Martinez

December 2014

Thesis Advisor: Peter C. Chu
Second Readers: Chenwu Fan
Ronald E. Betsch

Approved for public release; distribution is unlimited

THIS PAGE INTENTIONALLY LEFT BLANK

REPORT DOCUMENTATION PAGE

Form Approved OMB No. 0704–0188

1. AGENCY USE ONLY *(Leave blank)*	**2. REPORT DATE** December 2014	**3. REPORT TYPE AND DATES COVERED** Master's Thesis

4. TITLE AND SUBTITLE
BIO-OPTICAL AND HYDROGRAPHIC CHARACTERISTICS OF THE WESTERN PACIFIC OCEAN FOR UNDERSEA WARFARE USING SEAGLIDER DATA

5. FUNDING NUMBERS

6. AUTHOR(S) Ramon P. Martinez

7. PERFORMING ORGANIZATION NAME(S) AND ADDRESS(ES)
Naval Postgraduate School
Monterey, CA 93943–5000

8. PERFORMING ORGANIZATION REPORT NUMBER

9. SPONSORING /MONITORING AGENCY NAME(S) AND ADDRESS(ES)
N/A

10. SPONSORING/MONITORING AGENCY REPORT NUMBER

11. SUPPLEMENTARY NOTES The views expressed in this thesis are those of the author and do not reflect the official policy or position of the Department of Defense or the U.S. Government. IRB Protocol number ____N/A____.

12a. DISTRIBUTION / AVAILABILITY STATEMENT
Approved for public release; distribution is unlimited

12b. DISTRIBUTION CODE

13. ABSTRACT (maximum 200 words)

Analysis of hydrographic and optical variability in the western Pacific Ocean region is conducted using data collected by Naval Oceanographic Office (NAVOCEANO) from March 2008 to November 2011. Temporal and spatial patterns of temperature, salinity, optical scattering, and fluorescence were examined. Vertical charts of each variable were produced for environmental and operational characterization. Histograms of the maxima and minima were plotted to examine the frequency of these variables. Furthermore, the vertical correlations among the variables were identified.

14. SUBJECT TERMS Oceanography, hydrography, optical oceanography.

15. NUMBER OF PAGES 97

16. PRICE CODE

17. SECURITY CLASSIFICATION OF REPORT	**18. SECURITY CLASSIFICATION OF THIS PAGE**	**19. SECURITY CLASSIFICATION OF ABSTRACT**	**20. LIMITATION OF ABSTRACT**
Unclassified	Unclassified	Unclassified	UU

NSN 7540–01–280–5500

Standard Form 298 (Rev. 2–89)
Prescribed by ANSI Std. 239–18

THIS PAGE INTENTIONALLY LEFT BLANK

Approved for public release; distribution is unlimited

BIO-OPTICAL AND HYDROGRAPHIC CHARACTERISTICS OF THE WESTERN PACIFIC OCEAN FOR UNDERSEA WARFARE USING SEAGLIDER DATA

Ramon P. Martinez
Lieutenant Commander, United States Navy
B.S., Mississippi State University, 2009

Submitted in partial fulfillment of the
requirements for the degree of

MASTER OF SCIENCE IN METEOROLOGY AND PHYSICAL OCEANOGRAPHY

from the

NAVAL POSTGRADUATE SCHOOL
December 2014

Author: Ramon P. Martinez

Approved by: Peter C. Chu
Thesis Advisor

Chenwu Fan
Ronald E. Betsch
Second Readers

Peter C. Chu
Chair, Department of Oceanography

THIS PAGE INTENTIONALLY LEFT BLANK

ABSTRACT

Analysis of hydrographic and optical variability in the western Pacific Ocean region was conducted using data collected by Naval Oceanographic Office from March 2008 to November 2011. Temporal and spatial patterns of temperature, salinity, optical scattering and fluorescence were examined. Vertical charts of each variable were produced for environmental and operational characterization. Histograms of the maxima and minima were plotted to examine the frequency of these variables. Furthermore, the vertical correlations among the variables were identified.

THIS PAGE INTENTIONALLY LEFT BLANK

TABLE OF CONTENTS

LIST OF FIGURES

ACKNOWLEDGMENTS

I would like to humbly thank Professor Peter Chu for his patience and guidance as I wound my way along the research path. I will remain forever grateful.

This project would simply not have been finished without the dedication and skill of Mr. Chenwu Fan. His complete mastery of MATLAB and all things oceanographic combined with his patience were paramount to the completion of the project. Words cannot adequately express my appreciation for his assistance.

My family has continually provided both the inspiration and loving support I needed to always keep striving. Thank you Ramon, Barbara, Frances, Savannah and Sierra, but most of all Salamat Po, Bonita Ko Ann! 143!

For Mom. You always knew, and you never lost faith. Ever.

THIS PAGE INTENTIONALLY LEFT BLANK

I. INTRODUCTION

A. OVERVIEW

The U.S. Navy operates across all the world oceans and seas; the ocean environment significantly affects all naval operations. Tactical advantages may be gained or lost via the understanding and leveraging of the various facets of the ocean environment. Direct observations of physical oceanographic parameters collected by the employment of satellite technology, shipboard sensors and remotely operated vehicles all play a role in helping to characterize the ocean environment (Russell 2012). These directly observed data are used to seed various computer models that are meant to predict oceanographic changes as well as indications of how various sensors and weapons systems will perform and react to the ever-changing oceanographic conditions (Russell 2012).

The SEAGLIDER underwater glider is one such remotely operated vehicle that is being used to collect and transmit various observed oceanic parameters for inclusion in computer models that predict oceanic conditions and weapon and sensor performance. The SEAGLIDER has the ability to transit the vast oceans and serially report temperature, salinity, conductivity, and optical properties such as blue and red light transmission values in real time (Eriksen et al. 2001). The Naval Oceanographic Office operates a fleet of SEAGLIDERs to collect oceanographic data around the globe (Russell 2012). Oceanographic modelers use the collected data to check model assumptions and update model performance while tactical oceanographers incorporate the data into various softwares to predict weapon and sensor performance (Russell 2012).

A temporal and spatial analysis of a collected SEAGLIDER data set from the western Pacific Ocean will provide a better understanding of the physical oceanographic environment in this strategically vital area. A correlation of observed parameters may facilitate the improvement of operational models used to predict oceanographic conditions. This study will perform an analysis of the collected data parameters and use various statistical correlation techniques to discover any correlations that may exist.

B. OBJECTIVES AND OUTLINE

The objectives of this research are: 1) to produce two-dimensional graphs and tabular results of the various seawater properties' data collected by the Naval Oceanographic Office using SEAGLIDER glides in the western Pacific Ocean from March 2008 through November 2011 2) to perform an analysis of the individual seawater properties to determine how the properties evolved over the course of seasonal change and 3) to statistically compare and identify relationships of the hydrographic, optical, and bio-optical seawater properties to one another to discover if optical and/or bio-optical properties can be inferred from given vertical profiles generated with the collected SEAGLIDER data.

This thesis will consist of six chapters. Chapter I will serve as an overview and introduction with a brief summary of the relevance of the research to various U.S. Navy warfighting communities and a discussion of the western Pacific region to include strategic relevance, geography, bathymetry, ocean circulation patterns and pertinent atmospheric forcing mechanisms. Chapter II will describe the SEAGLIDER and the instrumentation used to collect the data with a discussion of the bio-optical and optical parameters. Chapter III will detail the data tracks and processing software, the method by which the SEAGLIDER determines its position within the water column, and the software and techniques used to sort and compare the data. Chapter IV presents the analysis of the various data and Chapter V concludes the research, presents findings, and provides recommendations for future research.

C. NAVAL RELEVANCE

Naval operations are of course conducted above, on, and beneath the surface of the world oceans. A greater understanding of the oceanic environment can and does facilitate the ability for one potential adversary to gain advantage over another. An analysis of the collected data set will foster greater understanding of the hydrographic, optical and bio-optical characteristics of the western Pacific Ocean which will in turn facilitate the ability of Anti-Submarine Warfare (ASW) planners to better achieve victory in any potential conflict.

One of the most important factors affecting the detection, counter detection, and avoidance of detection of deployed submarines is the manner in which sound propagates and the pathways sound follows through the seawater (DOSITS 2013). The seawater temperature, salinity and pressure vertical and horizontal profile throughout the areal ocean water column determines the varying paths through which sound will travel through the ocean (DOSITS 2013). Any efforts that increase the data points within the water column for these parameters will aid both ocean modelers and tactical decision makers attempting to find submarines in the ocean using sound-based techniques.

Bio-optical and optical properties of the ocean also play an important and significant role in a hunt for submerged submarines employing non-acoustic search techniques (Naval Research Lab 2012). The potential correlation of bio-optical and/or optical parameters to specific temperature, salinity and pressure values within the water column will both aid model development and facilitate better prediction of where submarines may be most easily detected.

Naval Special Warfare (NSW) operations by their very nature are quite sensitive to oceanographic environmental conditions, particularly bio-optical properties in the littoral region. Accurate observation and model based prediction of these parameters will aid special warfare operators to safely complete their mission while avoiding detection and unnecessary risk. This study will not incorporate littoral observations, but the potential correlations of temperature, salinity, and depth profiles to bio-optical and optical properties may aid better understanding and model prediction of the environment where NSW operators typically perform their assigned missions.

Both acoustic and non-acoustic methods are employed in the hunt for sea mines (Bachkosky et al. 2000). Sea mines can be deployed on the bottom, attached to an anchor to lurk within the water column or on the sea surface, or left to drift upon the ocean current. A characterization of the water column’s acoustic and non-acoustic properties is paramount to finding deployed sea mines. Underwater glider collected data will aid the classification of the oceanographic environment to ensure Mine Counter Measure (MCM) planners are best able to counter deployed sea mines (Bachkosky et al. 2000).

D. THE WESTERN PACIFIC OCEAN

The western Pacific Ocean region and the surrounding land areas are some of the most geophysically and economically dynamic areas of the world. The region serves as a global trade route and economic base to numerous countries and peoples. Each year, the area is home to some of the most intense tropical cyclones on Earth and the oceanographic conditions are widely varying and dynamic over relatively short areal distances.

1. Strategic Location

The western Pacific Ocean east of the Ryuku Islands and south of Japan is a vitally strategic area of the world (Figure 1). “The trans-Pacific ocean shipping market is by far North America’s largest trade lane, accounting for nearly 20 million 20-foot-equivalent container units in the U.S. trade alone in 2012” (Journal of Commerce 2014). Important U.S. trade partners making use of these trade routes include China and the ASEAN member nations of Japan, Republic of Korea, Taiwan and Canada (Office of U.S. Trade Representative 2014). Petroleum products that have been shipped through the Strait of Malacca from southwest Asia also must transit this area enroute to Korea, Japan and North America. U.S. policy and strategy has recently increased focus toward Asia and the United States National Security Strategy directs a deepening engagement in the Asian region (Campbell and Andrews 2013). National economies that depend on either imports or exports or both are vulnerable to a disruption in seaborne trade (UNDP 2011). This study will better characterize the oceanographic properties of this important international water space.

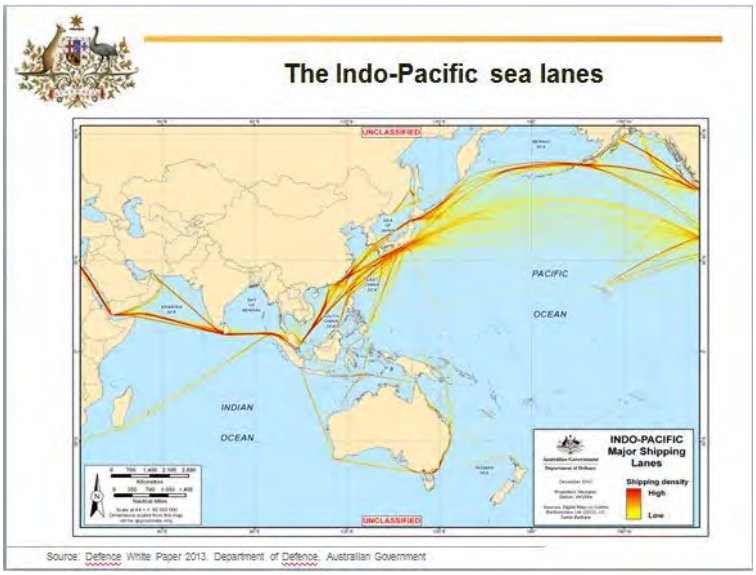

Figure 1. Indo-Pacific sea lanes (from Defence White Paper 2013, Department of Defence, Australian Government).

2. Geography

The area of study comprises over 435 x 10^3 km^2 of the western Pacific Ocean stretching from 122 E to 139 E longitudes and from 21 N to 34 N latitudes. The data is collected primarily from a concentrated swath along a corridor from near 20 N 122 E to the east of Taiwan extending northeast just east of the Ryuku Island chain to near 34 E 133 E just south of central Japan. The Ryuku chain is comprised of over 100 separate volcanic and coral islands stretching from Taiwan to Japan; the Ryuku Island chain separates the East China Sea from the Philippine Sea (Figure 2).

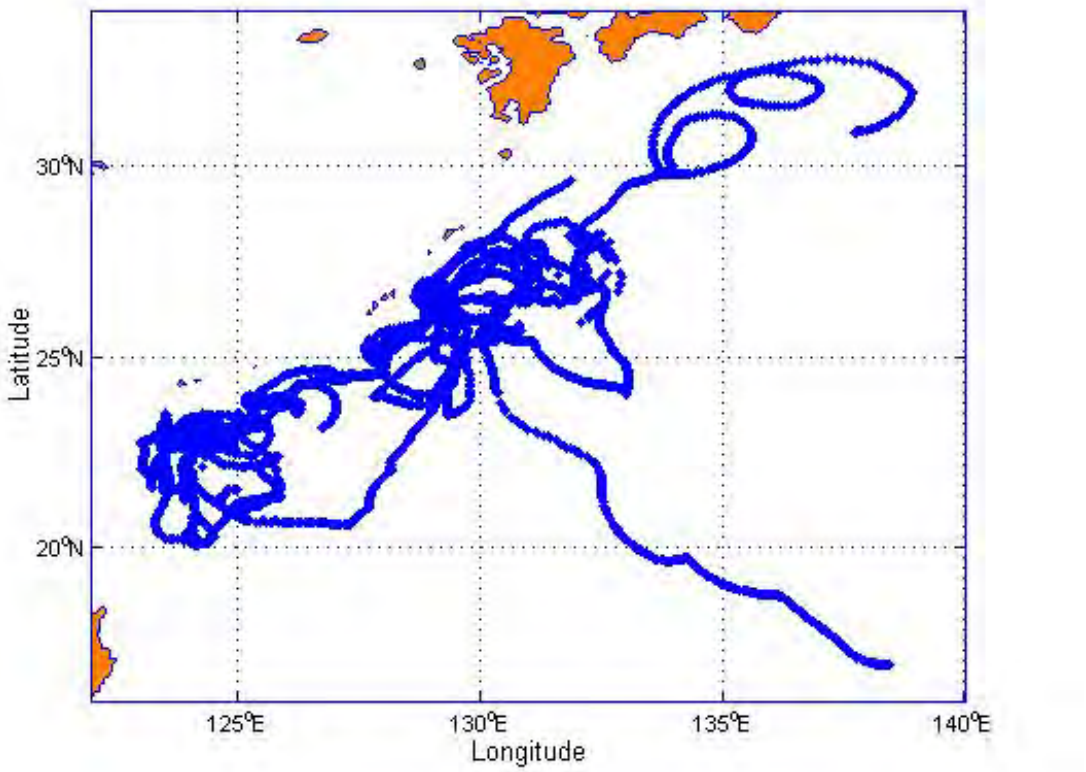

Figure 2. SEAGLIDER tracks along the Ryuku Islands and south of Japan.

3. Bathymetry

The bathymetry of the western Pacific Ocean (Figure 3) in the area of interest is comprised of deep abyssal plain rising to a plateau bounding the Ryuku Island ridge that extends from Asia under the East China Sea. A series of east-west oriented ridges are located under the north central Philippine Sea extending northward toward southern Japan. The Shikoku Basin extends southward from the waters off of south central Japan. The Shikoku basin is bounded on the east by the Izu-Bonin-Marianas oceanic ridge which extends southward from central Japan to the Marianas Islands along the western boundary of the Marianas Trench. The bathymetry of the area of study is therefore mixed and varied.

Figure 3. Bathymetry of the Western Pacific. The blue arrows indicate the Kuroshio warm current (from COMET Program n.d.).

4. Atmospheric Forcing Over Western Pacific

The atmospheric meteorological condition over the area of the study is climatologically controlled by the subtropical high pressure regime that rotates anticyclonically over the western Pacific Ocean. Easterly trade winds blow across the tropical portion of the gyre and become southerly and southwesterly at the western continental boundary. Cold air outbreaks originating over Asia serially track over the northern area of interest in the autumn through spring months to produce northwesterly winds and seas. Migratory cyclonic low pressure systems both transit and are spawned over the area of interest to produce gale to storm force winds and seas as large as 6 to 8 meters.

The annual Asian monsoon pattern heavily influences meteorological conditions over the western Pacific Ocean. The winter or Northeast monsoon develops in autumn and typically lasts into spring. In response to surface cooling induced by a seasonal reduction of solar radiation over the Asian continent, the Siberian high builds over Asia to produce anticyclonic northerly flow over the area of interest. The western Pacific subtropical high weakens and retreats eastward (Figure 4). As Asia begins to rewarm in the spring as the sun angle increases and the days lengthen, the Siberian high weakens,

the Asiatic thermally induced low pressure develops over the Himalayan region, and the subtropical West Pacific high rebuilds and moves westward to produce southwesterly flow over the area of interest (Figure 5).

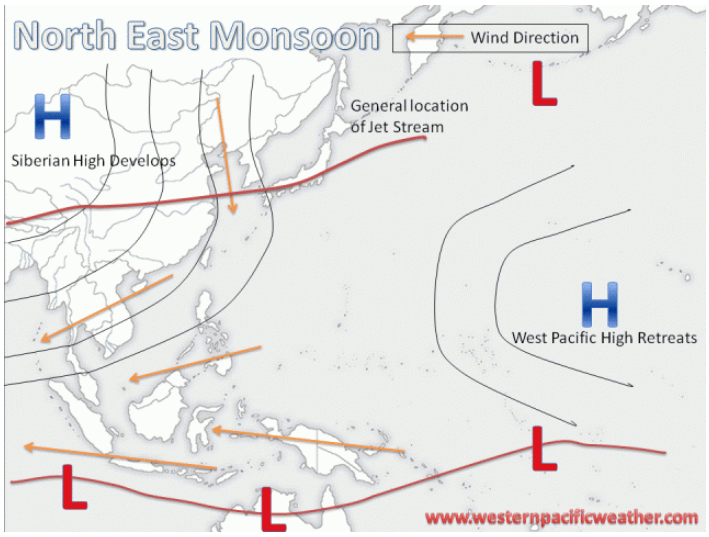

Figure 4. Northeast Monsoon pattern. The northern red line indicates the general Jet Stream location. The southern red line indicates the general location of the Inter Tropical Convergence Zone (from Westpacwx.com n.d).

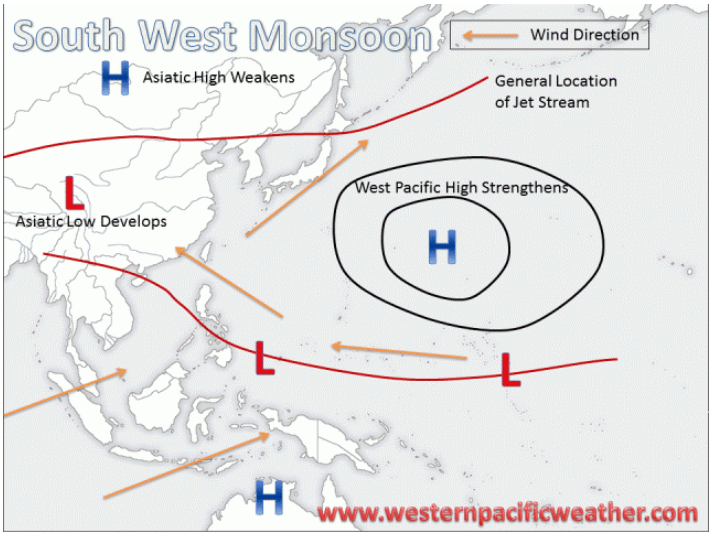

Figure 5. Southwest Monsoon pattern. The northern red line indicates the general Jet Stream location. The southern red line indicates the general location of the Inter Tropical Convergence Zone (from Westpacwx.com n.d).

The western Pacific Ocean is the most active tropical cyclogenesis region in the world. Tropical cyclones climatologically form in the western Pacific throughout the year with maxima from June to November and minima during February and March. The western Pacific Ocean typically produces the most, 30% of the annual global total, tropical cyclones in any given year (McBride 1995). Tropical cyclones annually transit the area of interest to produce very intense winds and very large waves sometimes in excess of 10 meters (Figure 6). Tropical cyclone passage can markedly change the characteristics of the temperature, salinity and depth vertical profile across an ocean area.

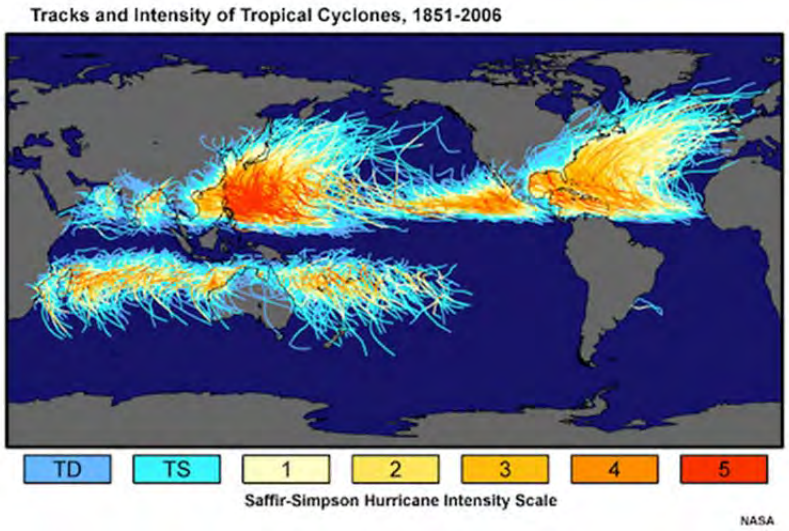

Figure 6. Global Tropical cyclone tracks 1851–2006. The Western Pacific is transited by numerous intense Category 5 tropical cyclones (from NASA n.d.).

5. Western North Pacific Oceanic Circulation Pattern

The oceanic circulation pattern of the western Pacific is dominated by the sub-tropical North Pacific gyre system. There are two primary ocean currents flowing near the area of the study, the warm core Kuroshio and the cold core Oyashio. The Equatorial current flows westward along the southern periphery of the North Pacific gyre. The gyre turns northward near the western ocean boundary east of Luzon and Taiwan to become the Kuroshio Current which flows northward through and east of the Ryuku Islands. The Kuroshio turns eastward along the southern Japanese coast and extends eastward across

the northern Pacific Ocean (Barkley 1970). The Oyashio Current originates in the northern Bering Sea and flows southward along the eastern Russian coast and the Kamchatka peninsula. A portion of the Oyashio flows into the Sea of Japan, while another significant branch turns eastward across the northern Pacific (Qiu 2001). The area of this study is dominated by the Kuroshio, but the interface along the Oyashio and Kuroshio currents' boundary produces both warm and cold core eddies which periodically meander through the area of the study (Figure 7).

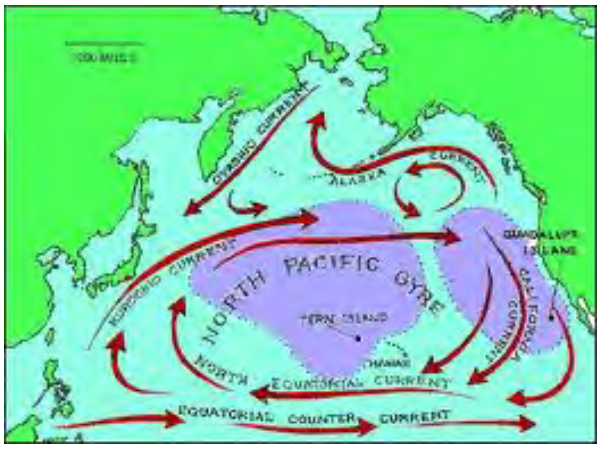

Figure 7. The North Pacific Gyre system (from Bear Springs Blossom http://www.nature-education.org/oceancurrents.html n.d.).

II. DATA COLLECTION

A. THE SEAGLIDER

Griffiths et al. provide an excellent overview of the general capabilities of undersea gliders. “Undersea gliders offer an alternative propulsion paradigm to the propeller driven autonomous underwater vehicle by using buoyancy change and wings to produce forward motion” (Griffiths et al. 2007). Undersea gliders operate at slow speed (< .5 m/s), provide long endurance (over six months or 3,000 km), and send their data to shore in near real time using two way satellite communication systems (Griffiths et al. 2007). Undersea gliders can operate in the entire world’s ocean to include the polar regions. Undersea gliders, using various sensor packages, can be used to collect a whole host of oceanographic data to facilitate study of, for example, ecosystem dynamics, ocean circulation patterns, and global climate change (Griffiths et al. 2007). Undersea gliders can also be used to provide data for ocean prediction models which can have tactical application to world Navies’ missions (Griffiths et al. 2007).

The SEAGLIDER is one such undersea ocean glider that was developed in the late 1990s at the University of Washington by a team comprised of Charles C. Eriksen, John W. Ballard, and Andres M. Chiodi of the University’s School of Oceanography, and T. James Osse, Russell D. Light, Timothy Wen, Thomas W. Lehman, and Peter L. Sabin of the University of Washington Applied Physics Laboratory (Eriksen et al. 2001). The SEAGLIDER was designed to serially profile the ocean to 1500 meters vertical depth while transiting over the course of a series of dive profiles up to 6000 kilometers horizontally (Eriksen et al. 2001). The SEAGLIDER consists of a pressure sealed hull enclosed by a fiber glass fairing to which wings, rudders, and a trailing antenna array are attached (Eriksen et al. 2001). SEAGLIDER propulsion through the water is conducted using a buoyancy control engine that changes the buoyancy of the vehicle to enable SEAGLIDER to become slightly negatively or positively buoyant within the relevant portion of the water mass (Eriksen et al. 2001). A battery powered mechanical control within the hull shifts the battery pack forward and aft and side to side to control the pitch and roll of the vehicle as it glides through the water (Figure 8). Shifting the pitch

downward while decreasing the buoyancy causes the SEAGLIDER to “glide” downward while setting the pitch upward while increasing the buoyancy causes the SEAGLIDER to “glide” upward within the water column (Eriksen et al. 2001). Similarly, the fore and aft and side to side positional shifts of the battery pack control the turning of the vehicle (Eriksen et al. 2001). The combination of fore and aft and side to side positioning of the battery pack with the buoyancy changes controls the SEAGLDIER on its programmed course to collect oceanographic data (Eriksen et al. 2001). The attached wings provide stability to the vehicle to prevent excessive rolling or yawing (Eriksen et al. 2001).

SEAGLIDER is remote operator programmed to perform a series of downward and upward glides while collecting various oceanographic data parameters using variable installed sensor packages (Eriksen et al. 2001). The SEAGLIDER can position itself at the ocean surface with a 45 degree downward angle to present the antenna array skyward to facilitate two way satellite communications (Figure 9). Remote operators can automatically download collected oceanographic data while optionally providing SEAGLIDER with updated mission profile instructions during the pre-programmed sea surface communication periods (Eriksen et al. 2001).

Figure 8. The SEAGLIDER and components (from SEAGLIDER Fabrication Center seaglider.washington.edu n.d.).

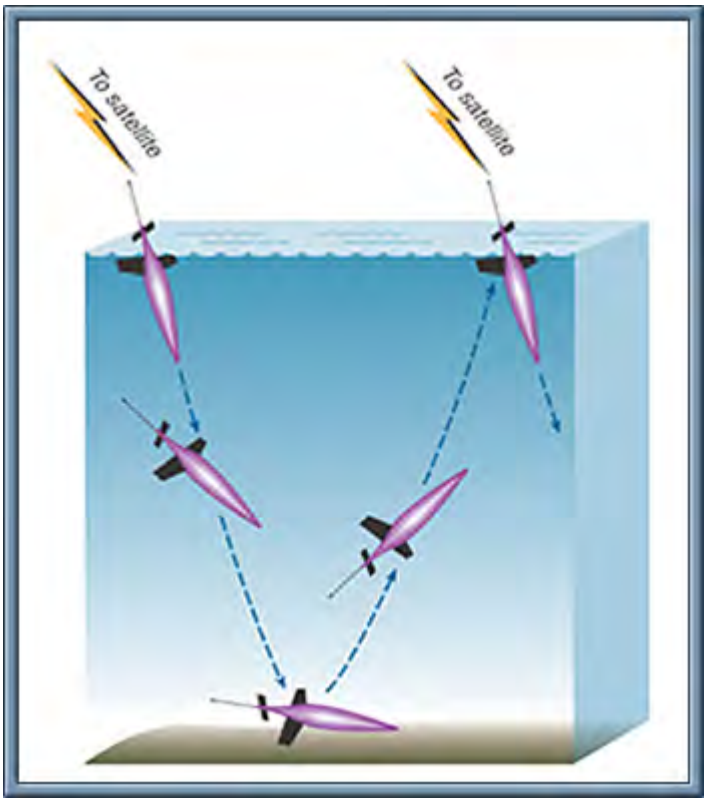

Figure 9. SEAGLIDER data collection and communication window glide profile. "After each dive SEAGLIDER dips its nose to raise its antenna out of the water. It determines its position via GPS, calls in via Iridium data telemetry satellite, uploads the oceanographic data" (from Applied Physics Laboratory www.apl.washington.edu n.d.).

The Naval Oceanographic Office's Glider Operations Center globally deploys and remotely operates a fleet of SEAGLIDERS to continually collect oceanographic data from the world's oceans. The data collected for this study was provided by the Naval Oceanographic Office Glider Operations Center.

B. HOW DOES SEAGLIDER KNOW WHERE IT IS?

SEAGLIDER uses a GPS fix at the start of each dive cycle to update its position (Eriksen et al. 2001). The vehicle uses a Kalman filter routine to predict the proper glider speed and heading or control vector for each operator indicated dive cycle (Eriksen et al. 2001). The SEAGLIDER navigational software chooses the control vector that will make the best progress toward the target location prescribed by the operator provided dive

profile for data collection (Eriksen et al. 2001). Once SEAGLIDER returns to the sea surface at the completion of a dive cycle, it again initiates a GPS fix (Eriksen et al. 2001). The GPS fix is compared to a dead reckoning position projection to determine how far the vehicle has transited horizontally from its anticipated position given the prescribed dive profile (Eriksen et al. 2001). The horizontal shift is then used to compute a depth integrated current to the dive profile. The collected oceanographic data is then correlated to the derived horizontal locations over the entire dive sequence (Eriksen et al. 2001). The SEAGLIDER then uploads the completed dive profile's data to the control station, initiates another GPS fix, and embarks on the next cycle in the operator prescribed series of data collection dives (Eriksen et al. 2001).

C. THE INSTRUMENTATION PACKAGE EMPLOYED TO COLLECT THE DATA

The SEAGLIDERs that collected the data used in this study were outfitted with two separate sensors which collected six different types of data throughout the vertical water column.

1. Conductivity, Temperature, Depth (CTD) Sensor

Twelve of the sixteen SEAGLIDERs employed to collect the data for the study were fitted with the Seabird Electronics SBE 41 CP CTD sensor. The SBE 41CP is designed to collect a continuous data profile, sampling at 1 Hz as the vehicle performs a dive cycle (Seabird Electronics, Inc. 2008). Seawater is not pumped past the CTD sensor during the glide cycle, water flow is provided by the gliding motion through the water column (Seabird Electronics, Inc. 2008). The data is stored in internal memory and the data controller requests and transmits the data when the SEAGLIDER reaches the surface and initiates two way communications (Seabird Electronics, Inc. 2008). The SBE 41CP can spot sample on command in addition to or in combination with continuous sampling (Seabird Electronics, Inc. 2008). For example, a SEAGLIDER can be programmed to spot sample in deep water, where parameters of interest are fairly stable, and then to perform a continuous profile as the vehicle ascends through shallower depths, providing

the desired level of detail while minimizing the data to be transmitted and conserving battery power (Seabird Electronics, Inc. 2008).

The SBE 41 CP temperature measurements were determined to be accurate to within 0.001 Celsius degrees and the salinity measurements were found accurate within 0.005 psu (practical salinity units) or better over several years (Janzen et al. 2008). The Practical Salinity Scale defines salinity in terms of the conductivity ratio of a sample to that of a solution of 32.4356 g of KCl at 15°C in a 1 kg solution (OSIL 2012). A sample of seawater at 15°C with conductivity equal to this KCl solution has a salinity of exactly 35 psu (OSIL 2012). In practice, salinity is determined from empirical relationships between temperature and the conductivity ratio of a sample to International Association for the Physical Sciences of the Ocean (IAPSO) Standard Seawater (OSIL 2012). Comparison of results with other laboratories requires all researchers to use the IAPSO Standard Seawater for calibration (Plaschke 1999). The pressure sensor used to derive glide profile depth is accurate to within 2 dbar (Seabird Electronics, Inc. 2008).

Four of the sixteen SEAGLIDERs employed to collect the data for the study were fitted with the Seabird Electronics Glider Payload CTD (GPCTD) sensor. The primary difference in the two sensors is that the GPCTD uses an onboard pump to ensure continuous water flow past the sensor (Seabird Electronics, Inc. 2008). The measurement specifications are similar (Seabird Electronics, Inc. 2008).

2. Flourometer and Optical Backscattering Meter

The SEAGLIDERs were also fitted with the WET Labs, Inc bb2fl ECO-puck. The Environmental Characterization Optics puck is comprised of three sensors (WET Labs, Inc, 2012). A flourometer measures the bio-optical parameter chlorophyll-a at 470/700 nm wavelengths and two separate and distinct optical sensors measure the optical backscattering coefficients at the 470 nm and 700 nm wavelengths (WET Labs, Inc. 2012). The deployed ECO-pucks collected data in the top 300 meters of the water column to preserve battery life and temporally extend the deployment cycles.

The flourometer senses chlorophyll-a from 0–30 µg/L and is accurate to within .015 µg/L (WET Labs, Inc 2012). Chlorophyll in its various forms is bound within the

cells of living organisms (YSI Environmental 2013). Chorophyll-a is the most abundant form of chlorophyll within photosynthetic organisms. In the ocean water column, the amount of chlorophyll-a content serves as an indicator of the vertical location of phytoplankton (YSI Environmental 2013). Chlorophyll fluoresces, when irradiated with light at a particular wavelength, chlorophyll then emits light at a higher wavelength (YSI Environmental 2013). The seawater is irradiated by the sensor at 470 nm and the chlorophyll-a induced irradiance is then measured at 650–700 nm, and the 470 nm wavelength light is filtered to discount backscatter.

The optical backscattering sensors sense from 0–5 m^-1 and are accurate to within .003 m^-1 (WET Labs, Inc 2014). The optical backscattering coefficient is measured so that oceanographers can discover various useful factors about the seawater that has been sampled. (Boss et al. 2004). Optical backscattering is created when a photon of light interacts with a particle either in the atmosphere or in water. Within the ocean, the particles can vary from water molecules to fish. When the photon strikes a particle it can either be absorbed, be redirected or "scattered," or continue to propagate in the same direction (Boss et al. 2004). The optical backscattering coefficient refers to all of the photons that have been redirected in the backward direction (Boss et al. 2004). Optical backscattering is defined as the fraction of incident light that has been scattered in the backward direction per unit distance travelled by the photons; the unit of measurement is the inverse meter (m^-1) (Boss et al. 2004). Many water constituents including water molecules, salts and other dissolved materials, organic and inorganic particles, and bubbles contribute to optical backscattering (Boss et al. 2004).

THIS PAGE INTENTIONALLY LEFT BLANK

III. DATA SET, SOFTWARE, AND ANALYSIS TECHNIQUES

A. THE SEAGLIDER DATA SET

The SEAGLIDER data set used in this study was collected during several western Pacific Ocean cruises conducted by the Naval Oceanographic Office from March 2008 to November 2011. Figure 2 indicates with a blue dot the location of each of 6573 SEAGLIDER glides that encompass the portion of the data set that is located in the western Pacific Ocean and the Philippine Sea. Figure 10 indicates a text listing of some of the NetCDF files that make up the data set. Each NetCDF file represents one SEAGLIDER glide cycle. The NetCDF data format is comprised of a set of software libraries and self-describing, machine-independent data formats that support the creation, access, and sharing of array oriented scientific data (Unidata 2014).

```
  1       4  sg128_2010_1021_1803_1280089E_250219N_00000050_edit.nc
  2       5  sg128_2010_1021_2245_1280009E_250305N_00000051_edit.nc
  3       6  sg128_2010_1022_0326_1279976E_250362N_00000052_edit.nc
  4       7  sg128_2010_1022_0812_1280030E_250498N_00000053_edit.nc
  5       8  sg128_2010_1022_1244_1280069E_250536N_00000054_edit.nc
  6       9  sg128_2010_1022_1713_1280284E_250579N_00000055_edit.nc
  7      10  sg128_2010_1022_2150_1280210E_250632N_00000056_edit.nc
  8      11  sg128_2010_1023_0228_1280061E_250715N_00000057_edit.nc
  9      12  sg128_2010_1023_0719_1279966E_250875N_00000058_edit.nc
 11      14  sg128_2010_1023_1656_1280108E_251112N_00000060_edit.nc
 12      15  sg128_2010_1023_2149_1280181E_251163N_00000061_edit.nc
 14      17  sg128_2010_1024_0718_1280192E_251271N_00000063_edit.nc
 15      18  sg128_2010_1024_1210_1280068E_251406N_00000064_edit.nc
 16      19  sg128_2010_1024_1701_1280098E_251494N_00000065_edit.nc
 17      20  sg128_2010_1024_2157_1280343E_251600N_00000066_edit.nc
 18      21  sg128_2010_1025_0252_1280351E_251740N_00000067_edit.nc
 19      22  sg128_2010_1025_0753_1280367E_251821N_00000068_edit.nc
 20      23  sg128_2010_1025_1253_1280368E_251856N_00000069_edit.nc
 34      57  sg128_2010_1102_1346_1277064E_251322N_00000103_edit.nc
 36      59  sg128_2010_1103_0046_1277037E_251251N_00000105_edit.nc
 40      63  sg128_2010_1103_2324_1276851E_251388N_00000109_edit.nc
 49      72  sg128_2010_1106_0240_1278354E_252712N_00000118_edit.nc
 50      73  sg128_2010_1106_0818_1278710E_252939N_00000119_edit.nc
 52      75  sg128_2010_1106_1936_1279479E_253416N_00000121_edit.nc
 54      77  sg128_2010_1107_0655_1280203E_253720N_00000123_edit.nc
 55      78  sg128_2010_1107_1224_1280495E_253789N_00000124_edit.nc
```

Figure 10. Listing of some SEAGLIDER NetCDF data files.

B. DATA PROCESSING SOFTWARE

MATLAB, a software package developed by the MathWorks company, is "a programming environment for algorithm development, data analysis visualization, and numeric computation" (MathWorks 2014). Several MATLAB programs, scripts and routines were developed to facilitate the processing and analysis of the NetCDF files comprising the collected SEAGLIDER data set.

C. DATA SORTING AND VISUALIZATION TECHNIQUES

Prior to actual analysis of the data, MATLAB programs were written to display the locations of each of the SEAGLIDER glides. The gliders were binned in files by specific SEAGLIDER and month for spatial and temporal reasons. In this way, the seawater characteristics could be analyzed by more specific time and location.

Once the binning process was complete, a MATLAB program was developed and used to assign a specific latitude and longitude to the glide cycles. In its raw form, each SEAGLIDER NetCDF file represents one complete dive cycle as the SEAGLIDER begins at the surface, dives to the assigned depth, and then returns to the surface at some distance from where it began the dive cycle. Figure 9 serves as a visualization of the typical SEAGLIDER dive profile. The raw NetCDF file assigns a specific latitude and longitude at both surface ends of the dive cycle. This presents a problem during vertical visualization and analysis of the seawater properties. The developed MATLAB program was used to separate each glide cycle into two halves using the maximum depth as the halfway cutoff point, and each half was then assigned the surface latitude and longitude of the surface end of that half of the cycle. In this way, each profile became two profiles, with two separate locations to facilitate the best potential vertical analysis of the seawater properties.

An eight panel visualization tool program was developed and used to visually inspect and bin each of the SEAGLIDER data profiles (Figure 11). The eight variables used in the visualization are location, temperature, conductivity, salinity, 470 nm optical backscatter coefficient, 700 nm optical backscatter coefficient, and chlorophyll content. If any of the data variables was corrupt or missing, that particular profile was binned

separately from those profiles that presented all data correctly. Of the 6573 initial data profiles, 2090 were determined to include all data with no errors.

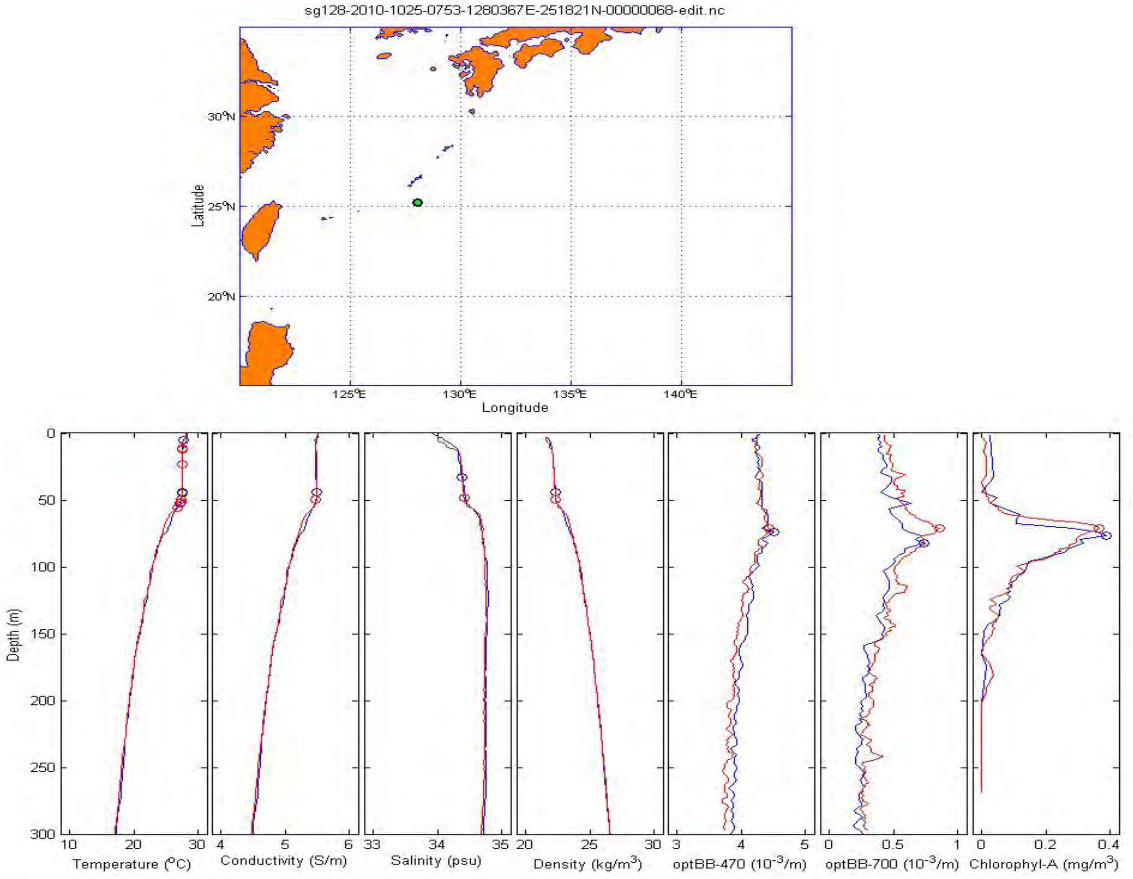

Figure 11. Eight-panel visualization tool.

Following the initial quality control inspection of all of the individual data profiles, an eight-panel monthly visualization tool was created and used to produce the analysis figures. The data was further separated by specific glider and by which method of six different and specific temperature based mixed layer depth methods was used in each panel. Figure 12 is 1 of 240 separate figure panels that were created to display the monthly data.

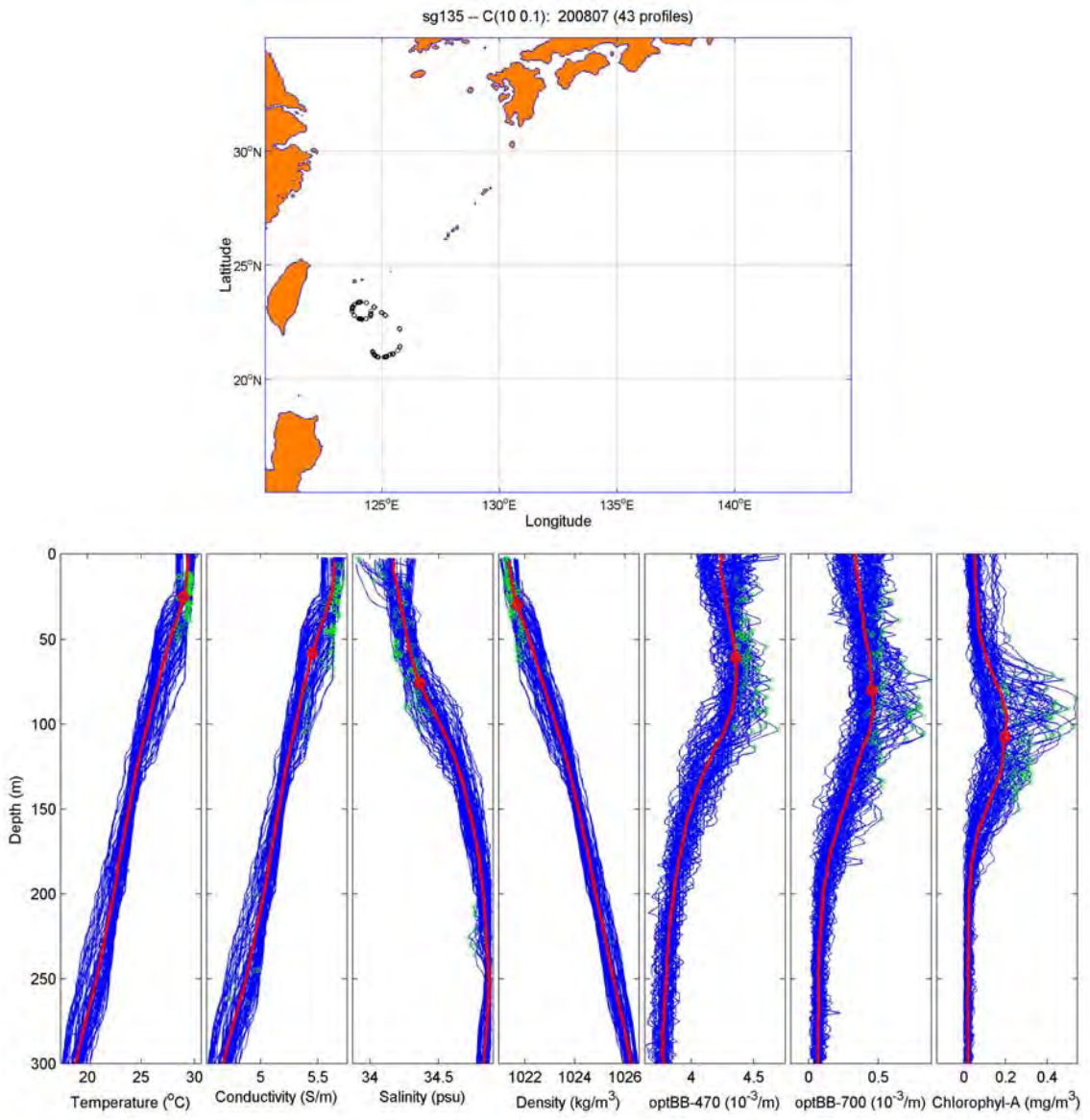

Figure 12. Monthly eight-panel visualization tool.

MATLAB programs were also developed to calculate and present each of the collected variables and methodologies in tabular form collated by specific glider and month. Finally, MATLAB scripts were used to perform a correlation analysis of the hydrographic, optical, and bio-optical parameters.

D. TEMPERATURE BASED MIXED LAYER DEPTH DETERMINATION METHODS

MATLAB was used to calculate six separate temperature methods used to determine the depth of the mixed layer depth. The Sprintall and Roerich method determines at which depth temperature decreases by .1 Celsius degree over 15 meters or more of depth from a reference temperature at 10 meters depth (Sprintall and Roerich 1999). Montegut et al. developed a similar method to determine the mixed layer depth; it simply determines at which depth the temperature decreases by .2 Celsius degrees from a reference temperature at 10 meters depth (Montegut et al. 2004). The Monterey and Levitus method determines at which depth the temperature decreases by .5 Celsius degrees from the sea surface temperature or SST (Monterey and Levitus 1997). Chu and Fan developed three different methods that were used in this analysis. The first is a determination at which depth temperature decreases by .8 Celsius degrees from the sea surface temperature (Chu and Fan 2011). Another is their Maximum Angle method where the angles created by successively coupled downward pointing vectors are compared. The depth of the maximum angle is determined as the mixed layer depth. Both temperature and density can be used as variables when using the Maximum Angle method; here temperature is used (Chu and Fan 2011). The third Chu and Fan method is the Optimal Linear Fitting method. The Root Mean Square error and the bias of the profile data are compared at successive depths of an optimally linear fitted polynomial temperature (or other variable) profile to determine the base of the mixed layer depth (Chu and Fan 2010).

E. DETERMINING MIXED LAYER DEPTH USING CONDUCTIVITY, SALINITY AND DENSITY

The depth of the mixed layer was also determined using the Chu and Fan Maximum Angle method (Chu and Fan 2011) and the three non-temperature hydrographic variables: conductivity, salinity, and density.

F. BIO-OPTICAL AND OPTICAL PROPERTIES' DEPTH OF PARAMETER MAXIMUM VALUE

A mixed layer depth per se was not calculated for the bio-optical or optical properties. However, a MATLAB script was developed and used to analyze these properties to determine at which depth the maximum value of each variable occurred within each specific profile.

IV. BIO-OPTICAL, OPTICAL, AND HYDROGRAPHIC CHARACTERISTICS

A. ANALYSIS OF MONTHLY VERTICAL PROFILES

Analysis of the spatial and temporal patterns of distribution of temperature, salinity, density, conductivity, optical backscattering coefficients at 470 and 700 nm, and chlorophyll concentration was conducted. The vertical structure of these variables was closely examined.

A representative figure and table for each month containing collected data is presented. The rest of the figure set will be presented in the appendix. Figure 13 displays the profiles collected by SEAGLIDER 131 in March 2008 with the temperature mixed layer depth computed using the Sprintall and Roerich method. The mean depths in meters of each parameter, indicated with a red dot in the eight-panel figures, are displayed in Table 1. The six temperature based mixed layer depth computation methods discussed previously are labeled as T1, T2, and etcetera across the top of the table followed by the maximum angle method computations for the salinity and density mixed layer depths. The table then indicates the depth in meters of the maximum value of the three bio-optical parameters: backscattering coefficient at 470 nm, backscattering coefficient at 700 nm, and chlorophyll content.

A brief qualitative analysis of each eight-panel figure and table pair is provided.

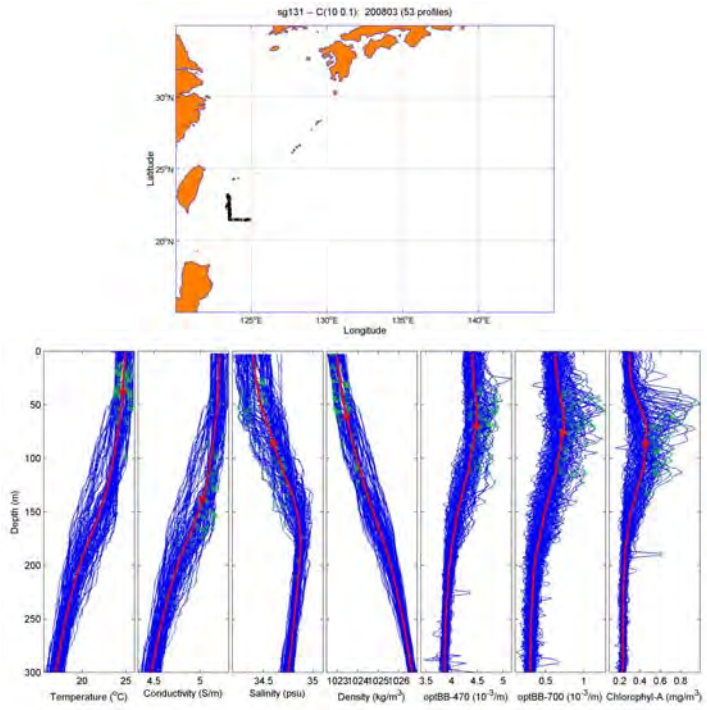

Figure 13. Eight-panel location and parameters for March 2008 Glider 131.

March 2008 Glider	TI MLD	T2 MLD	T3 MLD	T4 MLD	T5 MLD	T6 MLD	SALINITY MLD	DENSITY MLD	470nm Maximum Value	700nm Maximum Value	Chlorophyll Maximum Value
131	**37**	**46**	**68**	**84**	**61**	**81**	**86**	**61**	**69**	**76**	**86**
132	**42**	**52**	**72**	**88**	**77**	**98**	**98**	**81**	**59**	**73**	**88**
133	**42**	**52**	**72**	**88**	**77**	**98**	**98**	**81**	**59**	**73**	**88**
134	**41**	**46**	**53**	**65**	**56**	**100**	**83**	**61**	**77**	**89**	**90**

Table 1. Parameter depth in meters for March 2008 by specific SEAGLIDER.

Kuroshio western boundary current water is indicated by location and profiles from March, 2008 with evidence of a deep mixed layer. The six mixed layer depth identification methods indicate the uncertainty of the mixed layer depth. The three optical parameter panels indicate successively deeper levels of the maximum value for each specific parameter.

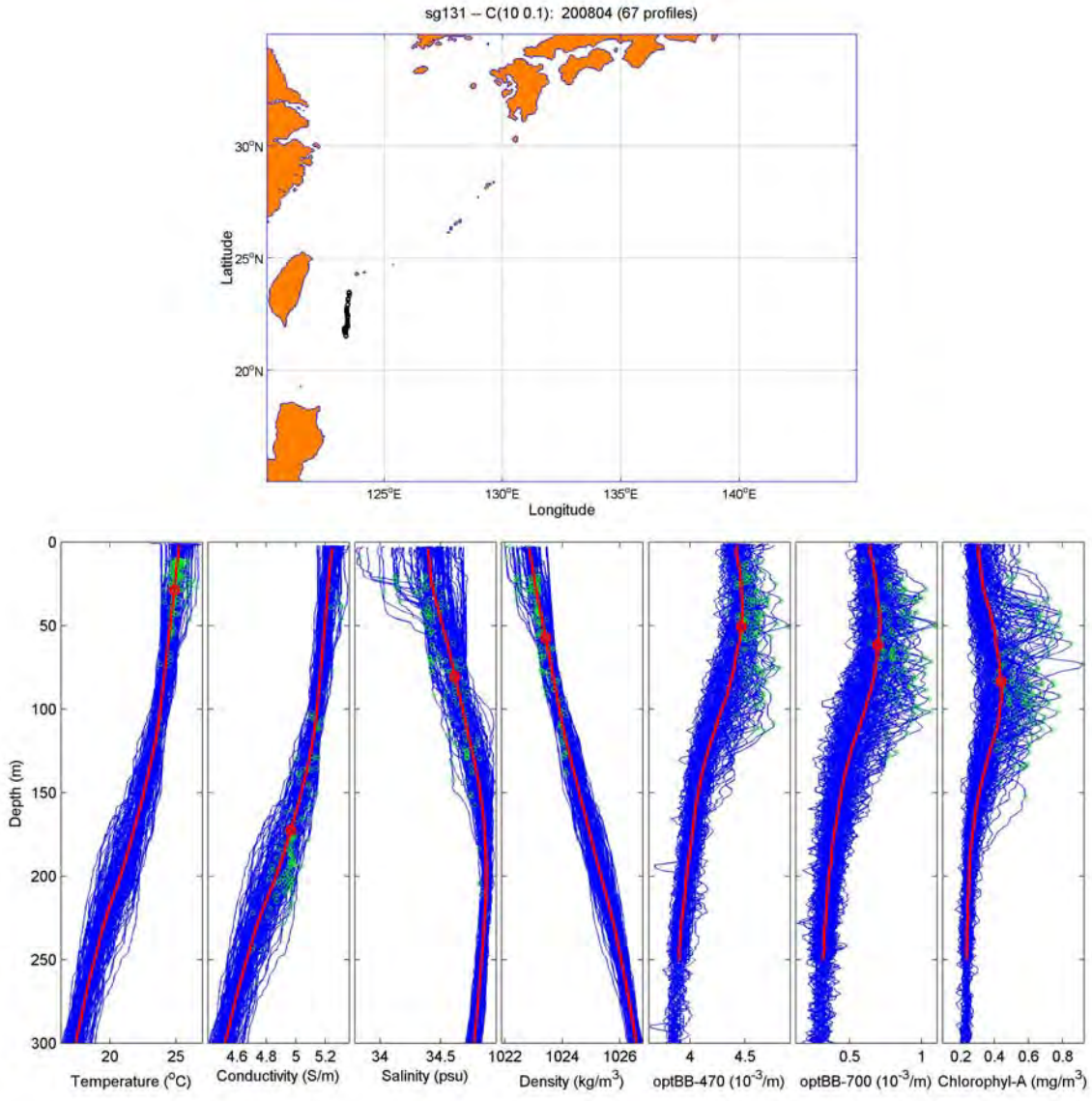

Figure 14. Eight-panel location and parameters for April 2008 Glider 131.

APRIL 2008 Glider	TI MLD	T2 MLD	T3 MLD	T4 MLD	T5 MLD	T6 MLD	SALINITY MLD	DENSITY MLD	470nm Maximum Value	700nm Maximum Value	Chlorophyll Maximum Value
131	26	34	46	63	55	98	80	57	50	61	83
132	16	19	22	31	22	72	50	23	89	98	104
133	29	37	39	56	45	72	70	42	51	88	99
134	19	22	25	31	27	63	67	26	75	90	93

Table 2. Parameter depth in meters for March 2008 by specific SEAGLIDER.

The SEAGLIDER 131 profiles for April 2008 presented in Figure 14 are indicating wide variance in the near surface salinity values. The mean depth of the T5 Chu and Fan maximum angle mixed layer depth calculation method is collocated with the density parameter calculated using the Chu and Fan maximum angle method and the max value method used for the optical backscattering parameters.

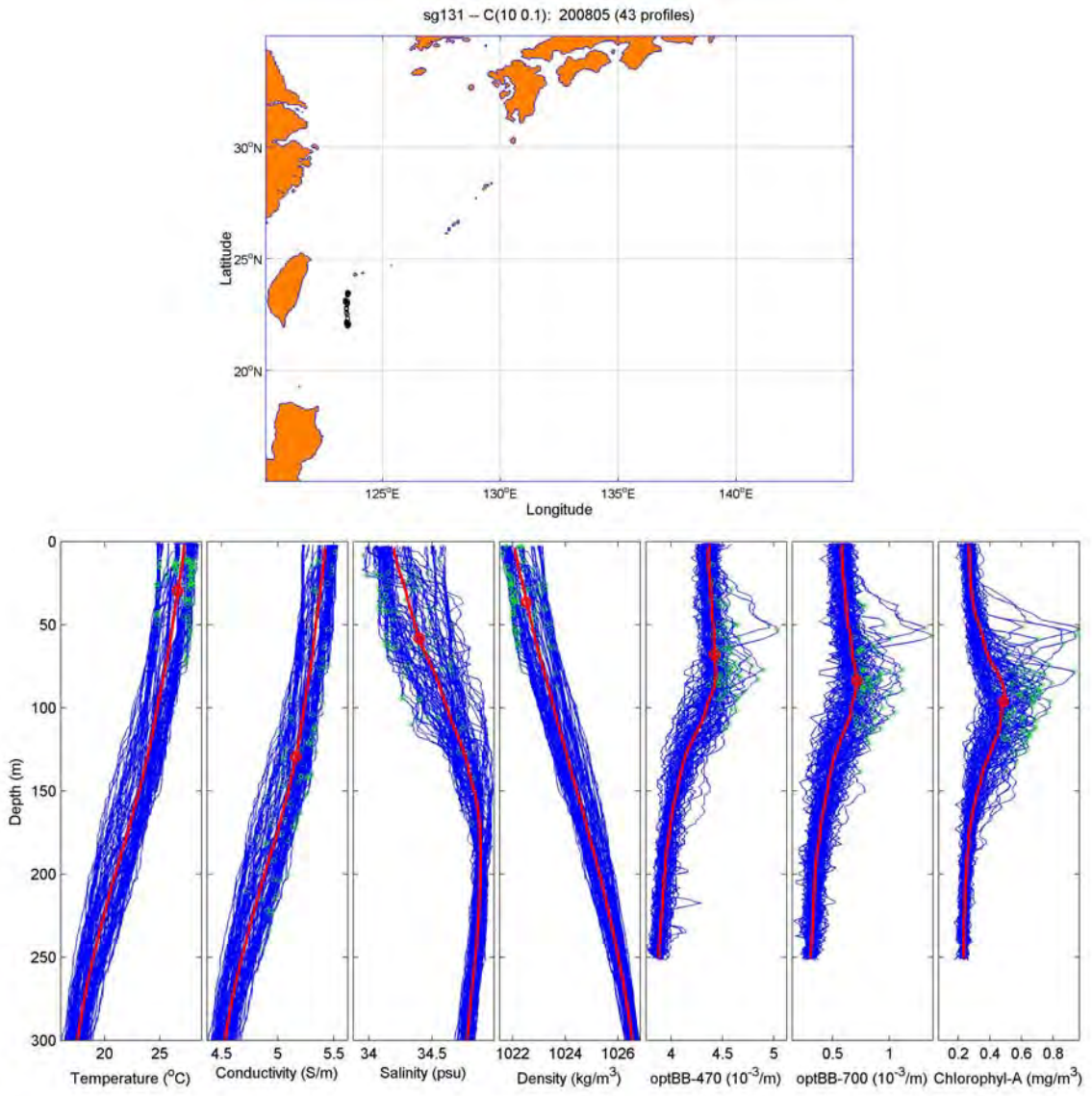

Figure 15. Eight-panel location and parameters for May 2008 Glider 131.

May 2008 Glider	TI MLD	T2 MLD	T3 MLD	T4 MLD	T5 MLD	T6 MLD	SALINITY MLD	DENSITY MLD	470nm Maximum Value	700nm Maximum Value	Chlorophyll Maximum Value
131	30	34	40	48	34	68	58	36	68	84	96
132	26	31	33	39	41	72	53	43	70	88	98
133	48	55	56	68	66	140	76	65	70	93	106

Table 3. Parameter depth in meters for May 2008 by specific SEAGLIDER.

The SEAGLIDER 131 profiles for May 2008 indicated in Figure 15 are indicating a surface temperature increase above 25 Celsius degrees. The salinity profiles are

indicating a wide near surface variability. The salinity mixed layer depth calculated using the Chu and fan maximum angle method is slightly deeper than the temperature based mixed layer depths and the density mixed layer depth calculated using the Chu and Fan maximum angle method. The optical parameters maximum value depths (i.e., backscattering at 470 nm, backscattering at 700 nm and chlorophyll) are all successively deeper in both Figure 15 and Table 3.

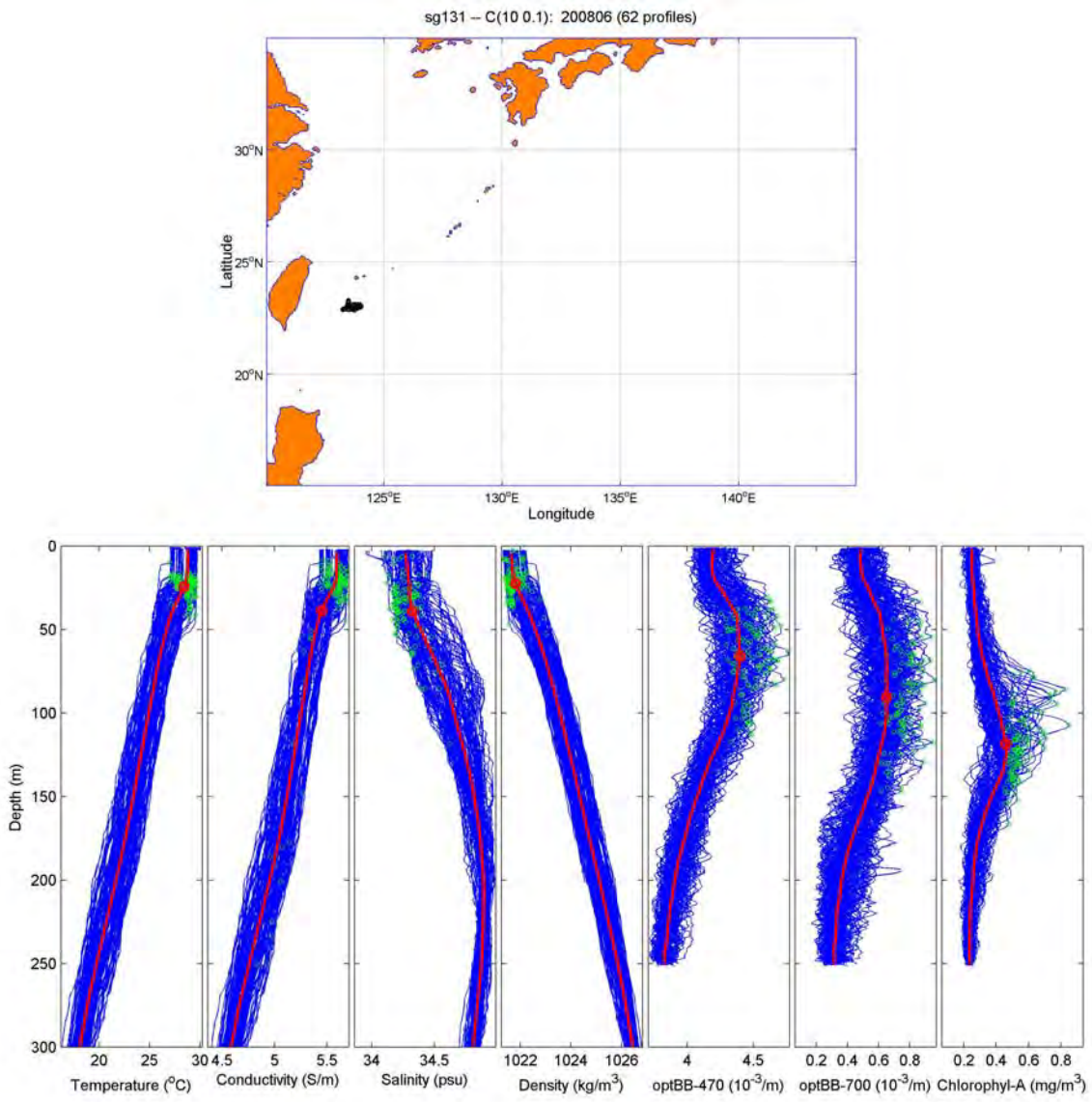

Figure 16. Eight-panel location and parameters for June 2008 Glider 131.

June 2008 Glider	TI MLD	T2 MLD	T3 MLD	T4 MLD	T5 MLD	T6 MLD	SALINITY MLD	DENSITY MLD	470nm Maximum Value	700nm Maximum Value	Chlorophyll Maximum Value
131	25	27	29	21	22	33	39	22	66	91	118
132	17	19	20	23	19	33	36	20	74	104	107
133	17	19	21	26	33	109	62	33	74	99	120

Table 4. Parameter depth in meters for June 2008 by specific SEAGLIDER.

Figure 16 and Table 4 indicate that all of the temperature based mixed layer depths for June of 2008 with the exception of the T6 Chu and Fan Optimal Linear Fitting method and the density mixed layer depth calculated with the Chu and Fan maximum angle method are all located in the 21 to 20 meter depth range. The optical parameters maximum value depths (i.e., backscattering at 470 nm, backscattering at 700 nm and chlorophyll) are all successively deeper in both Figure 16 and Table 4.

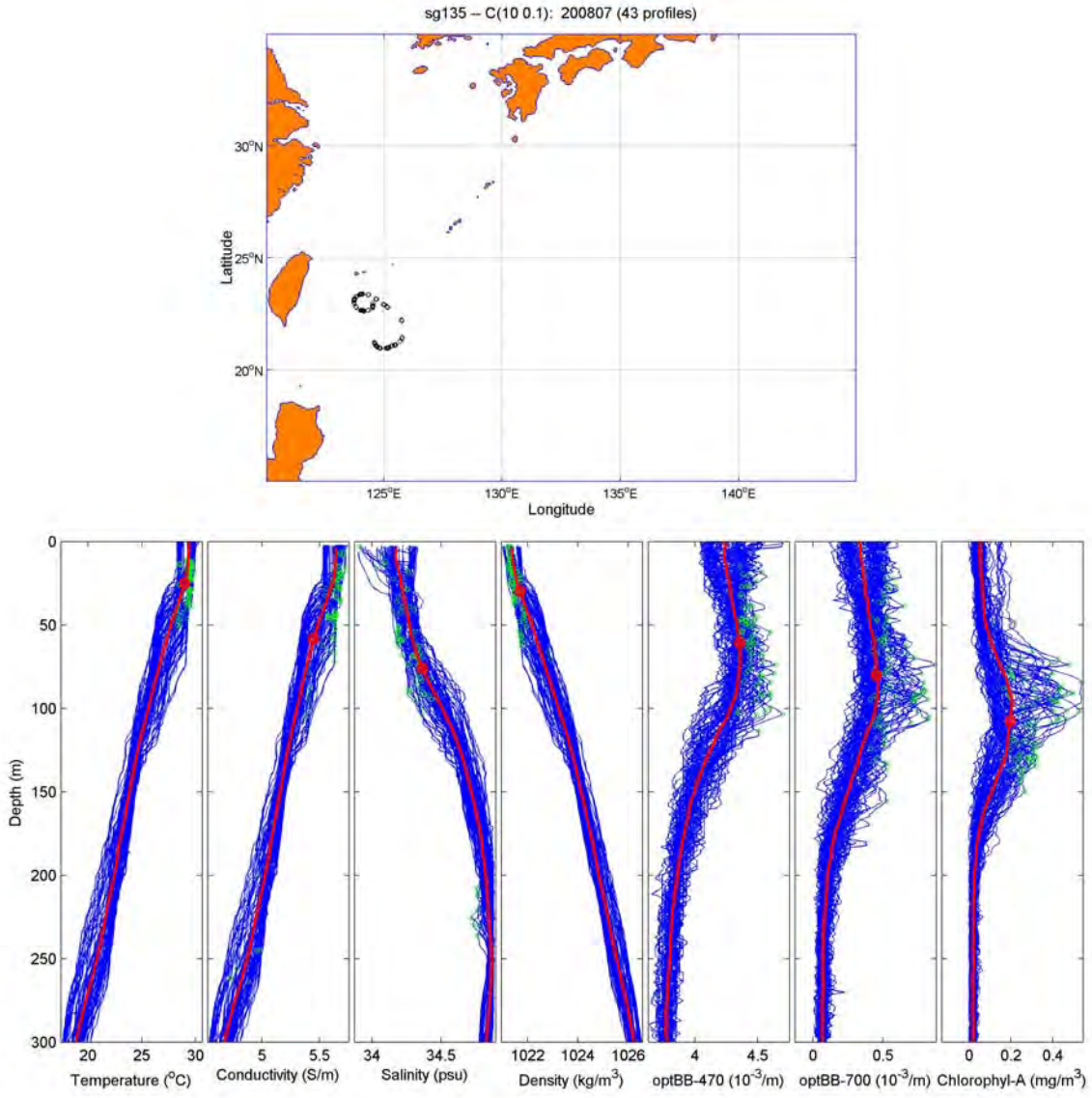

Figure 17. Eight-panel location and parameters for July 2008 Glider 135.

July 2008 Glider	TI MLD	T2 MLD	T3 MLD	T4 MLD	T5 MLD	T6 MLD	SALINITY MLD	DENSITY MLD	470nm Maximum Value	700nm Maximum Value	Chlorophyll Maximum Value
135	25	30	38	44	27	36	76	30	61	80	108

Table 5. Parameter depth in meters for July 2008 by specific SEAGLIDER.

Figure 17 and Table 5 displaying the data collected in July 2008 indicates that the sea surface temperature has warmed to above 28 degrees Celsius in most profiles. The temperature based mixed layer depth calculations all indicate mixed layer depths greater than 25 meters. The optical parameters maximum value depths (i.e., backscattering at 470 nm, backscattering at 700 nm and chlorophyll) are all successively deeper in both Figure 17 and Table 5. The temperature and the depth of the near surface mixed layer indicate a vertical temperature structure that is favorable for the formation and strengthening of tropical cyclones (Lin et al. 2012).

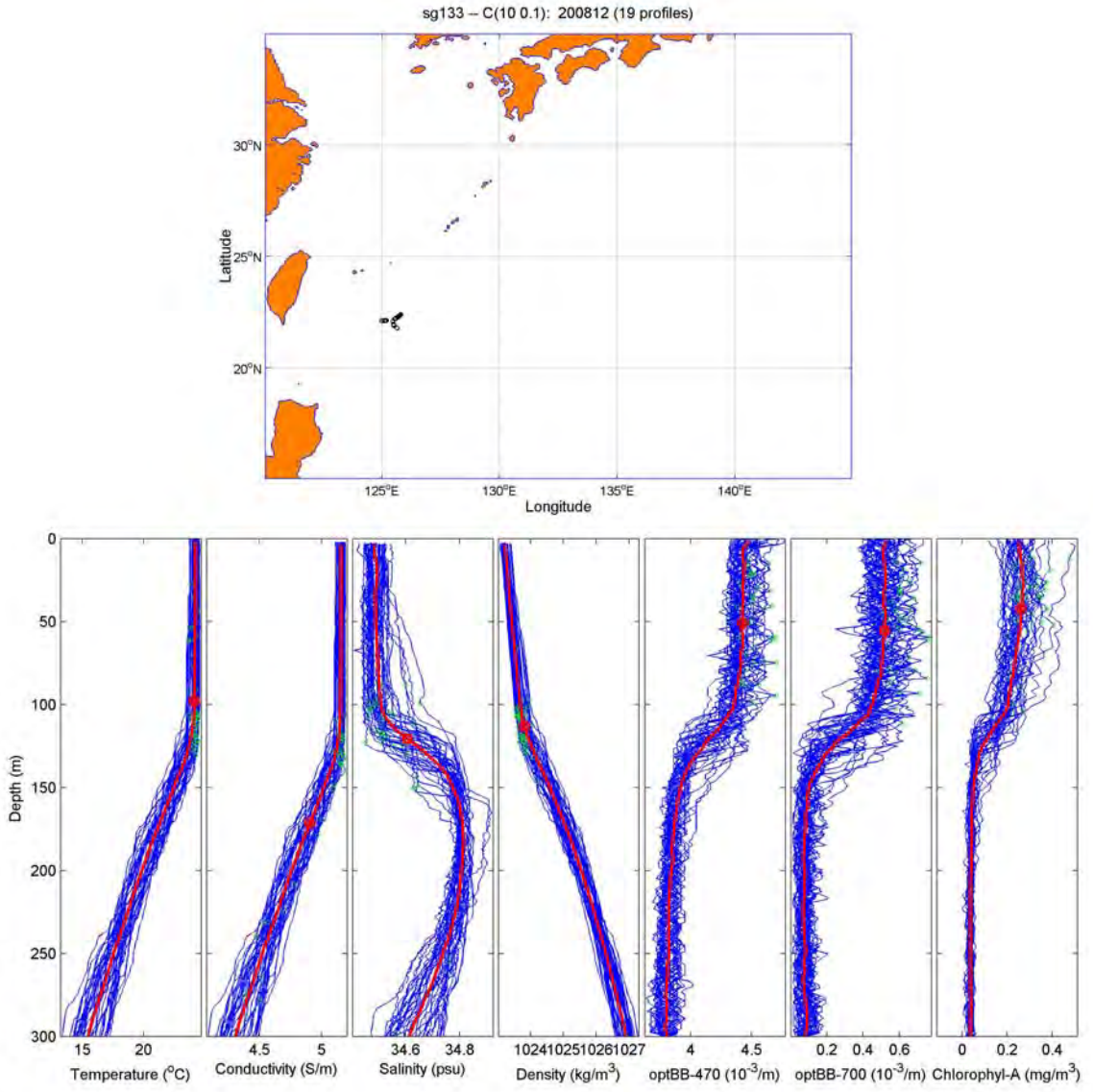

Figure 18. Eight-panel location and parameters for December 2008 Glider 133.

December 2008 Glider	TI MLD	T2 MLD	T3 MLD	T4 MLD	T5 MLD	T6 MLD	SALINITY MLD	DENSITY MLD	470nm Maximum Value	700nm Maximum Value	Chlorophyll Maximum Value
133	98	105	124	133	114	126	121	113	51	56	42
138	96	106	122	128	109	109	120	110	48	53	55

Table 6. Parameter depth in meters for December 2008 by specific SEAGLIDER.

Figure 18 and Table 6 displaying data from December 2008 indicate that there is a deep temperature, density and salinity mixed layer in excess of 100 m. The optical parameters are well distributed throughout the depth of the temperature and salinity surface based iso-layer, but the optical profile curve indicates a significant reduction of values below the mixed layer depths of the hydrographic properties.

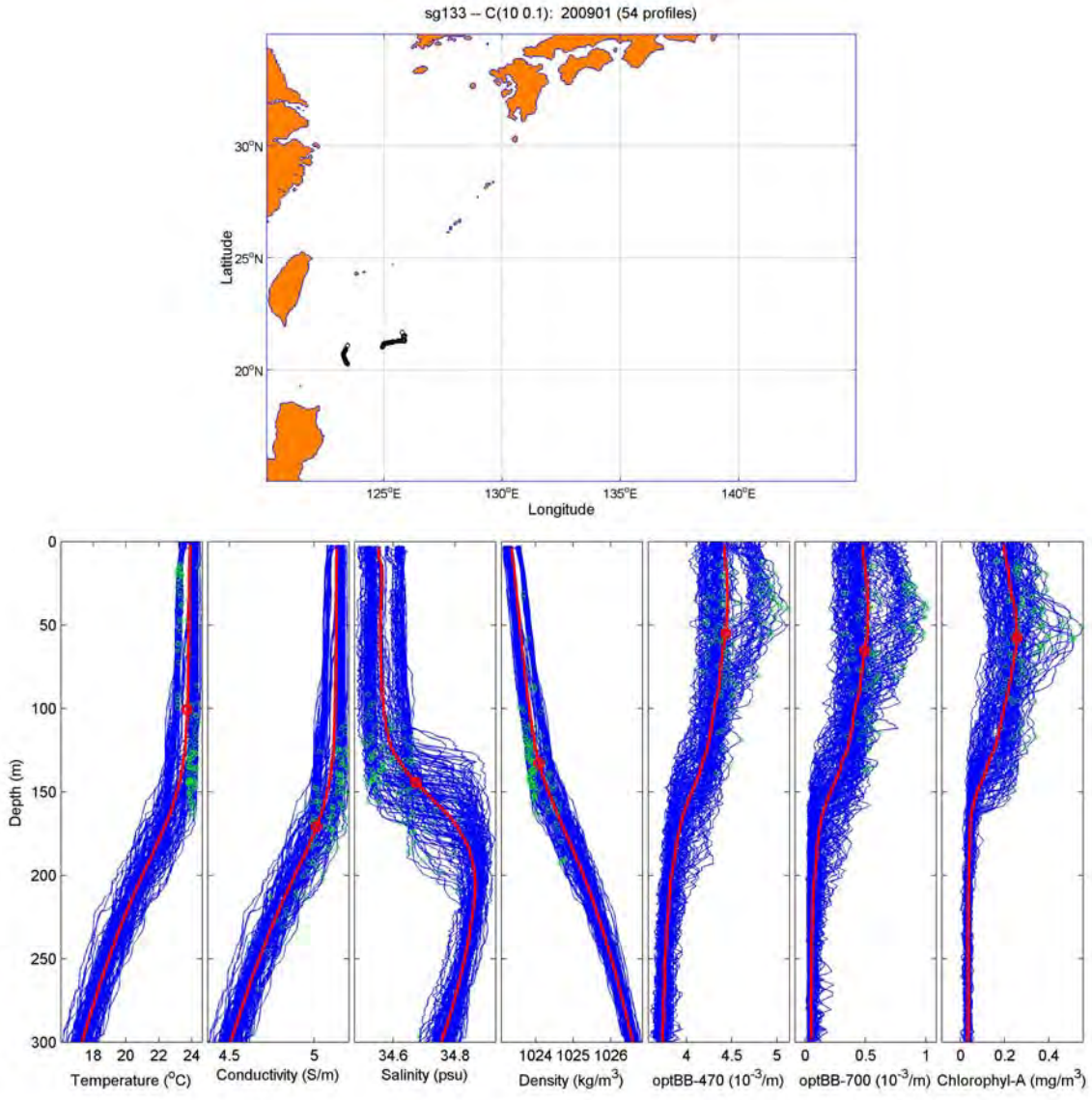

Figure 19. Eight-panel location and parameters for January 2009 Glider 133.

January 2009 Glider	TI MLD	T2 MLD	T3 MLD	T4 MLD	T5 MLD	T6 MLD	SALINITY MLD	DENSITY MLD	470nm Maximum Value	700nm Maximum Value	Chlorophyll Maximum Value
133	101	113	133	149	124	141	144	133	55	66	56
138	132	138	148	156	137	137	155	137	54	71	54

Table 7. Parameter depth in meters for January 2009 by specific SEAGLIDER.

Figure 19 and Table 7 displaying data from January 2009 indicate that there is a deep temperature, density and salinity mixed layer in excess of 100 meters across all temperature mixed layer depth calculation methods, which is very similar to the December 2008 data. The spatial separation of the profiling locations is indicated within the vertical profiles quantitative results, but qualitatively, the profiles are all similar. The optical parameters are well distributed throughout the depth of the temperature and salinity surface based iso-layer, but the optical profile curve indicates a significant reduction of values below the mixed layer depths of the hydrographic properties. This is especially evident in the chlorophyll content panel.

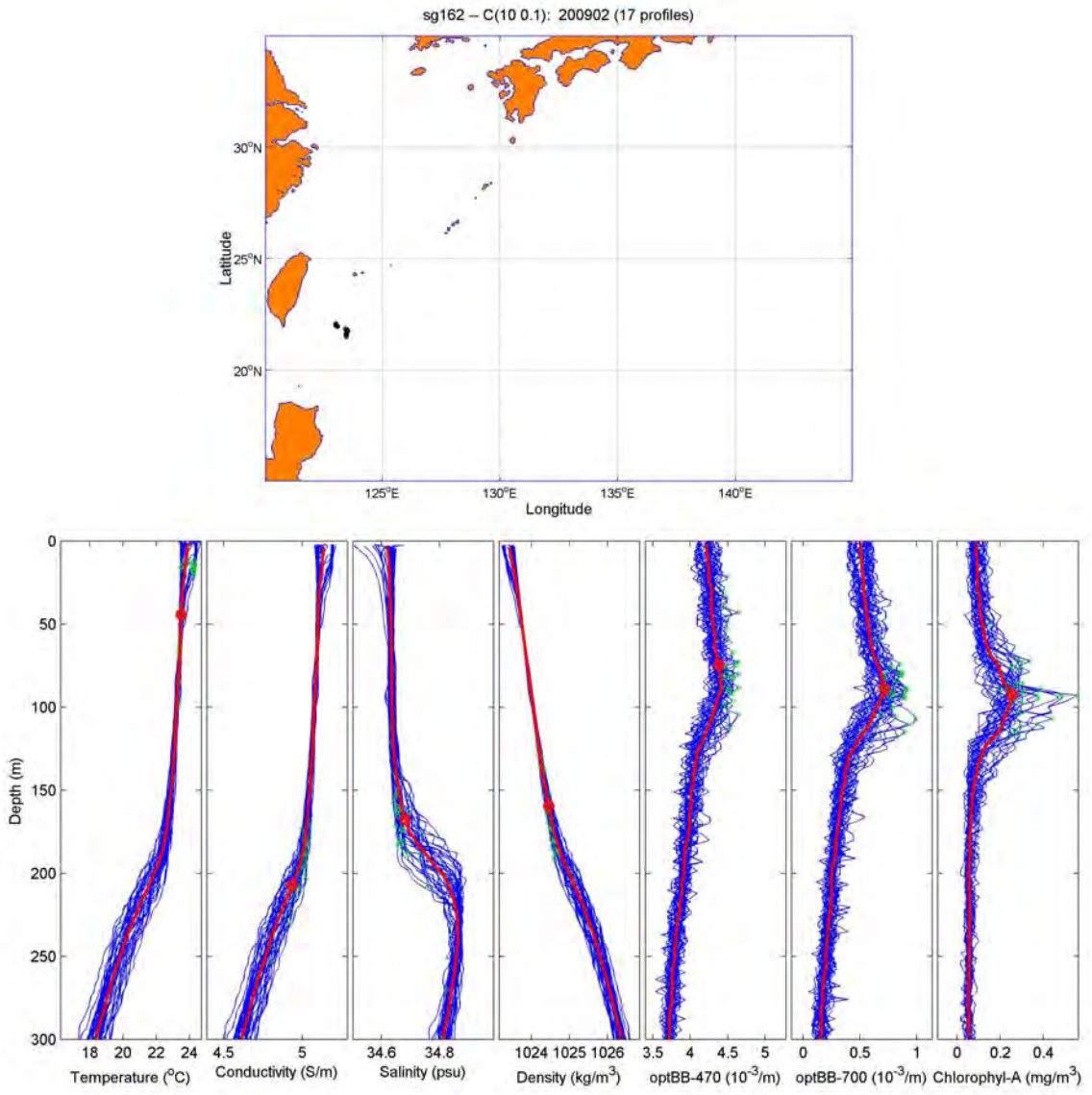

Figure 20. Eight-panel location and parameters for February 2009 Glider 162.

February 2009 Glider	TI MLD	T2 MLD	T3 MLD	T4 MLD	T5 MLD	T6 MLD	SALINITY MLD	DENSITY MLD	470nm Maximum Value	700nm Maximum Value	Chlorophyll Maximum Value
133	52	65	100	141	136	151	157	142	80	83	84
161	24	33	63	121	149	206	194	175	64	74	83
162	44	55	88	118	146	165	168	160	75	89	92

Table 8. Parameter depth in meters for February 2009 by specific SEAGLIDER.

The data from February 2009 presented in Figure 20 and Table 8 indicate a shallow surface layer residing over top of a deep isothermal isohaline layer with depths approaching and exceeding 200 meters in numerous individual profiles. The optical parameters maximum value depths (i.e., backscattering at 470 nm, backscattering at 700 nm and chlorophyll) are all successively deeper in both Figure 20 and Table 8. Similar to December 2008 and January 2009, there is a significant reduction in optical parameter values below the base of the deep isothermal and isohaline layer.

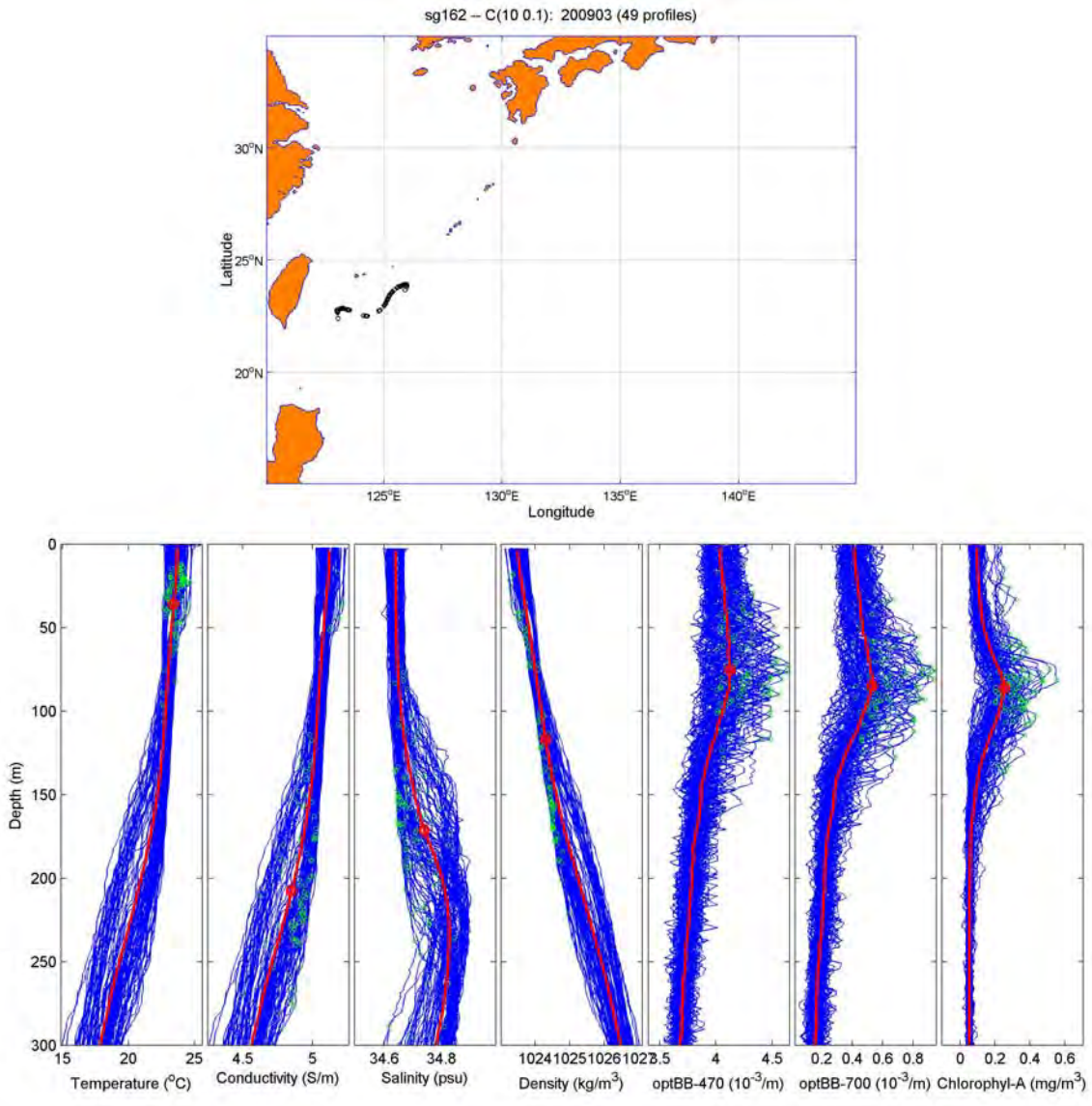

Figure 21. Eight-panel location and parameters for March 2009 Glider 161.

March 2009 Glider	TI MLD	T2 MLD	T3 MLD	T4 MLD	T5 MLD	T6 MLD	SALINITY MLD	DENSITY MLD	470nm Maximum Value	700nm Maximum Value	Chlorophyll Maximum Value
161	50	73	88	107	112	143	175	130	63	75	84
162	35	44	72	102	92	142	171	117	75	85	86

Table 9. Parameter depth in meters for March 2009 by specific SEAGLIDER.

The data from March 2009 presented in Figure 21 and Table 9 is similar to that of February 2009 and indicates a shallow surface layer residing over top of a deep isothermal isohaline layer with depths approaching and exceeding 200 meters in numerous individual profiles. The optical parameters maximum value depths (i.e., backscattering at 470 nm, backscattering at 700 nm and chlorophyll) are all successively deeper in both Figure 21 and Table 9. Similar to January 2009 and February 2009, there is a significant reduction in optical parameter values below the base of the deep isothermal and isohaline layer.

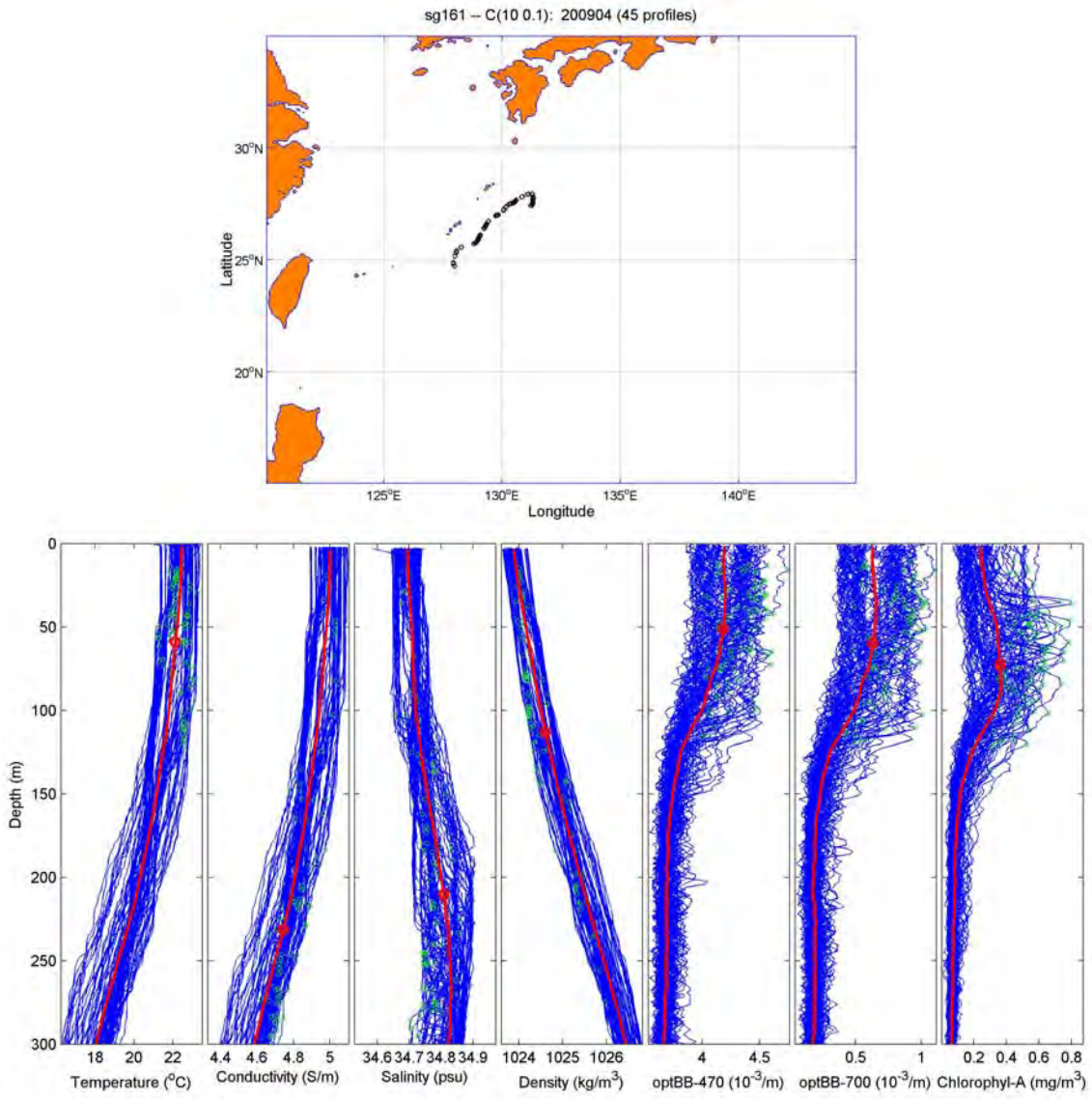

Figure 22. Eight-panel location and parameters for April 2009 Glider 161.

April 2009 Glider	TI MLD	T2 MLD	T3 MLD	T4 MLD	T5 MLD	T6 MLD	SALINITY MLD	DENSITY MLD	470nm Maximum Value	700nm Maximum Value	Chlorophyll Maximum Value
161	59	66	86	107	84	129	210	113	51	60	73
162	35	46	62	81	73	101	126	74	53	64	77

Table 10. Parameter depth in meters for April 2009 by specific SEAGLIDER.

The data from April 2009 presented in Figure 22 and Table 10 is similar to that of March 2009. Spatial separation from south to north is represented in the difference in the sea surface temperature values in the profiles. While there is a wider range of sea surface temperatures presented, the qualitative presentation of the data profiles is similar. The optical parameters are presenting evidence of a spring bloom as the sun angle over the area has increased from the data set profiles that were collected in the winter months (Kudo 1999).

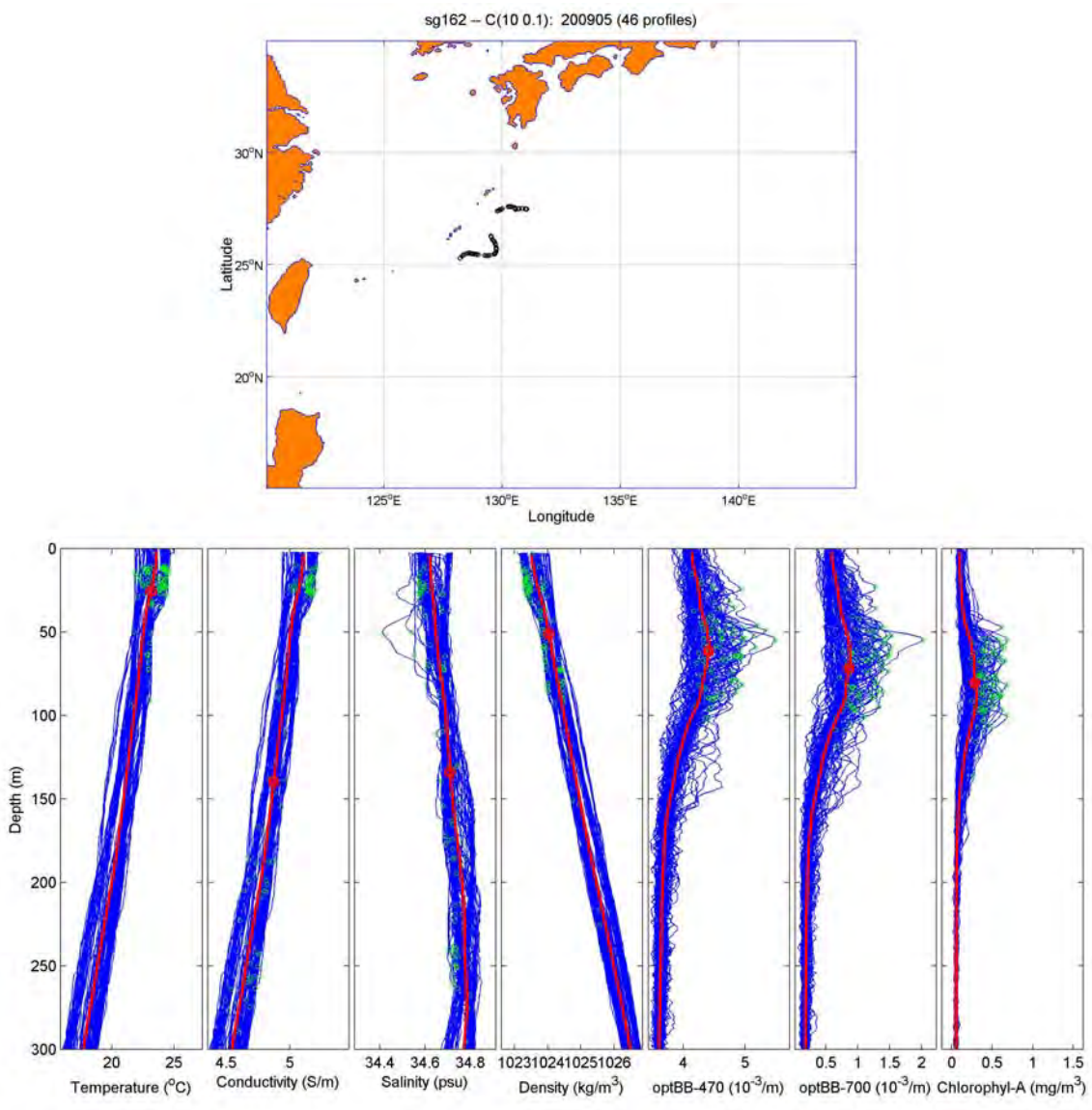

Figure 23. Eight-panel location and parameters for May 2009 Glider 162.

May 2009 Glider	TI MLD	T2 MLD	T3 MLD	T4 MLD	T5 MLD	T6 MLD	SALINITY MLD	DENSITY MLD	470nm Maximum Value	700nm Maximum Value	Chlorophyll Maximum Value
161	27	30	33	40	38	70	121	43	62	67	74
162	26	32	43	54	43	70	134	51	61	72	81

Table 11. Parameter depth in meters for May 2009 by specific SEAGLIDER.

Figure 23 and Table 11 present data from May 2009. There is some spatial separation induced variance which is evident as two distinct groupings of profiles, particularly in the temperature and salinity panels. Similar to April 2009, the profiles are qualitatively similar even though there is variance in the absolute values of the sea surface temperatures noted in the two distinct profile groupings. The spring warming of air and the increased solar angle has increased the sea surface temperatures which is in turn producing a sea surface based mixed layer evident in the profiles and tabular data. The optical parameters maximum value depths (i.e., backscattering at 470 nm, backscattering at 700 nm and chlorophyll) are all successively deeper in both Figure 23 and Table 11.

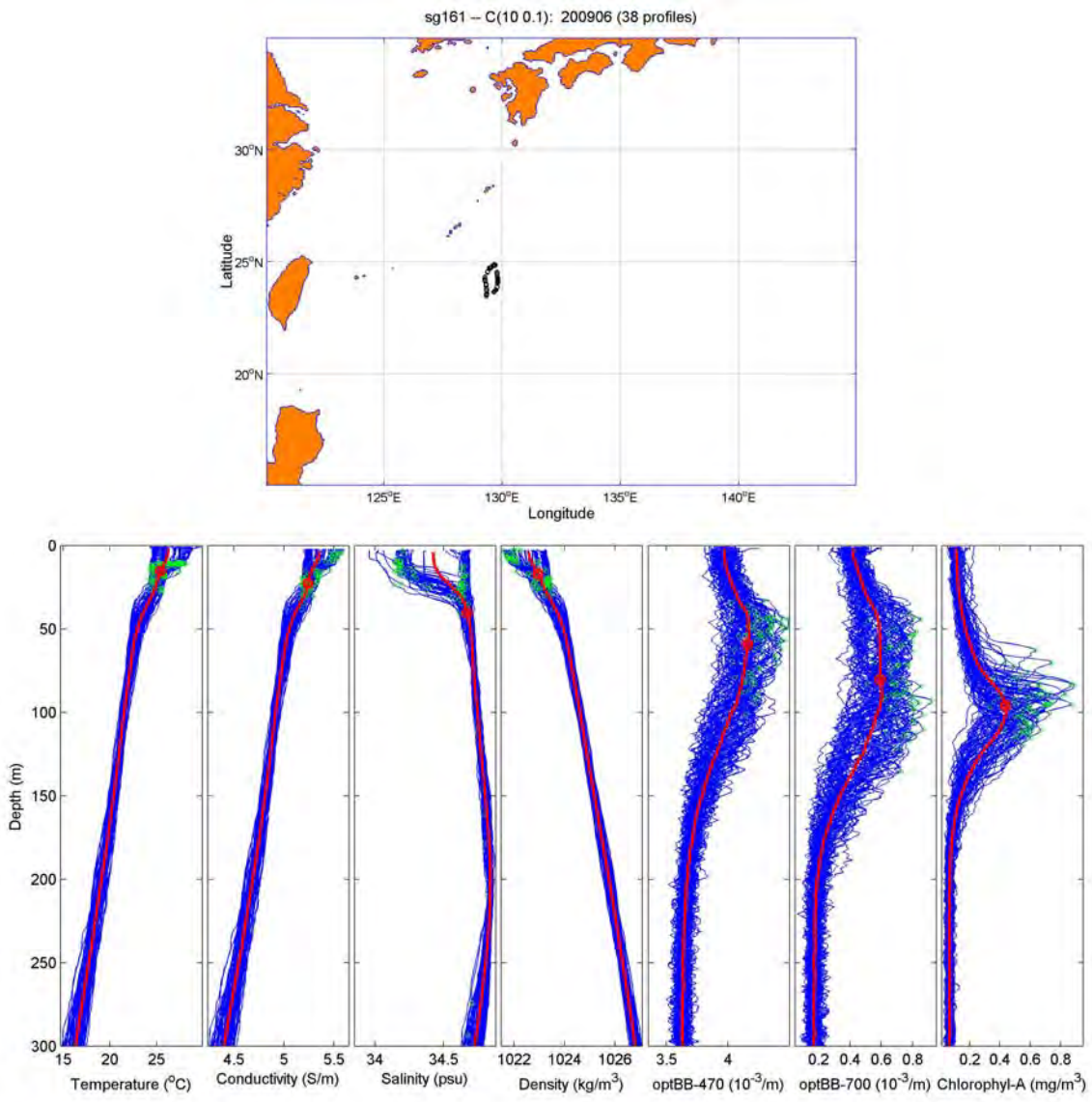

Figure 24. Eight-panel location and parameters for June 2009 Glider 161.

June 2009 Glider	TI MLD	T2 MLD	T3 MLD	T4 MLD	T5 MLD	T6 MLD	SALINITY MLD	DENSITY MLD	470nm Maximum Value	700nm Maximum Value	Chlorophyll Maximum Value
161	15	18	19	22	18	23	40	17	59	80	96
162	212	25	30	34	25	32	67	25	70	85	85

Table 12. Parameter depth in meters for June 2009 by specific SEAGLIDER.

Figure 24 and Table 12 display data from June 2009. There is some south to north as well as east to west spatial separation induced variance which, similar to May 2009, is evident as two distinct groupings of profiles, particularly in the temperature and salinity panels. Similar to May 2009, the profiles are qualitatively similar even though there is variance in the absolute values of the sea surface temperatures and the near surface salinity values noted in the two distinct profile groupings. The continued late spring warming of air and the further increase in the solar angle has further increased the sea surface temperatures which is in turn producing a sea surface based mixed layer evident in the profiles and tabular data. The optical parameters maximum value depths) i.e., backscattering at 470 nm, backscattering at 700 nm and chlorophyll) are all successively deeper in both Figure 24 and Table 11. The chlorophyll panel is indicating a well developed layer of maximum chlorophyll values vertically centered near 95 meters.

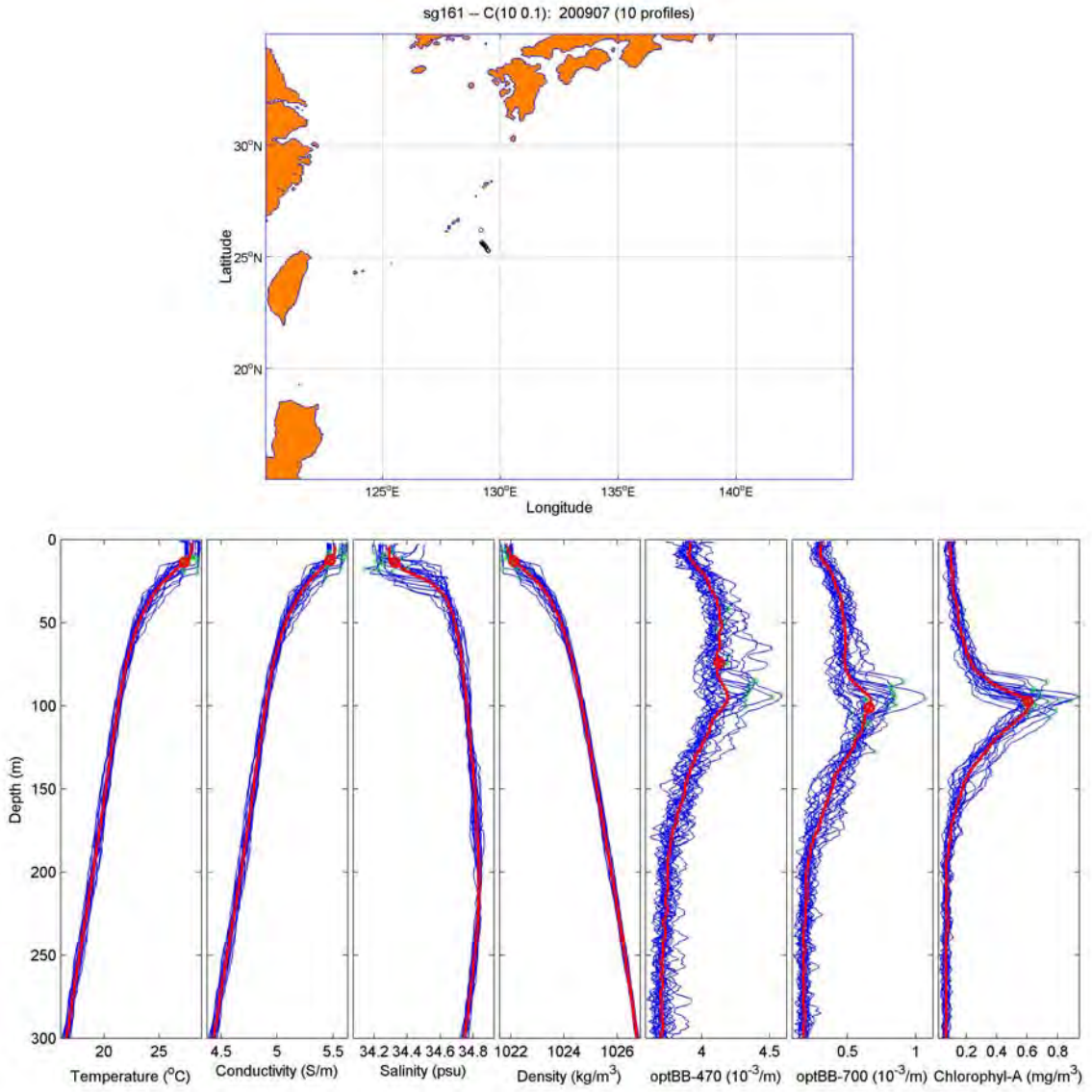

Figure 25. Eight-panel location and parameters for July 2009 Glider 161.

July 2009 Glider	TI MLD	T2 MLD	T3 MLD	T4 MLD	T5 MLD	T6 MLD	SALINITY MLD	DENSITY MLD	470nm Maximum Value	700nm Maximum Value	Chlorophyll Maximum Value
161	14	14	16	17	13	14	14	13	74	101	97

Table 13. Parameter depth in meters for July 2009 by specific SEAGLIDER.

Data presented in Figure 25 and Table 13 for July 2009 is indicating a very pronounced surface mixed layer with sea surface temperatures in excess of 29 Celsius degrees in several of the individual profiles. The temperature drops rapidly between 15 and 45 meters below the warm near surface layer. The optical backscattering at 470 and 700 nm and the chlorophyll content optical properties have a deep maximum value level near 100 meters.

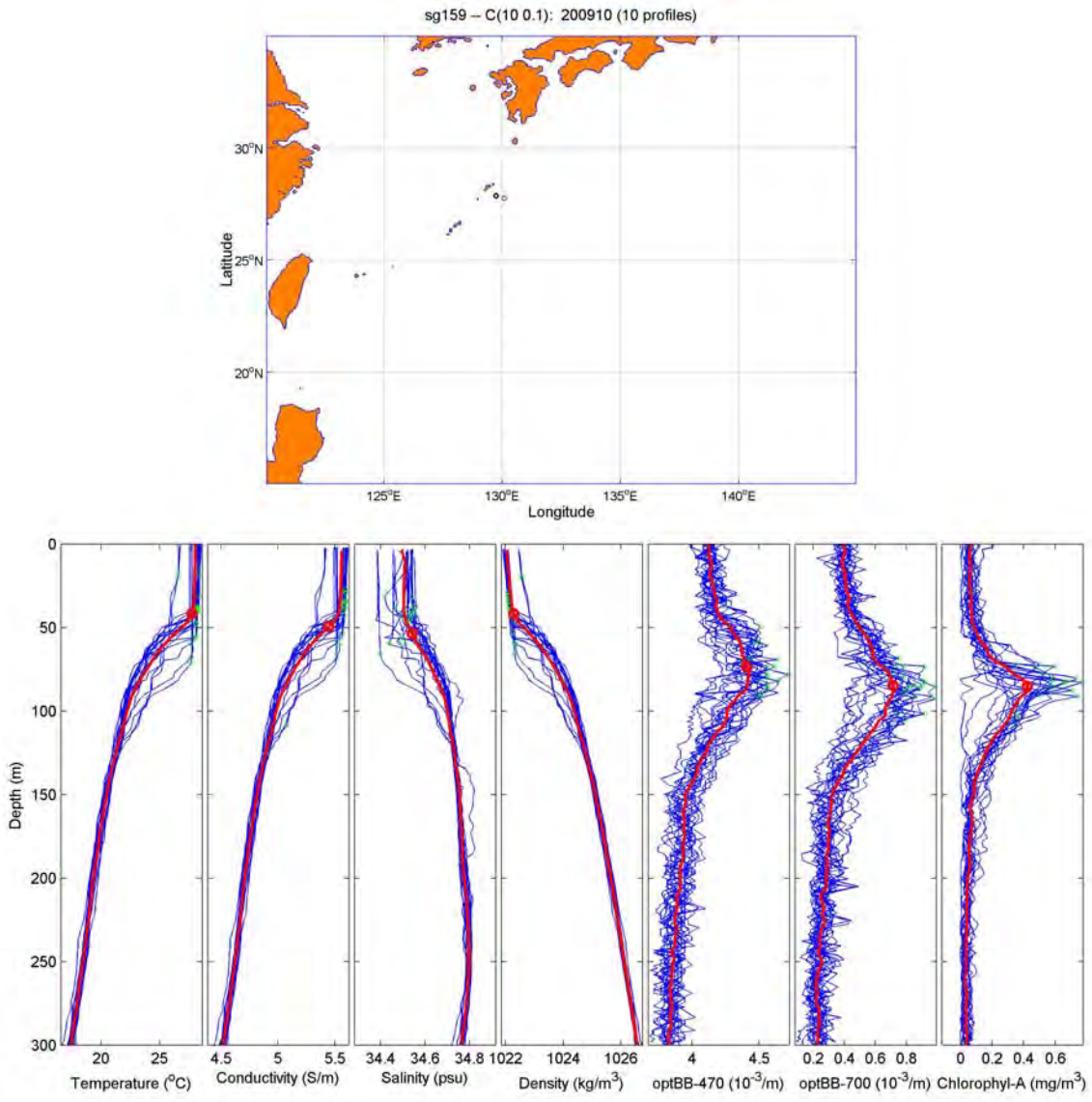

Figure 26. Eight-panel location and parameters for October 2009 Glider 159.

October 2009 Glider	TI MLD	T2 MLD	T3 MLD	T4 MLD	T5 MLD	T6 MLD	SALINITY MLD	DENSITY MLD	470nm Maximum Value	700nm Maximum Value	Chlorophyll Maximum Value
159	41	44	49	51	41	46	54	42	74	85	85

Table 14. Parameter depth in meters for October 2009 by specific SEAGLIDER.

The data for October 2009 presented in Figure 26 and Table 14 is depicting a very pronounced surface based mixed temperature and salinity layer near 45–55 in all profiles. The optical parameters maximum value depths (i.e., backscattering at 470 nm, backscattering at 700 nm and chlorophyll) are all successively deeper in both Figure 26 and Table 14 from 75 to 95 meters.

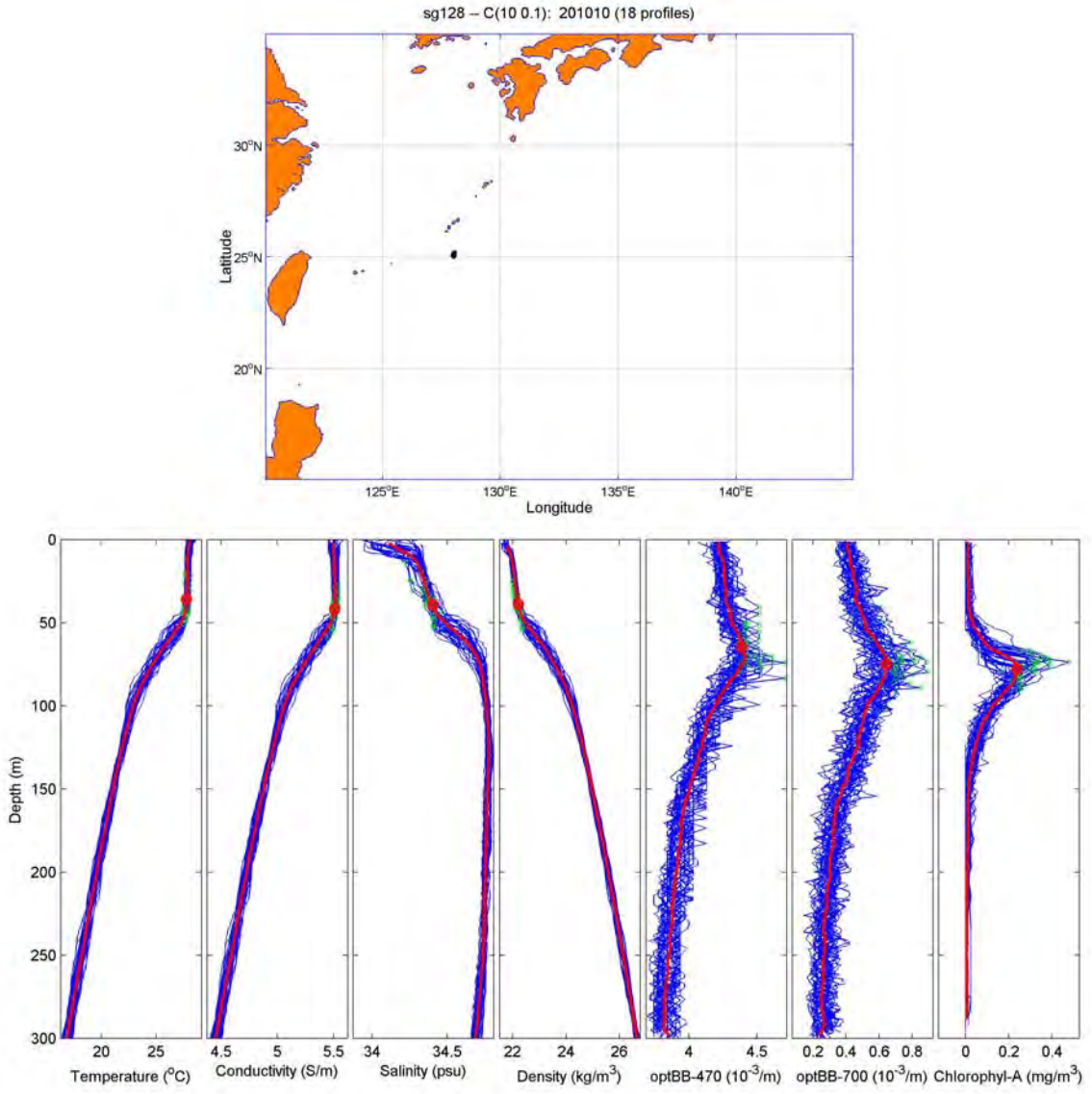

Figure 27. Eight-panel location and parameters for October 2010 Glider 128.

October 2010 Glider	TI MLD	T2 MLD	T3 MLD	T4 MLD	T5 MLD	T6 MLD	SALINITY MLD	DENSITY MLD	470nm Maximum Value	700nm Maximum Value	Chlorophyll Maximum Value
128	45	43	45	52	39	46	40	39	65	75	78

Table 15. Parameter depth in meters for October 2010 by specific SEAGLIDER.

The temperature profile data for October 2010 presented in Figure 27 and Table 15 is depicting a very pronounced surface based mixed temperature layer near 45–55 meters in all profiles. The salinity values are widely distributed in the upper 10–15 meters of the data set, but there is a similar structure below 15 meters with a pronounced halocline near 45 meters. The optical parameters maximum value depths (i.e., backscattering at 470 nm, backscattering at 700 nm and chlorophyll) are all successively deeper in both Figure 27 and Table 15 from 65 to 78 meters.

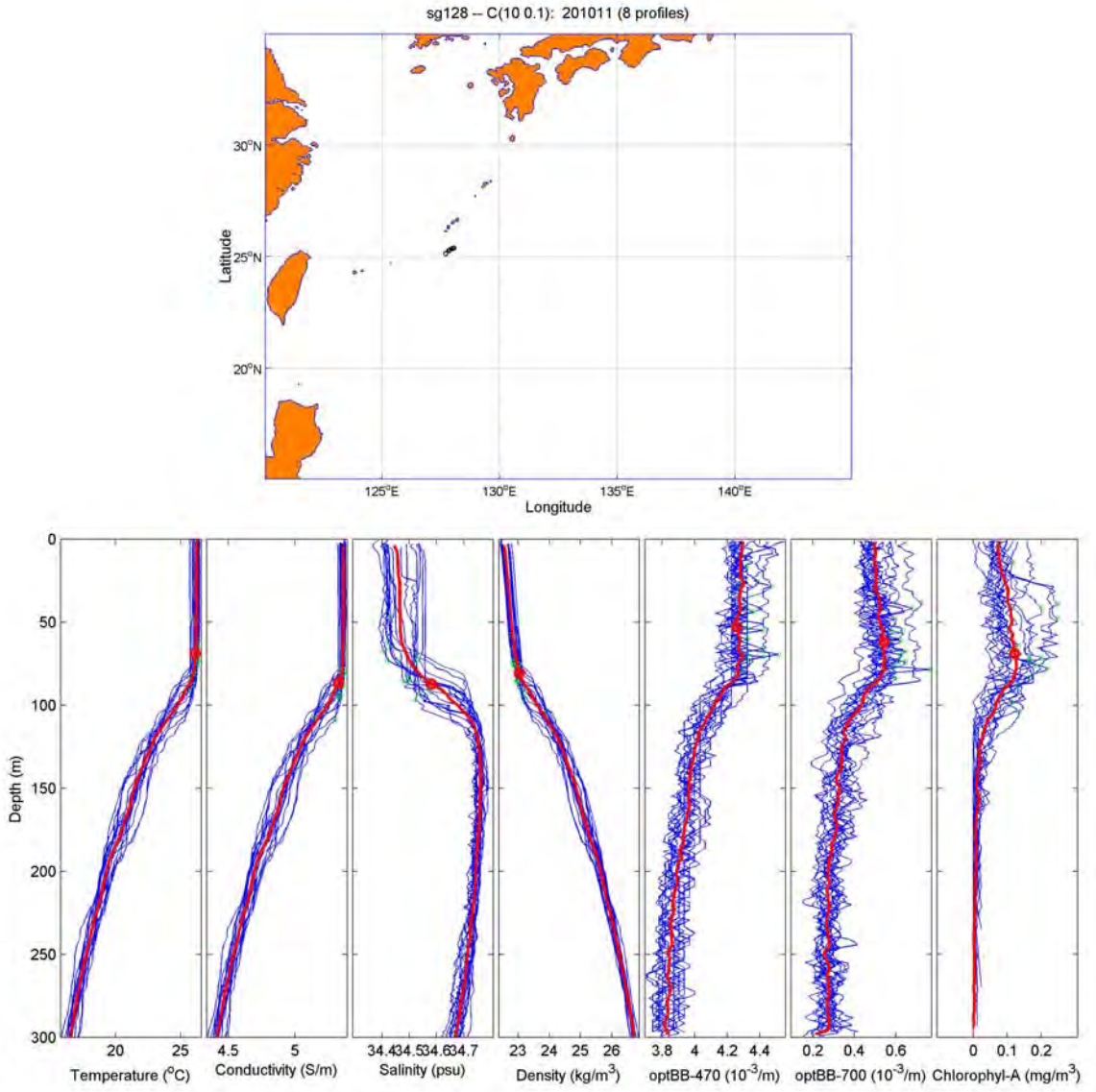

Figure 28. Eight-panel location and parameters for November 2011 Glider 128.

November 2011 Glider	TI MLD	T2 MLD	T3 MLD	T4 MLD	T5 MLD	T6 MLD	SALINITY MLD	DENSITY MLD	470nm Maximum Value	700nm Maximum Value	Chlorophyll Maximum Value
128	69	78	88	92	82	81	87	81	53	62	69

Table 16. Parameter depth in meters for November 2011 by specific SEAGLIDER.

The data profiles collected in November 2011 presented in Figure 28 and Table 16 indicate a deep and pronounced surface based isothermal and isohaline layer from 70 to 90 meters. The thermocline and halocline is quite sharp with a steep decline in temperature and salinity values. The three optical property profiles indicate well vertically distributed levels of backscatter and chlorophyll content in the surface layer with a pronounced decrease in values near the base of the surface thermal, salinity and density mixed layer.

B. SEASONAL VARIATION

Seasonal changes were noted among the hydrographic, optical, and bio-optical parameters. A season by season discussion of the observed parameter vertical profile structures is provided.

1. Winter

The prepared winter profiles are generally marked by a deep mixed layer in excess of 100 meters. The salinity profile in Figure 18 in particular indicates a sharp base with a steep salinity gradient decreasing below the base of the isohaline layer. The temperature and density profiles are all similar, but the gradients are not as steep as in the salinity profile.

The winter bio-optical parameter profiles all indicate the parameter values well distributed within the water column above 100 meters. The optical backscattering coefficient curves for 470 nm and 700 nm as well as the chlorophyll concentration curves are vertically well mixed in the upper 100 meters, but there is an observed base coincident with the base of the hydrographic parameter bases. Below this base, the bio-

optical profiles indicate a rapid decline in values with increasing depth to near 150 meters, below which the curves become isovalued for all three optical and bio-optical parameters.

2. Spring

The spring season hydrographic profiles indicate a sea surface temperature increase above 25°C in response to the higher solar radiation. Warmer spring air masses are preventing ocean surface cooling typically observed in the winter months when Asian continental cold air masses move over the area of the study. The vertical structures of the hydrographic profiles are similar to the winter profiles with a deep mixed layer, but the bases of the mixed layer are not as pronounced. Some salinity profiles are indicating a wide near surface variability. The salinity mixed layer depth calculated using the Maximum Angle method (Chu and Fan 2011) is slightly deeper than the temperature based mixed layer depths and the density mixed layer depth calculated using the Maximum Angle method (Chu and Fan 2011).

The optical backscattering and chlorophyll concentration parameter profiles indicate a well mixed vertical structure above 115 meters depth. There is a marked increase in chlorophyll content in response to the spring phytoplankton bloom. Below 115 meters, there is a gradual decrease in all three parameters to a depth of 150 meters below which all three parameters become vertically uniform.

3. Summer

The Summer hydrographic parameter profiles indicate a marked change from the typical winter and spring scenarios. The sea surface temperature warms above 28°C and there is a near surface mixed layer 20–25 meters deep. The salinity profiles indicate a near surface less saline layer above 20–25 meters below which salinity values rapidly increase with a sharp and steep gradient to near 50 meters. The conductivity and density curves both indicate a similar structure with a well mixed surface layer above 20–25 meters with a rapid change in values to near 50 meters below which all hydrographic parameter gradients become less pronounced.

The optical backscattering and chlorophyll concentration profiles indicate a prominent layer of increased values near 100 meters depth, with a sharp and pronounced gradient of decreasing values to near 150 meters. Below this depth, the three parameters become vertically uniform.

4. Autumn

The autumn hydrographic profiles are marked by a surface based mixed layer structure to 50 meters depth. This structure is evident in all four hydrographic variables. Below the surface mixed layer, there is a sharp steep gradient to near 85 meters below which the decline in values becomes more gradual. Sea surface temperatures are 28–30 Celsius degrees.

The optical backscattering and the chlorophyll content vertical profiles curves are similar to the summer profiles discussed above in the summer section, but the chlorophyll content maxima is shallower and located near 85 meters. The parameter values decrease rapidly to near 140 meters depth below which the curves become vertically uniform.

C. STATISTICAL HYDROGRAPHIC AND OPTICAL RELATIONSHIP

Correlation analysis of hydrographic and optical parameters was performed. There was not any consistent data set wide correlation of the depth or qualitative presentation of the profiles of any particular hydrographic variable such as temperature, conductivity, salinity or density profiles to the profiles or depths of the bio-optical or optical properties (i.e., optical backscattering at 470 nm and 700 nm or chlorophyll content vertical profiles).

However, under certain conditions, such as those evident in December 2008, January 2009 and November 2011 in Figures 18, 19 and 28, the depths of the bases of the hydrographic property mixed layer depths coincided with the depths of a pronounced decrease in the values of the bio-optical properties. Qualitatively, these three months all are marked by deep isothermal and isohaline structures from the surface to depths in excess of 100 meters. Below the bases of the isothermal and isohaline layers, the thermocline and haloclines are both pronounced with a steep thermal and haline gradient.

The bio-optical and optical properties all visually present a “valuecline” in that the two backscattering coefficients and the chlorophyll concentration profiles quickly reduce to minima with a shape presentation similar to that of the thermoclines and haloclines evident in the hydrographic profiles.

D. STATISTICAL CHLOROPHYLL AND OPTICAL RELATIONSHIP

MATLAB script was used to determine the Pearson correlation coefficient (Ingram 1974) for the depth of the maximum value of chlorophyll concentration compared to the depth of the maximum value of the optical backscattering coefficient at 470 nm. Separately, the depth of the maximum value of chlorophyll content was compared to the depth of the maximum value of the backscattering coefficient at 700 nm. The Pearson correlation coefficient is given by the equation below.

$$r = \frac{\sum_{i=1}^{n}(X_i - \bar{X})(Y_i - \bar{Y})}{\sqrt{\sum_{i=1}^{n}(X_i - \bar{X})^2}\sqrt{\sum_{i=1}^{n}(Y_i - \bar{Y})^2}}$$

The MATLAB script calculated result is presented in Figure 29. The blue dots represent the depth in meters of maximum chlorophyll content on the x axis with the depths of the respective optical backscattering coefficients along the y axis for each dive profile within the data set. The 470 nm backscattering coefficient is .313 with a mean rate, or slope, of .81, and the 700 nm backscattering coefficient is .525 with a mean rate, or slope, of .97. These results indicate that the depth of the max 700 nm backscattering coefficient more closely correlates to the depth of the maximum chlorophyll content. The results confirm the qualitative visual interpretation of the bio-optical properties in the eight-panel figures presented above.

In simple terms, the depth of the maximum backscatter coefficient at 470 nm is typically found above the depth of the maximum backscatter coefficient at 700 nm which is in turn found above the depth of the maximum chlorophyll content. There is typically less vertical separation between the depths of the maximum backscatter coefficient at 700 nm and the maximum values of chlorophyll content. See Figure 25 above for an excellent example of this phenomenon.

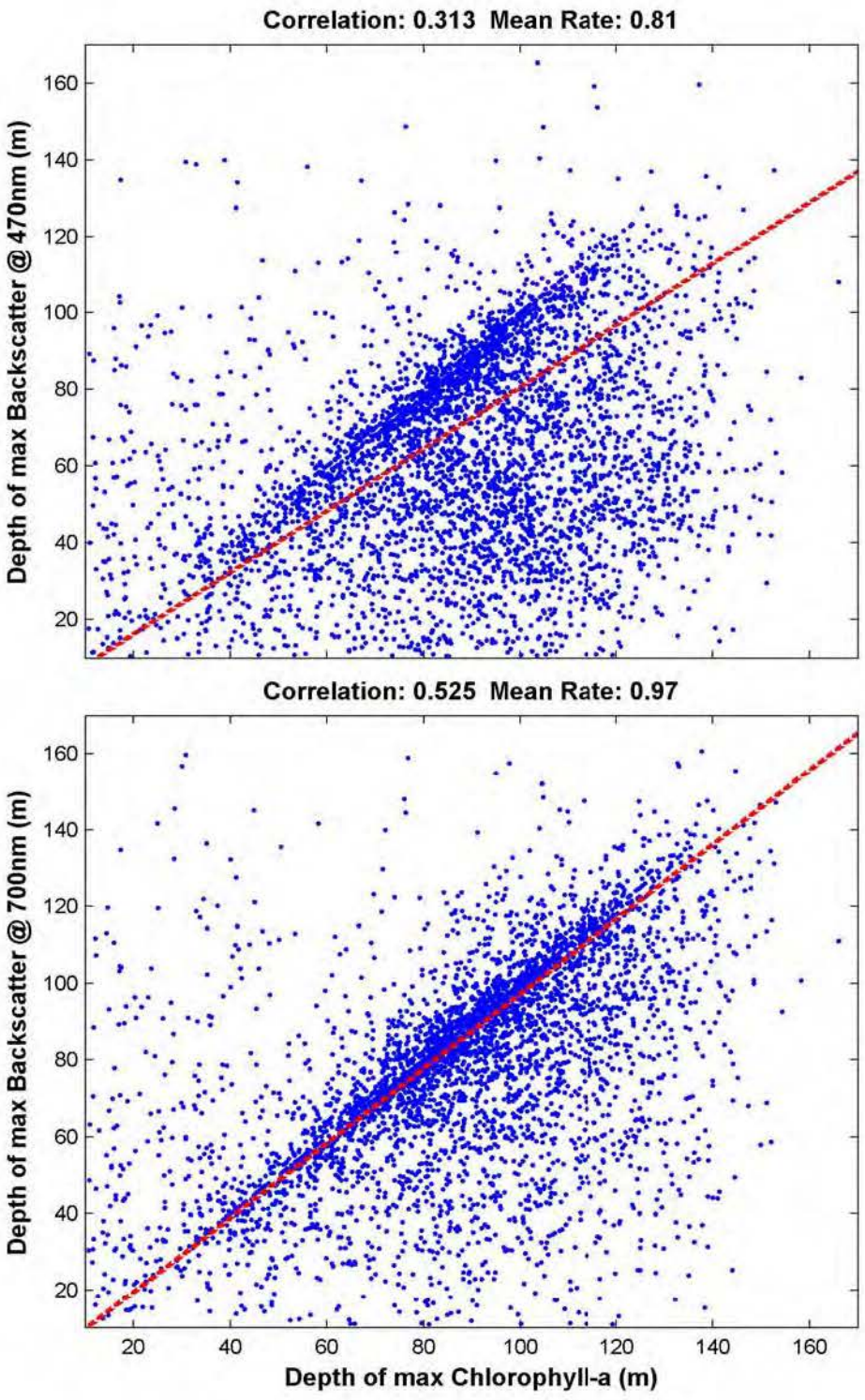

Figure 29. Depth of maximum value of chlorophyll content correlated to depth of maximum values of backscattering coefficients at 470 and 700 nm.

The data set was reduced by visual inspection using the previously discussed MATLAB program to view individual dive profiles. Data profiles that presented potentially corrupted bio-optical curves were discarded. The Pearson linear coefficient (Ingram 1974) MATLAB routine discussed above was then applied to this reduced data set. The result is presented in Figure 30.

The result is similar to that of the larger data set. The 470 nm backscattering coefficient is .317 with a mean rate, or slope, of .83, and the 700 nm backscattering coefficient is .522 with a mean rate, or slope, of 1. These results indicate that the vertical depth of the max 700 nm backscattering coefficient correlates to the depth of the maximum chlorophyll content.

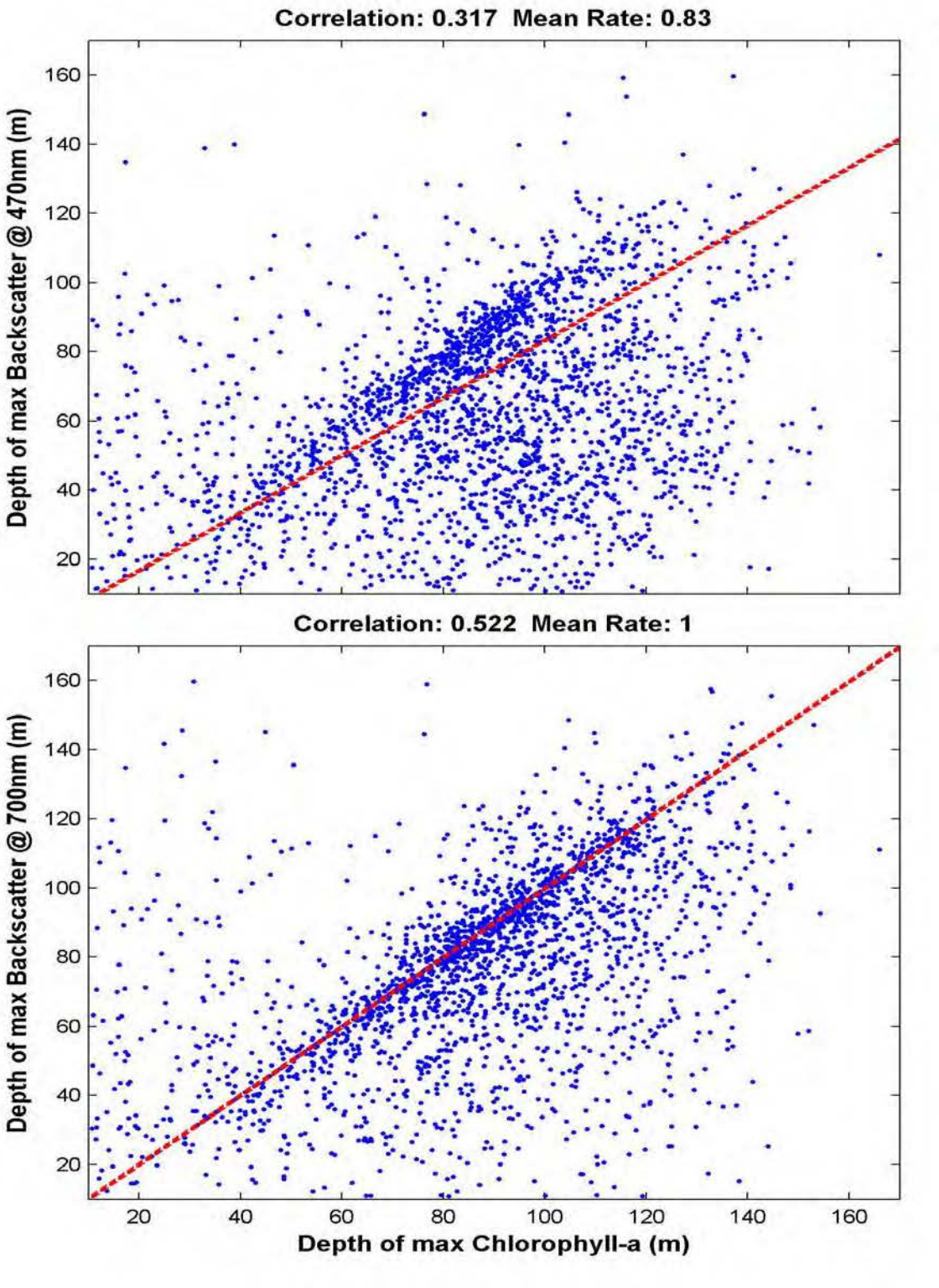

Figure 30. Reduced set depth of maximum value of chlorophyll content correlated to depth of maximum values of backscattering coefficients at 470 and 700 nm.

V. CONCLUSIONS AND FUTURE WORK

A. CONCLUSIONS

The U.S. Navy operates across all the world oceans and seas; the ocean environment significantly affects all naval operations. Naval operations are of course conducted above, on, and beneath the surface of the world oceans. The SEAGLIDER is a remotely operated vehicle that is being used to collect and transmit various observed oceanic parameters for inclusion in computer models that predict oceanic conditions and weapon and sensor performance. An analysis of a collected SEAGLIDER data set will foster greater understanding of the hydrographic, optical and bio-optical characteristics of the western Pacific Ocean which will help understanding of the ocean environment and will in turn facilitate the ability of naval warfighters and planners to better achieve victory in any potential conflict.

For these reasons, a temporal and spatial analysis of a collected SEAGLIDER data set from the western Pacific Ocean was performed to provide a better understanding of the physical oceanographic environment in this strategically vital area. The two dimensional monthly graphs of the various hydrographic and bio-optical parameters will improve the operational and situational awareness regarding the oceanographic conditions among the oceanography and various warfighting communities.

Furthermore, a correlation of observed parameters was completed to facilitate the improvement of operational models used to predict oceanographic conditions. Additionally, the completed analysis of the seasonal variability of the hydrographic and bio-optical conditions can facilitate the better understanding of how expected conditions can change over the course of the year.

Across the entirety of the analyzed data set, the depth of the maximum values of the analyzed bio-optical properties could not be linked to a particular hydrographic profile. There was not any consistent data set wide correlation of the depth or qualitative presentation of the profiles of any particular hydrographic variable such as temperature, conductivity, salinity or density profiles to the profiles or depths of the bio-optical or

optical properties (i.e., optical backscattering at 470 nm and 700 nm or chlorophyll content vertical profiles).

However, certain hydrographic profiles occurring in the winter months did qualitatively coincide with the depths of the maximum values of the bio-optical properties. The depths of the bases of the hydrographic property mixed layer depths coincided with the depths of a pronounced decrease in the values of the bio-optical properties. Qualitatively, these three months all are marked by deep isothermal and isohaline structures from the surface to depths in excess of 100 meters. Below the bases of the isothermal and isohaline layers, the thermocline and haloclines are both pronounced with a steep thermal and haline gradient.

There is correlation of the optical backscattering coefficients and the chlorophyll concentration within the analyzed data set. In simple terms, the depth of the maximum backscatter coefficient at 470 nm is typically found above the depth of the maximum backscatter coefficient at 700 nm which is in turn found above the depth of the maximum chlorophyll content. There is typically less vertical separation between the depths of the maximum backscatter coefficient at 700 nm and the maximum values of chlorophyll content. See Figure 25 above for an excellent example of this phenomenon.

In short, the hydrographic and bio-optical conditions in the western Pacific Ocean are important considerations for naval operators. Hopefully, this analysis will improve operators' environmental awareness and facilitate better operational and tactical planning decisions.

B. FUTURE WORK

There is potential for several follow on research and data analysis projects. A similar data set has been collected from the South China Sea region and is ready to be analyzed. Once complete, the result of that study could be compared to the results of this project to determine what, if any, similarities exist between the respective water masses.

A portion of the data set used in this analysis had corrupted or missing bio-optical property data. A study focusing solely on the collected conductivity, temperature, and density portion of the data set would be useful for inclusion in a climatological data base.

A study to determine if bio-optical max value layers vertically propagate within the water column when perturbed could prove useful to naval planners.

A study to determine if the depth of the maximum value layers of bio-optical properties could be sensed from altitude could also prove useful to naval planners as well as other scientific and economic communities.

THIS PAGE INTENTIONALLY LEFT BLANK

APPENDIX. MONTHLY EIGHT-PANEL FIGURES

The remainder of the monthly eight-panel figures is presented on the following pages.

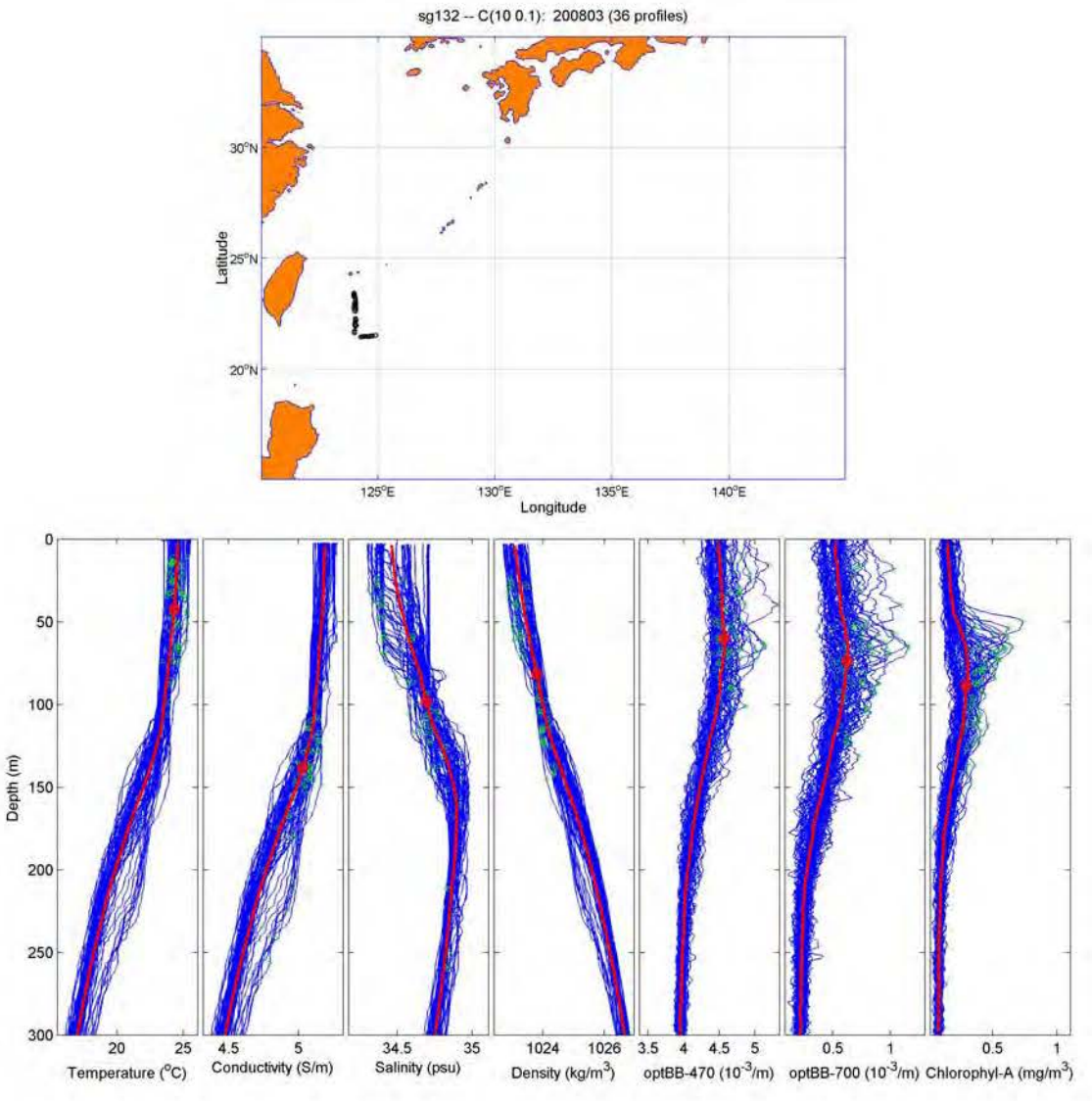

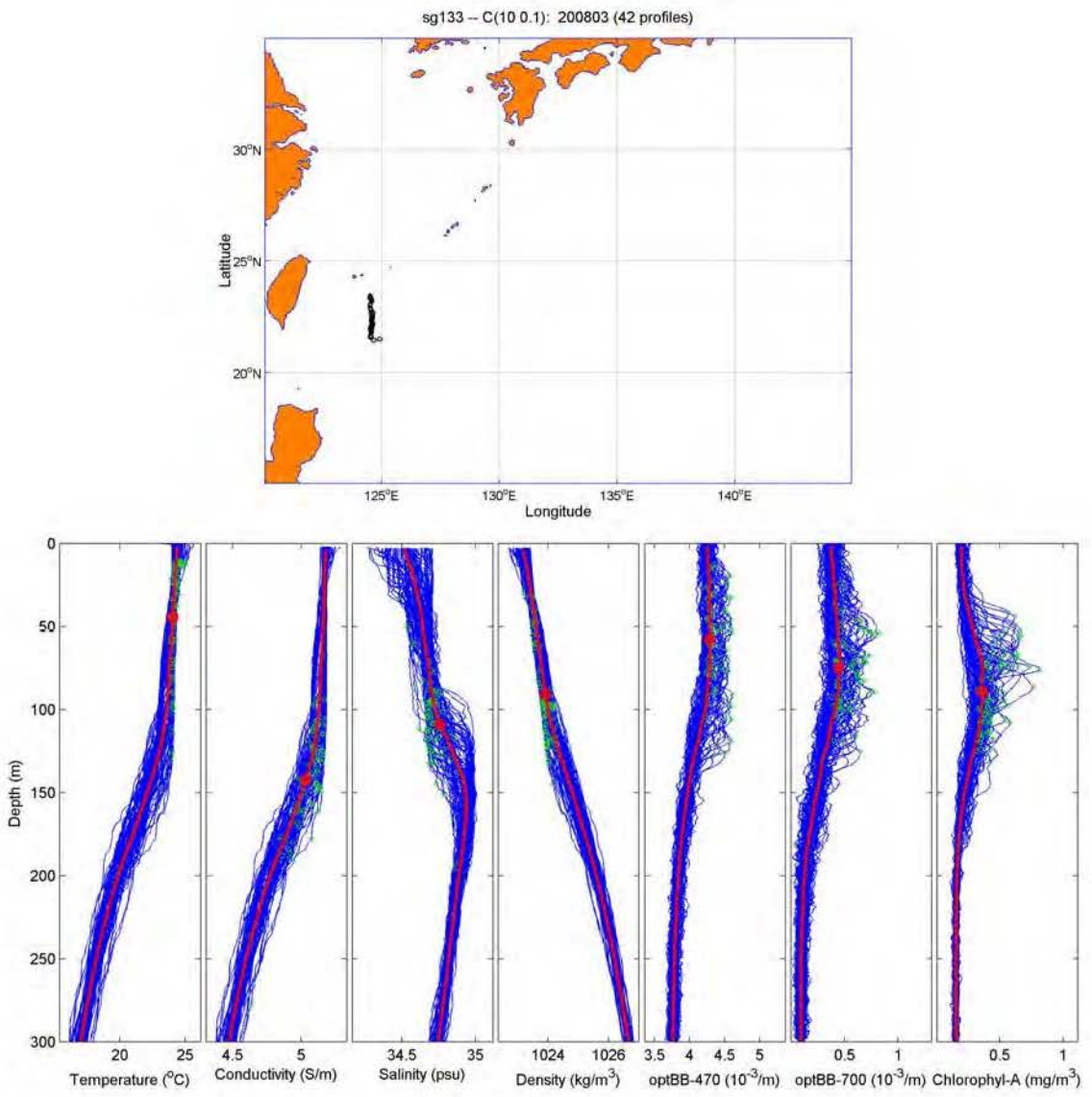
sg133 -- C(10 0.1): 200803 (42 profiles)
30°N
25°N
20°N
Latitude
125°E
130°E
135°E
140°E
Longitude
Depth (m)
0
50
100
150
200
250
300
20
25
Temperature (°C)
4.5
5
Conductivity (S/m)
34.5
35
Salinity (psu)
1024
1026
Density (kg/m3)
3.5
4
4.5
5
optBB-470 (10-3/m)
0.5
1
optBB-700 (10-3/m)
0.5
1
Chlorophyl-A (mg/m3)

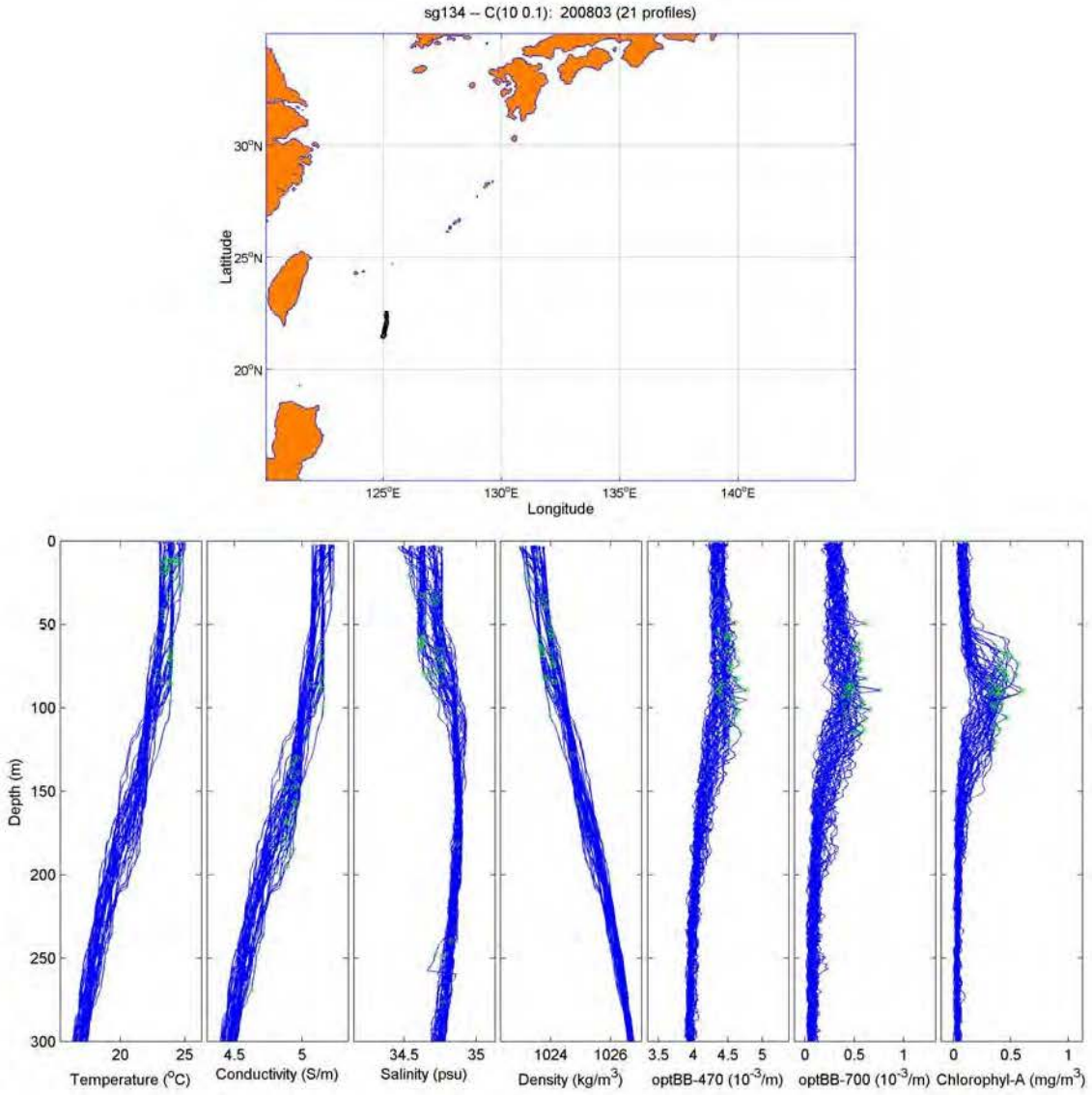
sg134 -- C(10 0.1): 200803 (21 profiles)
30°N
25°N
20°N
Latitude
125°E
130°E
135°E
140°E
Longitude
Depth (m)
0
50
100
150
200
250
300
20
25
Temperature (°C)
4.5
5
Conductivity (S/m)
34.5
35
Salinity (psu)
1024
1026
Density (kg/m3)
3.5
4
4.5
5
optBB-470 (10-3/m)
0
0.5
1
optBB-700 (10-3/m)
0
0.5
1
Chlorophyl-A (mg/m3)

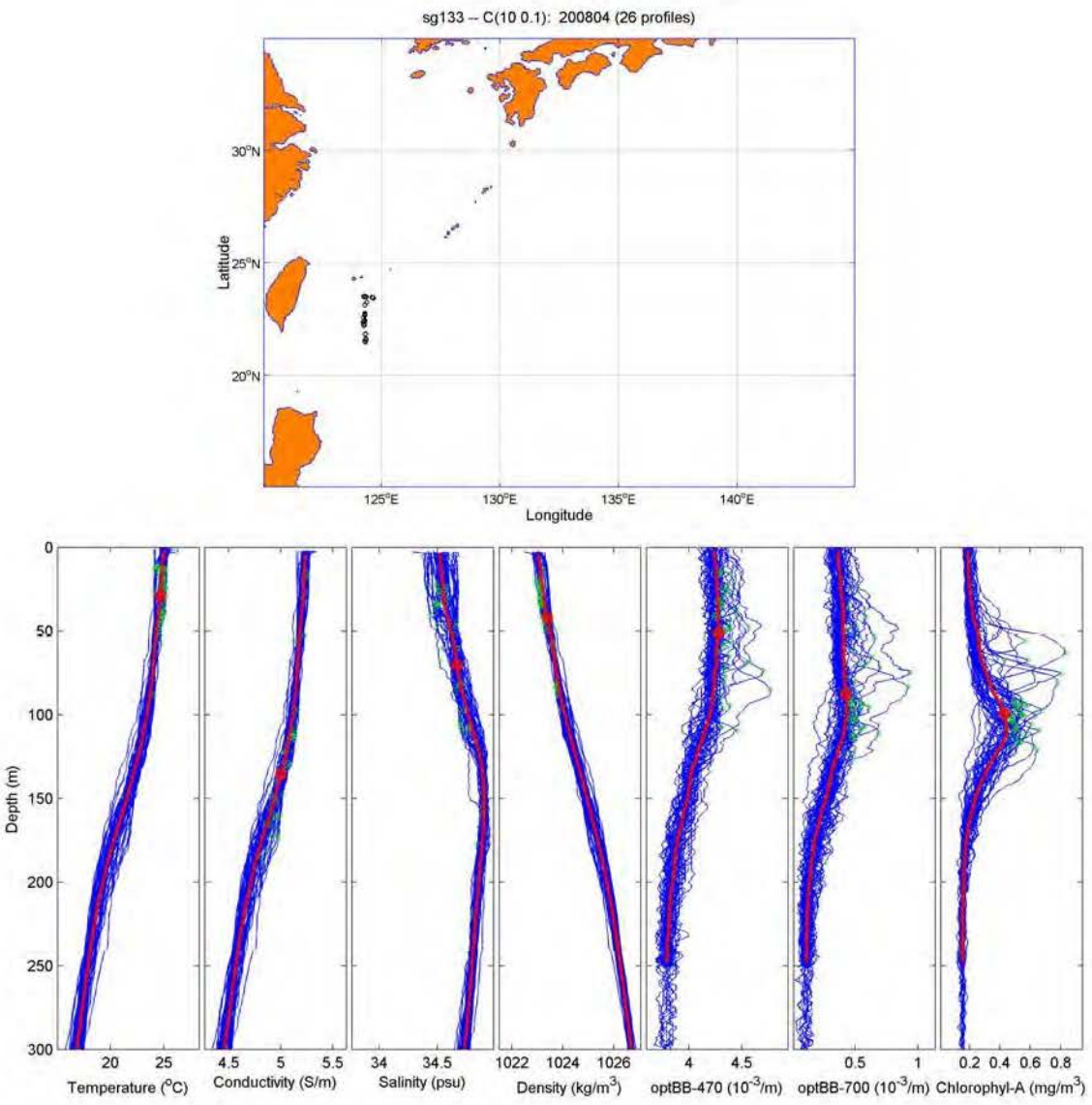
sg133 -- C(10 0.1): 200804 (26 profiles)
30°N
25°N
20°N
Latitude
125°E
130°E
135°E
140°E
Longitude
Depth (m)
0
50
100
150
200
250
300
20
25
Temperature (°C)
4.5
5
5.5
Conductivity (S/m)
34
34.5
Salinity (psu)
1022
1024
1026
Density (kg/m3)
4
4.5
optBB-470 (10-3/m)
0.5
1
optBB-700 (10-3/m)
0.2
0.4
0.6
0.8
Chlorophyl-A (mg/m3)

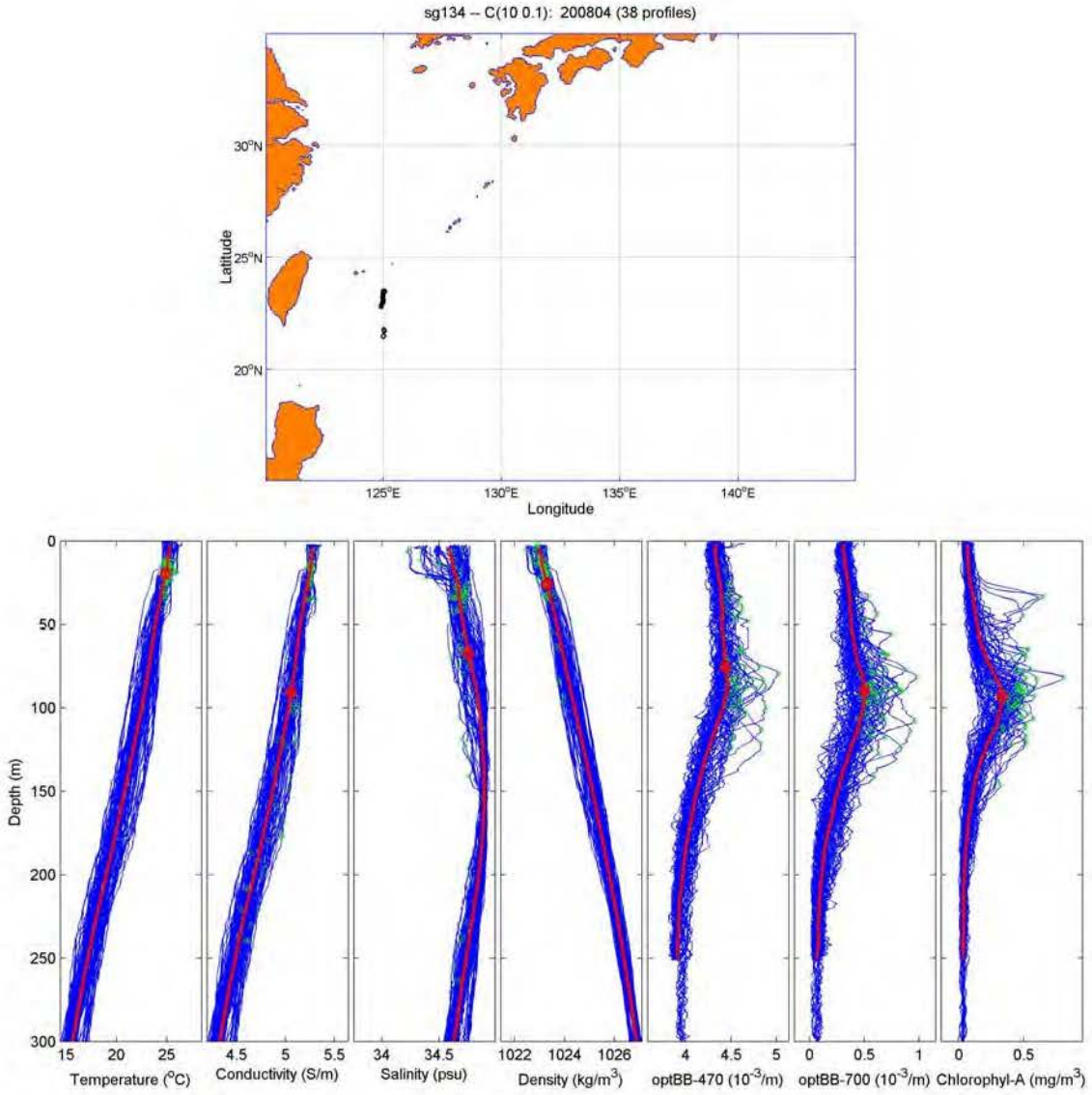
sg134 -- C(10 0.1): 200804 (38 profiles)
30°N
25°N
20°N
Latitude
125°E
130°E
135°E
140°E
Longitude
Depth (m)
0
50
100
150
200
250
300
15 20 25
Temperature (°C)
4.5 5 5.5
Conductivity (S/m)
34 34.5
Salinity (psu)
1022 1024 1026
Density (kg/m3)
4 4.5 5
optBB-470 (10-3/m)
0 0.5 1
optBB-700 (10-3/m)
0 0.5
Chlorophyl-A (mg/m3)

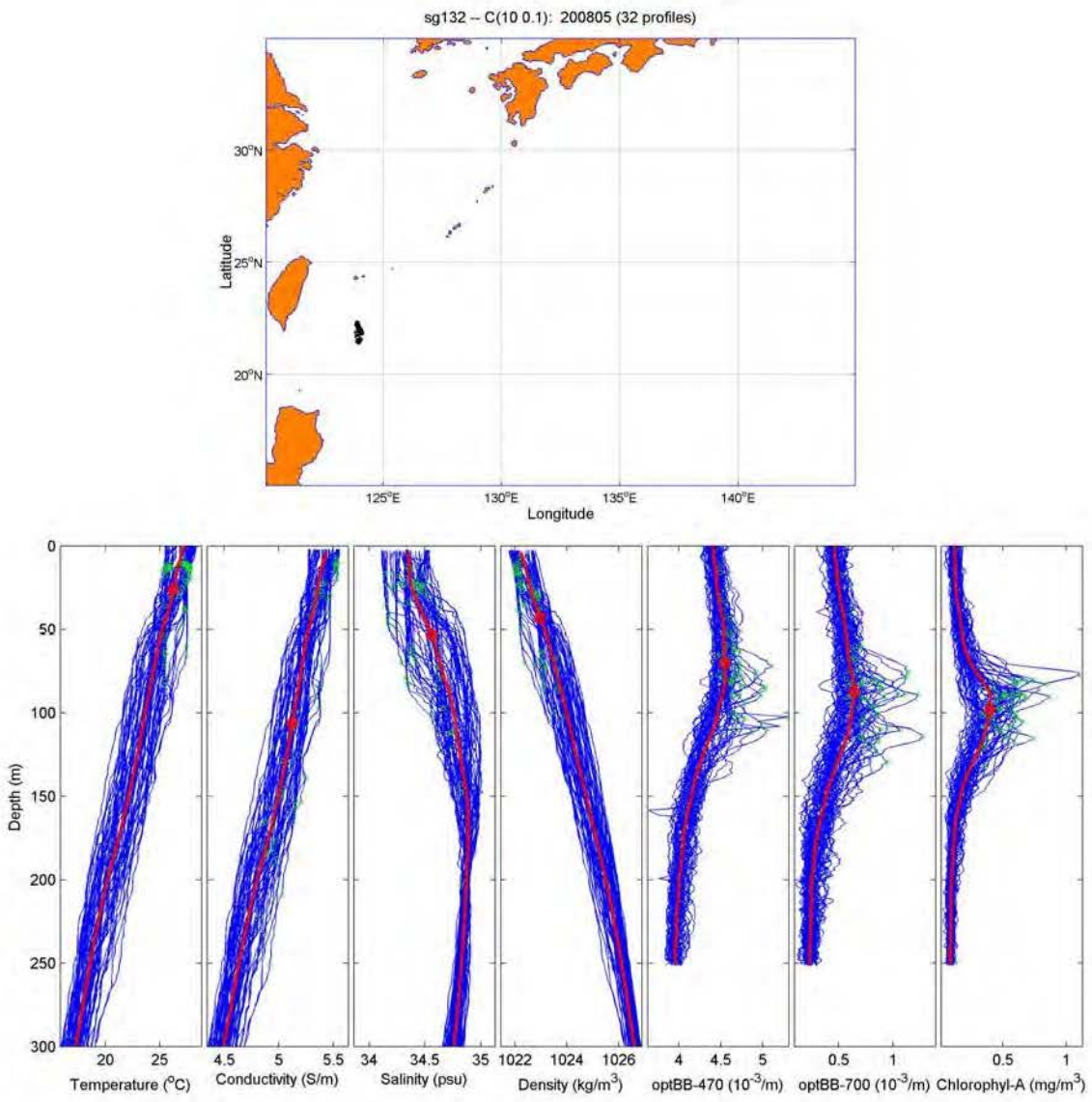
sg132 -- C(10 0.1): 200805 (32 profiles)
30°N
25°N
20°N
Latitude
125°E
130°E
135°E
140°E
Longitude
Depth (m)
0
50
100
150
200
250
300
20
25
Temperature (°C)
4.5
5
5.5
Conductivity (S/m)
34
34.5
35
Salinity (psu)
1022
1024
1026
Density (kg/m3)
4
4.5
5
optBB-470 (10-3/m)
0.5
1
optBB-700 (10-3/m)
0.5
1
Chlorophyl-A (mg/m3)

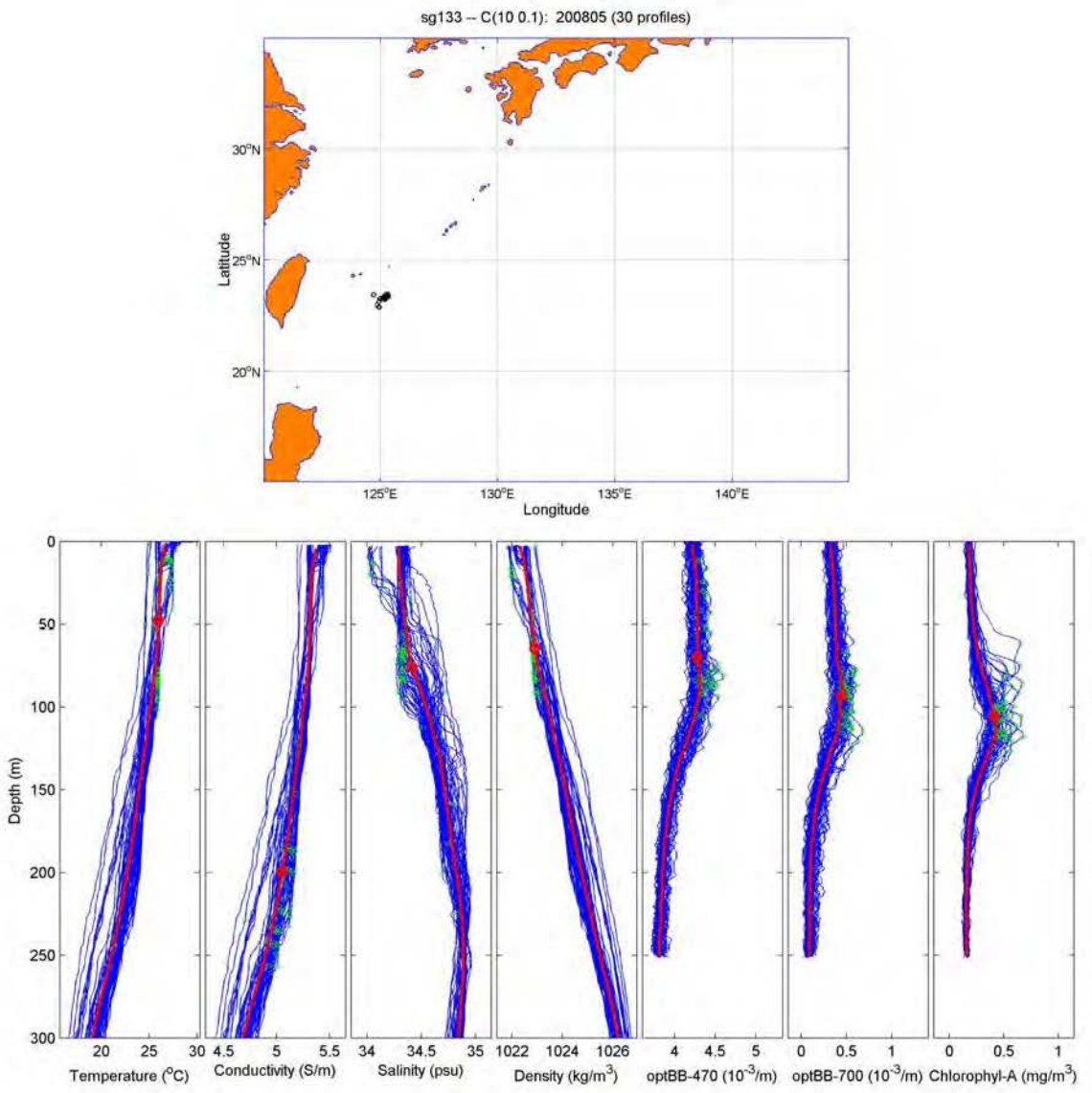
sg133 -- C(10 0.1): 200805 (30 profiles)
30°N
25°N
20°N
Latitude
125°E
130°E
135°E
140°E
Longitude
Depth (m)
0
50
100
150
200
250
300
20 25 30
Temperature (°C)
4.5 5 5.5
Conductivity (S/m)
34 34.5 35
Salinity (psu)
1022 1024 1026
Density (kg/m3)
4 4.5 5
optBB-470 (10-3/m)
0 0.5 1
optBB-700 (10-3/m)
0 0.5 1
Chlorophyl-A (mg/m3)

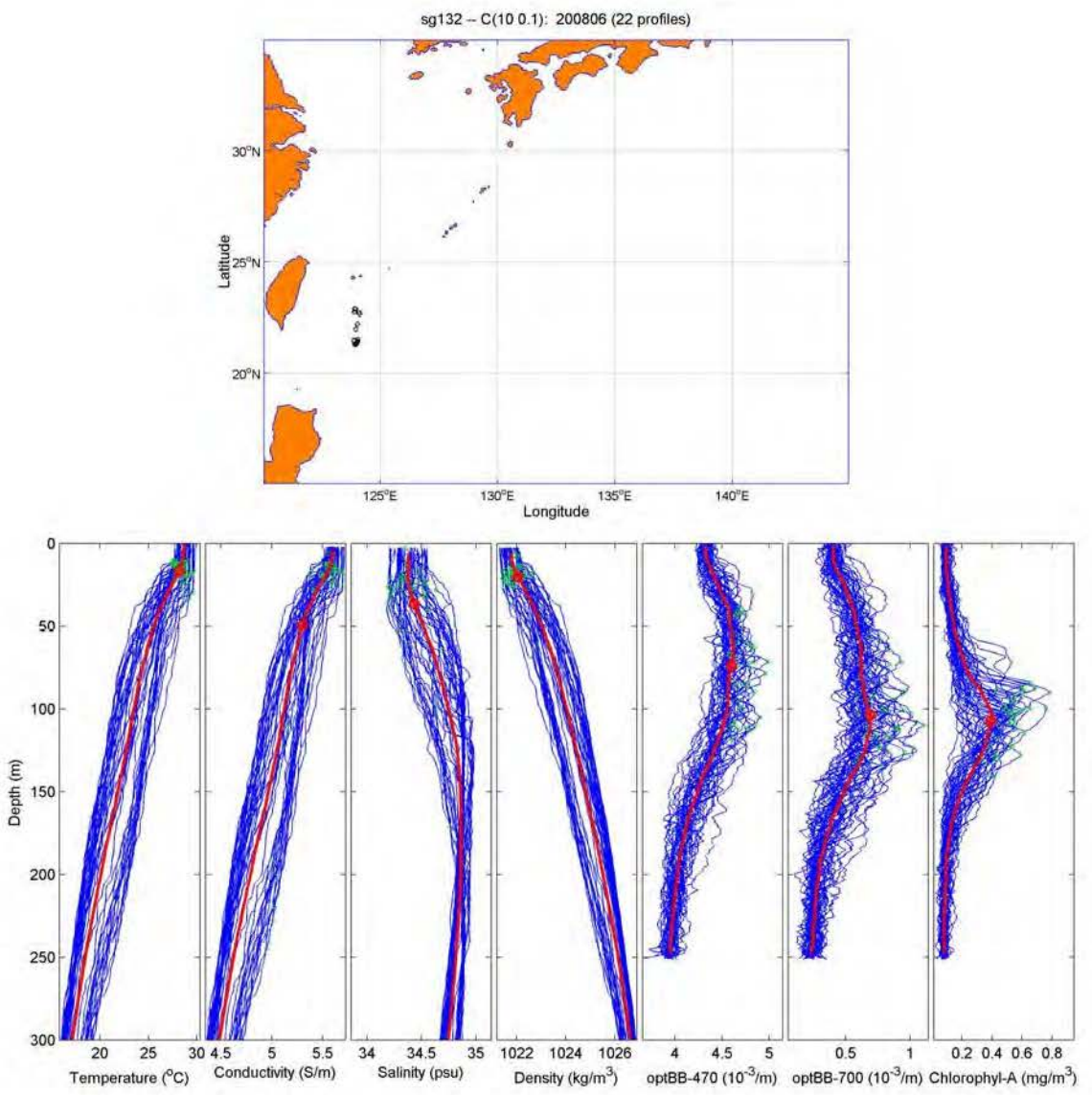
sg132 -- C(10 0.1): 200806 (22 profiles)
30°N
25°N
20°N
Latitude
125°E
130°E
135°E
140°E
Longitude
Depth (m)
0
50
100
150
200
250
300
20 25 30
Temperature (°C)
4.5 5 5.5
Conductivity (S/m)
34 34.5 35
Salinity (psu)
1022 1024 1026
Density (kg/m3)
4 4.5 5
optBB-470 (10-3/m)
0.5 1
optBB-700 (10-3/m)
0.2 0.4 0.6 0.8
Chlorophyl-A (mg/m3)

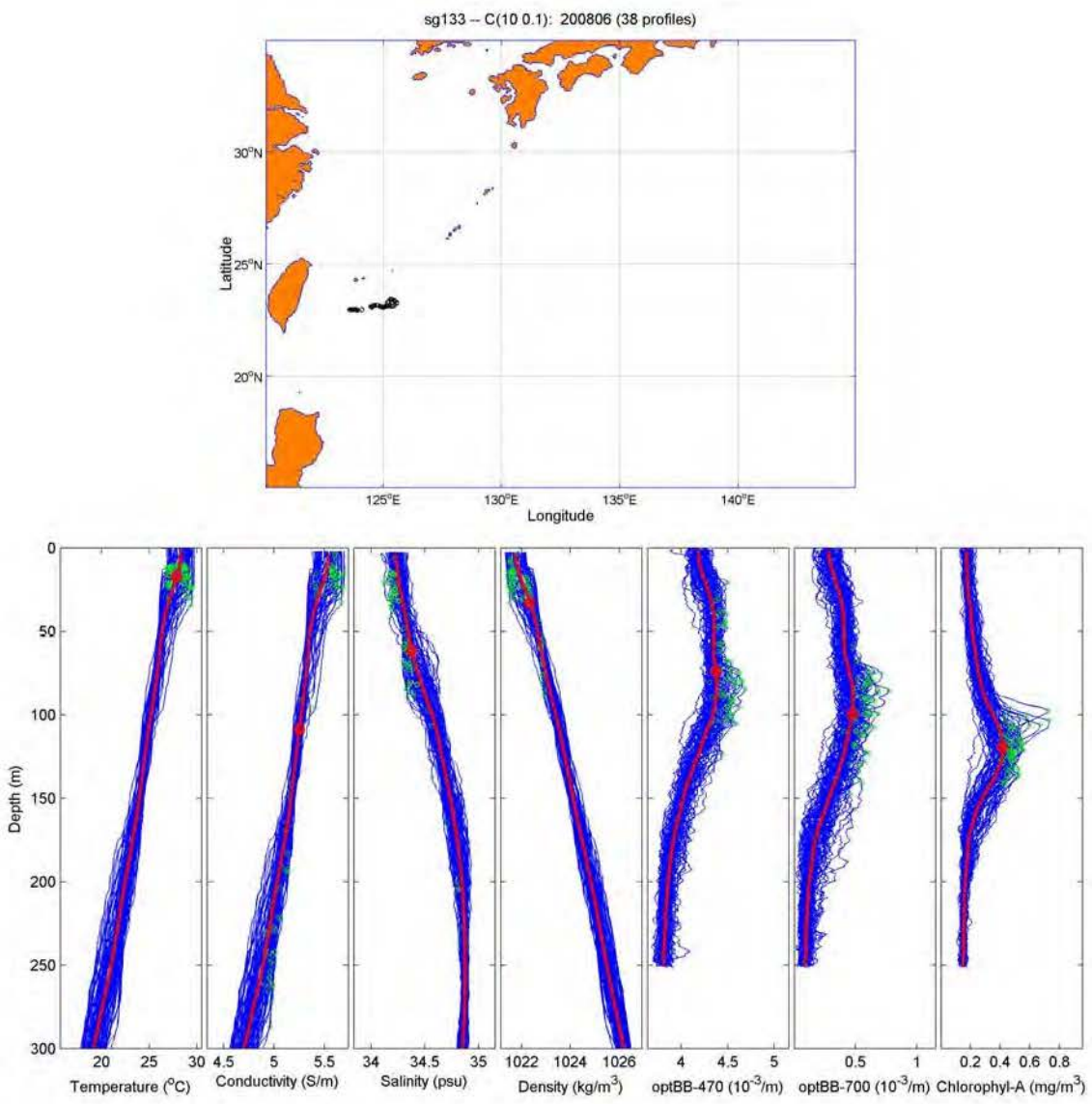
sg133 -- C(10 0.1): 200806 (38 profiles)
30°N
25°N
20°N
Latitude
125°E
130°E
135°E
140°E
Longitude
Depth (m)
0
50
100
150
200
250
300
20 25 30
Temperature (°C)
4.5 5 5.5
Conductivity (S/m)
34 34.5 35
Salinity (psu)
1022 1024 1026
Density (kg/m3)
4 4.5 5
optBB-470 (10-3/m)
0.5 1
optBB-700 (10-3/m)
0.2 0.4 0.6 0.8
Chlorophyl-A (mg/m3)

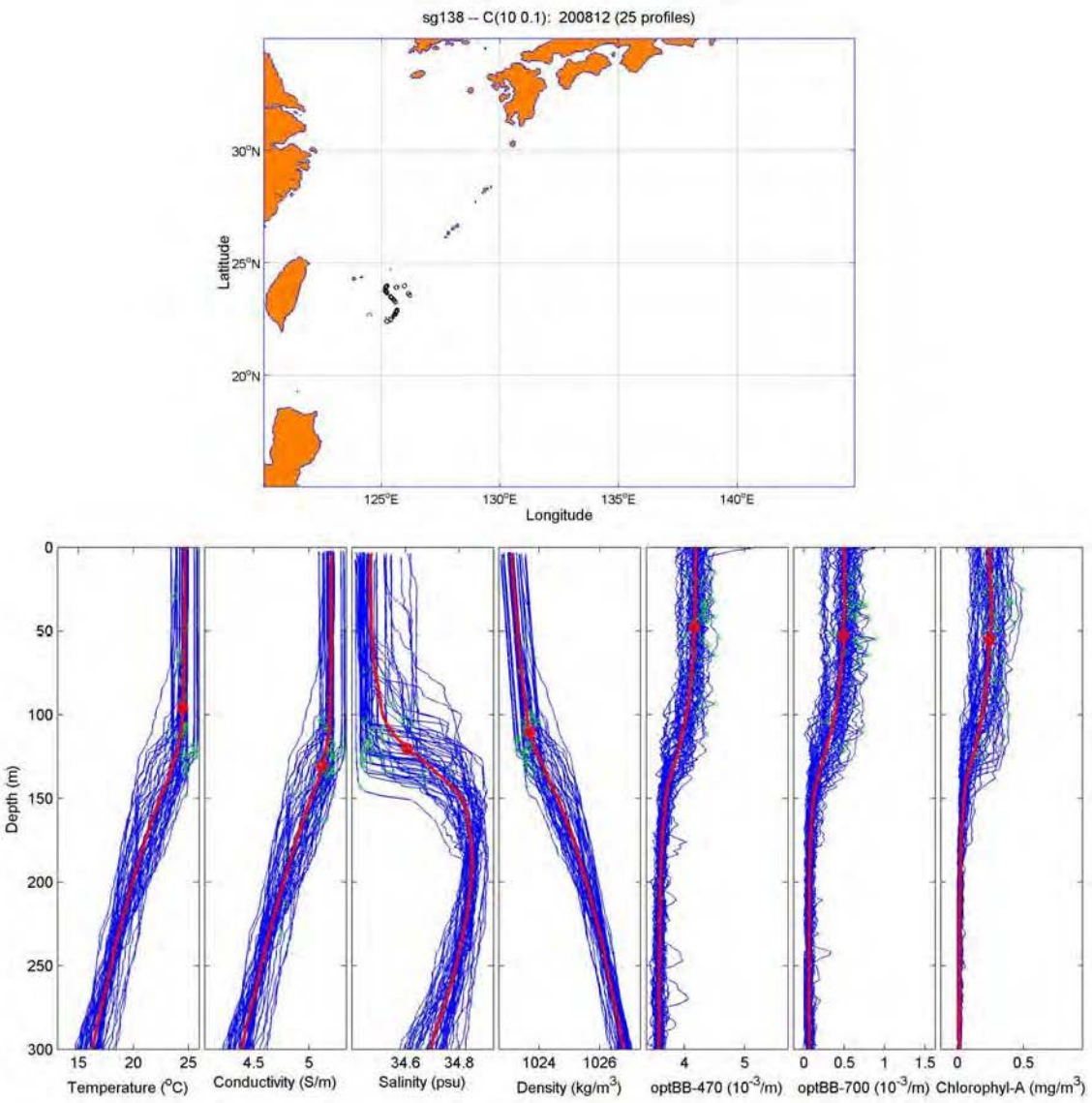
sg138 -- C(10 0.1): 200812 (25 profiles)
30°N
25°N
20°N
Latitude
125°E
130°E
135°E
140°E
Longitude
Depth (m)
0
50
100
150
200
250
300
15
20
25
Temperature (°C)
4.5
5
Conductivity (S/m)
34.6
34.8
Salinity (psu)
1024
1026
Density (kg/m3)
4
5
optBB-470 (10-3/m)
0
0.5
1
1.5
optBB-700 (10-3/m)
0
0.5
Chlorophyl-A (mg/m3)

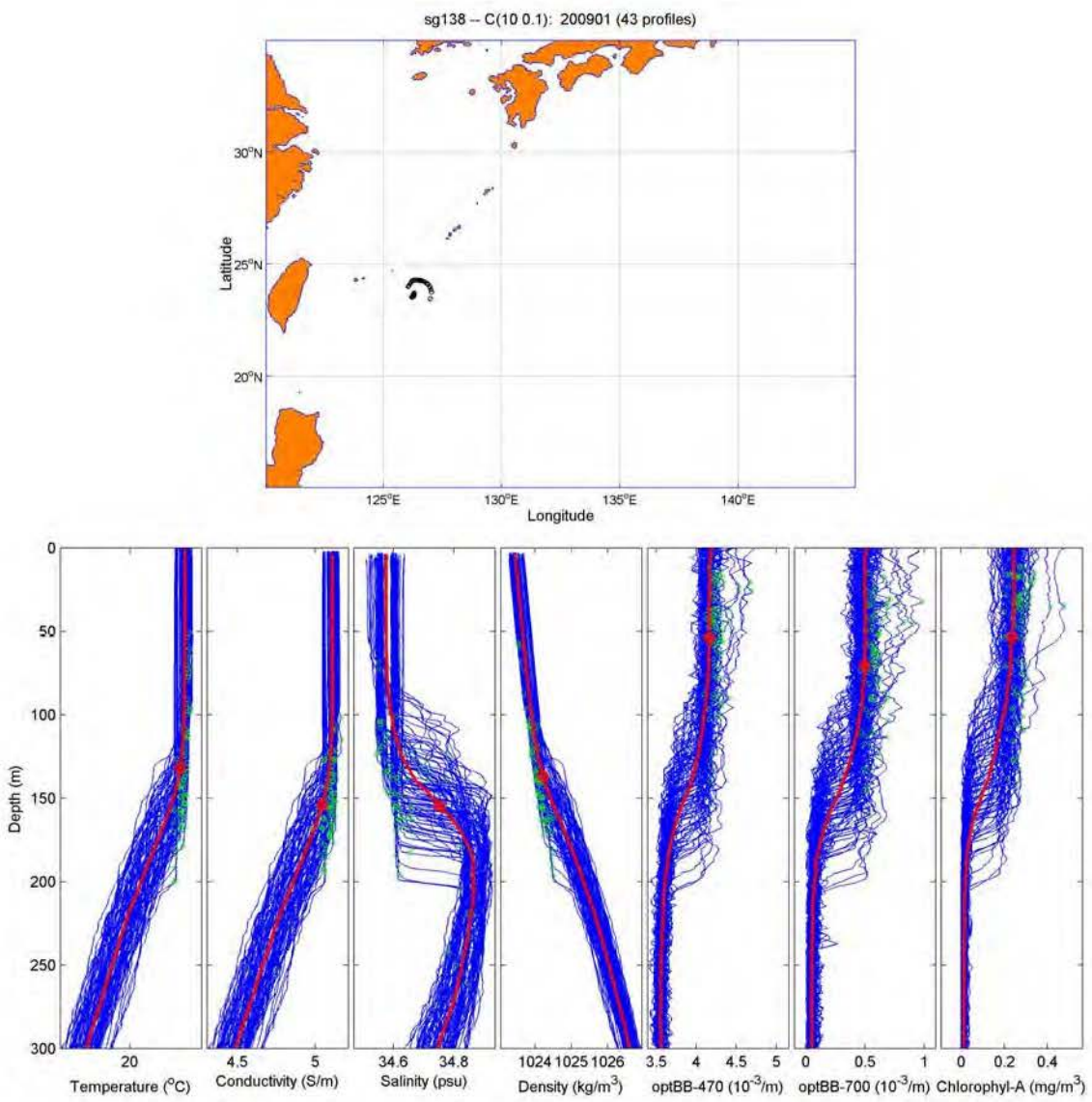
sg138 -- C(10 0.1): 200901 (43 profiles)
30°N
25°N
20°N
Latitude
125°E
130°E
135°E
140°E
Longitude
Depth (m)
0
50
100
150
200
250
300
20
Temperature (°C)
4.5
5
Conductivity (S/m)
34.6
34.8
Salinity (psu)
1024
1025
1026
Density (kg/m3)
3.5
4
4.5
5
optBB-470 (10-3/m)
0
0.5
1
optBB-700 (10-3/m)
0
0.2
0.4
Chlorophyl-A (mg/m3)

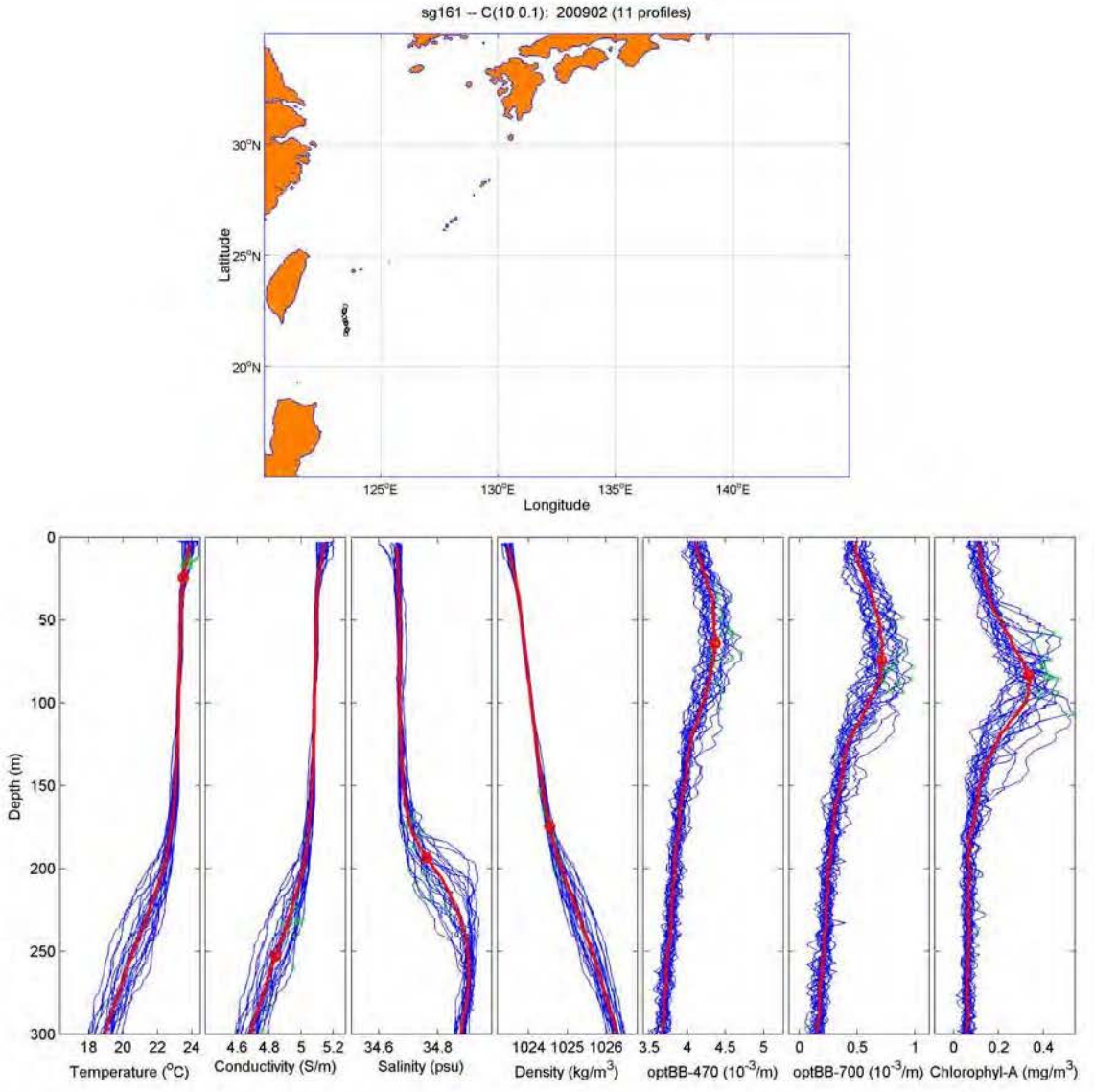
sg161 -- C(10 0.1): 200902 (11 profiles)
30°N
25°N
20°N
Latitude
125°E
130°E
135°E
140°E
Longitude
Depth (m)
0
50
100
150
200
250
300
18 20 22 24
Temperature (°C)
4.6 4.8 5 5.2
Conductivity (S/m)
34.6 34.8
Salinity (psu)
1024 1025 1026
Density (kg/m3)
3.5 4 4.5 5
optBB-470 (10-3/m)
0 0.5 1
optBB-700 (10-3/m)
0 0.2 0.4
Chlorophyl-A (mg/m3)

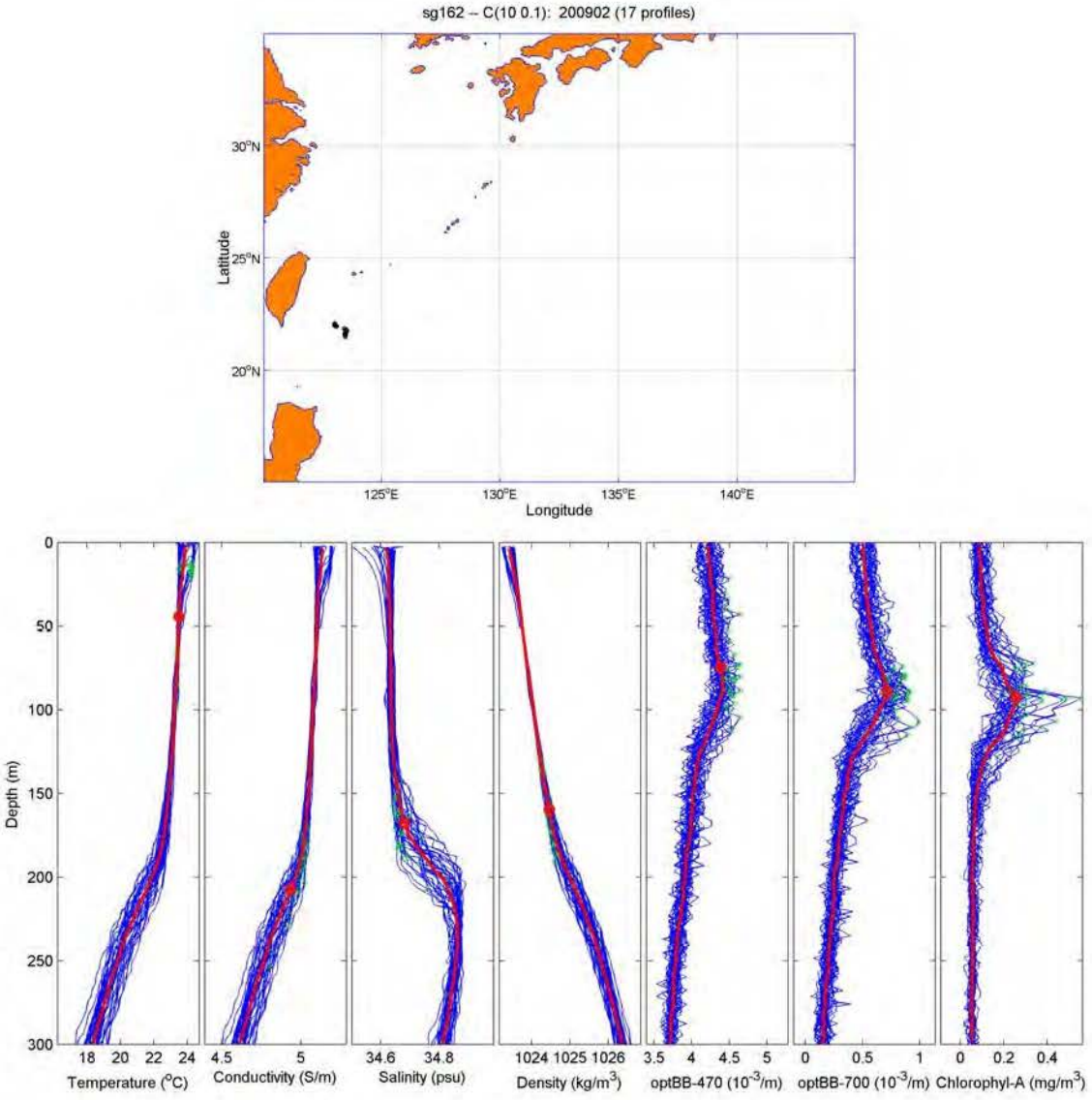
sg162 -- C(10 0.1): 200902 (17 profiles)
30°N
25°N
20°N
Latitude
125°E
130°E
135°E
140°E
Longitude
Depth (m)
0
50
100
150
200
250
300
18 20 22 24
Temperature (°C)
4.5 5
Conductivity (S/m)
34.6 34.8
Salinity (psu)
1024 1025 1026
Density (kg/m3)
3.5 4 4.5 5
optBB-470 (10-3/m)
0 0.5 1
optBB-700 (10-3/m)
0 0.2 0.4
Chlorophyl-A (mg/m3)

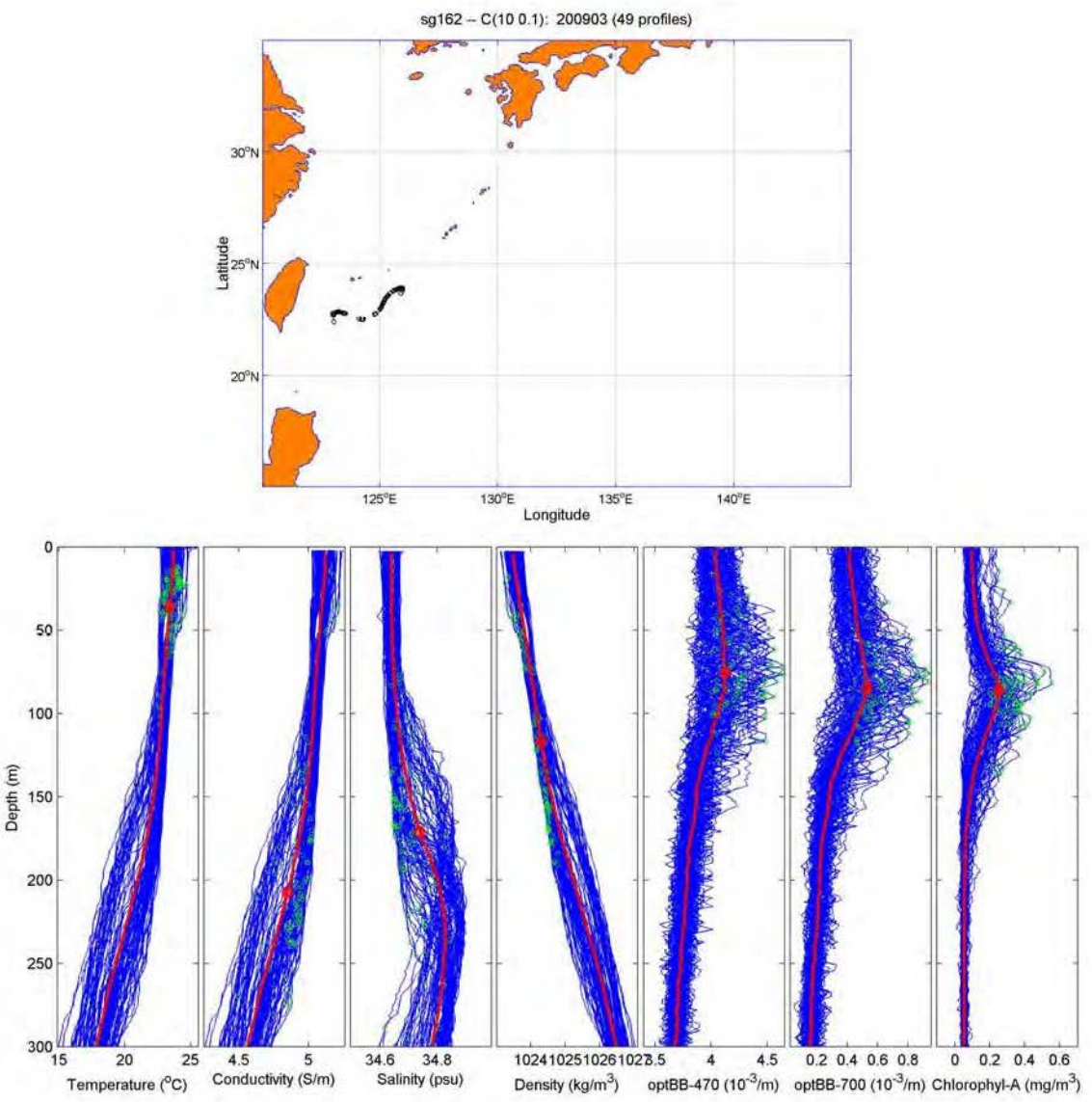
sg162 -- C(10 0.1): 200903 (49 profiles)
30°N
25°N
20°N
Latitude
125°E
130°E
135°E
140°E
Longitude
Depth (m)
0
50
100
150
200
250
300
15
20
25
Temperature (°C)
4.5
5
Conductivity (S/m)
34.6
34.8
Salinity (psu)
1024
1025
1026
1027
Density (kg/m3)
3.5
4
4.5
optBB-470 (10-3/m)
0.2
0.4
0.6
0.8
optBB-700 (10-3/m)
0
0.2
0.4
0.6
Chlorophyl-A (mg/m3)

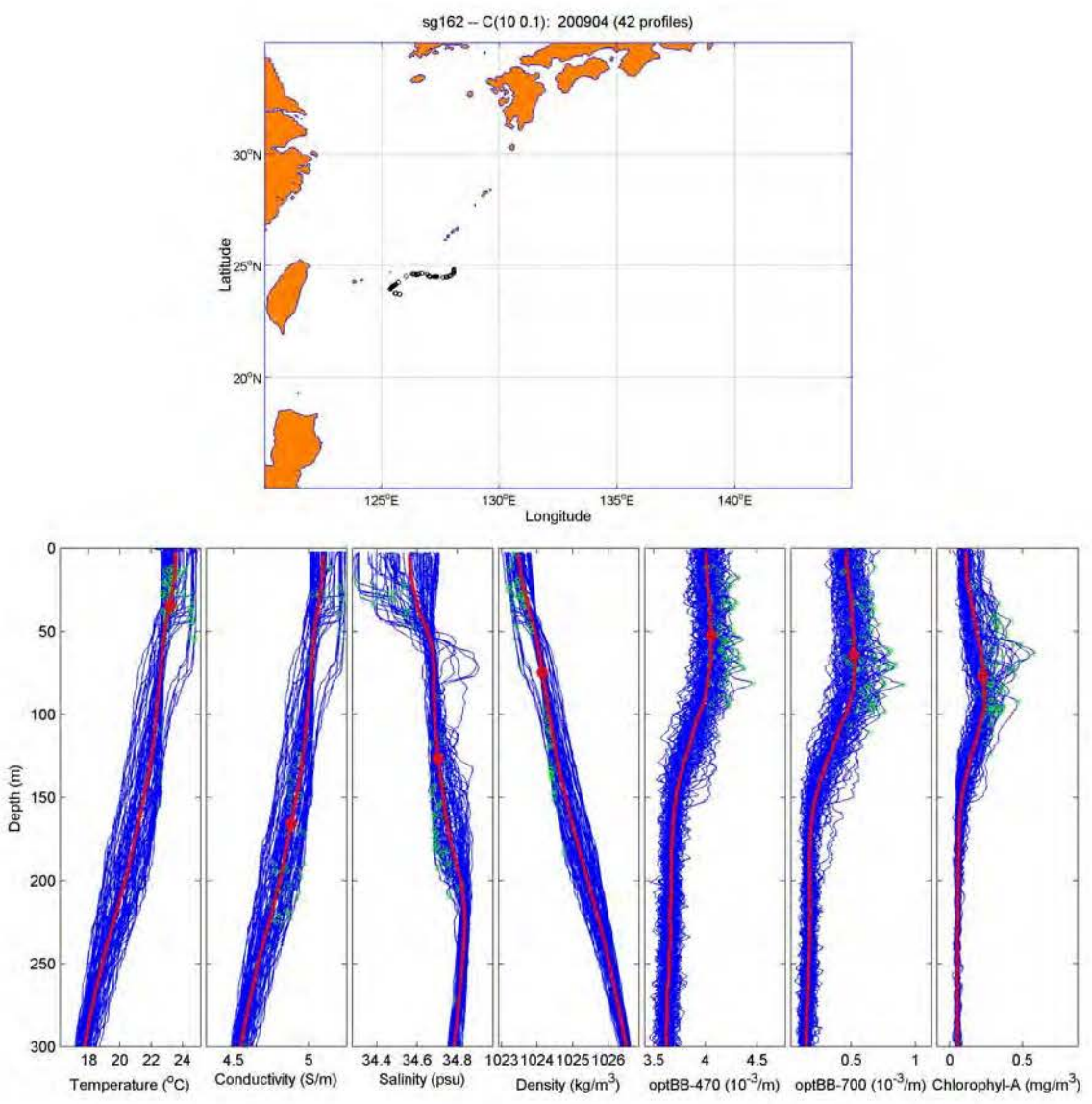
sg162 -- C(10 0.1): 200904 (42 profiles)
30°N
25°N
20°N
Latitude
125°E
130°E
135°E
140°E
Longitude
Depth (m)
0
50
100
150
200
250
300
18 20 22 24
Temperature (°C)
4.5 5
Conductivity (S/m)
34.4 34.6 34.8
Salinity (psu)
1023 1024 1025 1026
Density (kg/m3)
3.5 4 4.5
optBB-470 (10-3/m)
0.5 1
optBB-700 (10-3/m)
0 0.5
Chlorophyl-A (mg/m3)

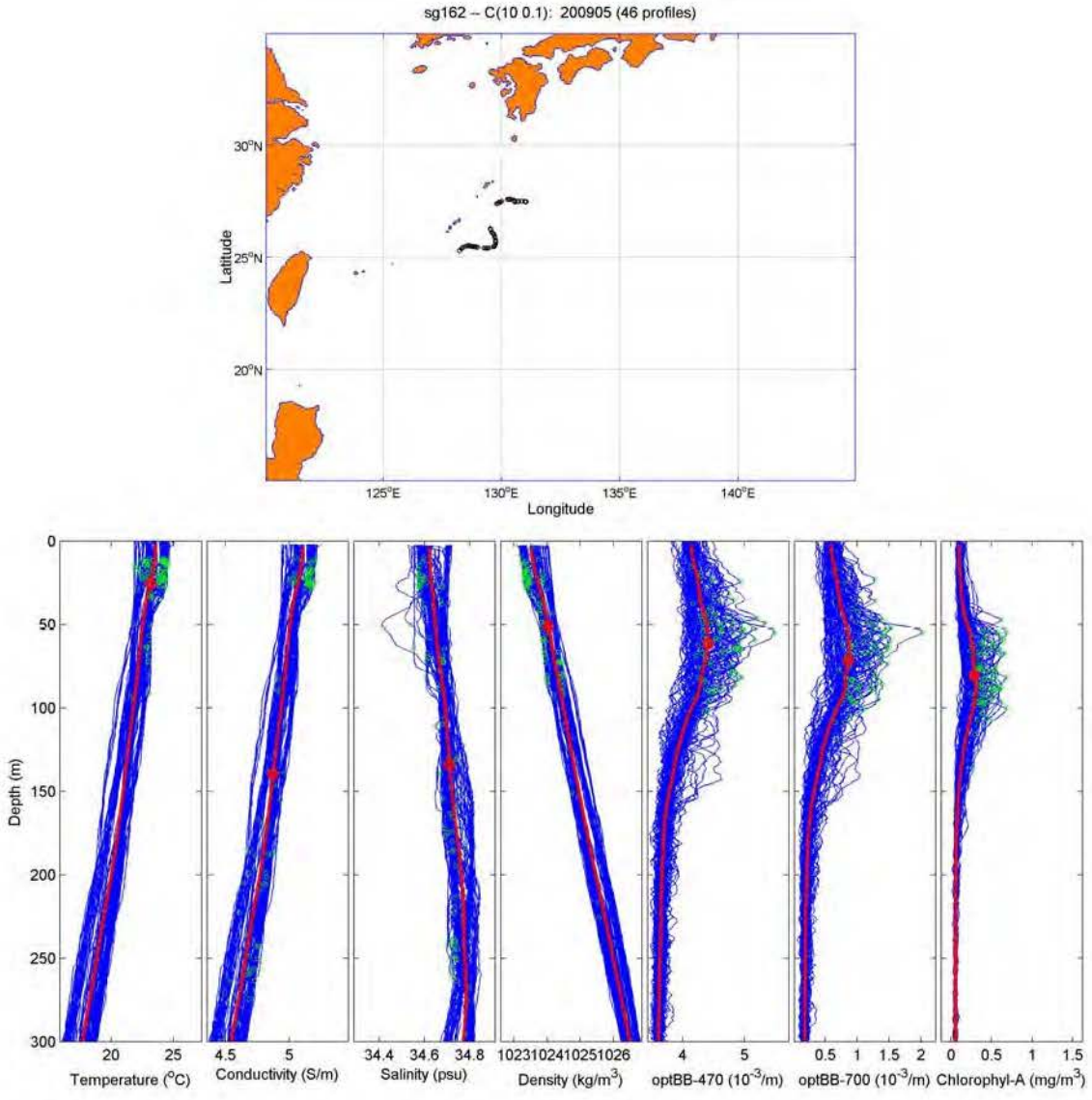
sg162 -- C(10 0.1): 200905 (46 profiles)
30°N
25°N
20°N
Latitude
125°E
130°E
135°E
140°E
Longitude
Depth (m)
0
50
100
150
200
250
300
20
25
Temperature (°C)
4.5
5
Conductivity (S/m)
34.4
34.6
34.8
Salinity (psu)
1023
1024
1025
1026
Density (kg/m3)
4
5
optBB-470 (10-3/m)
0.5
1
1.5
2
optBB-700 (10-3/m)
0
0.5
1
1.5
Chlorophyl-A (mg/m3)

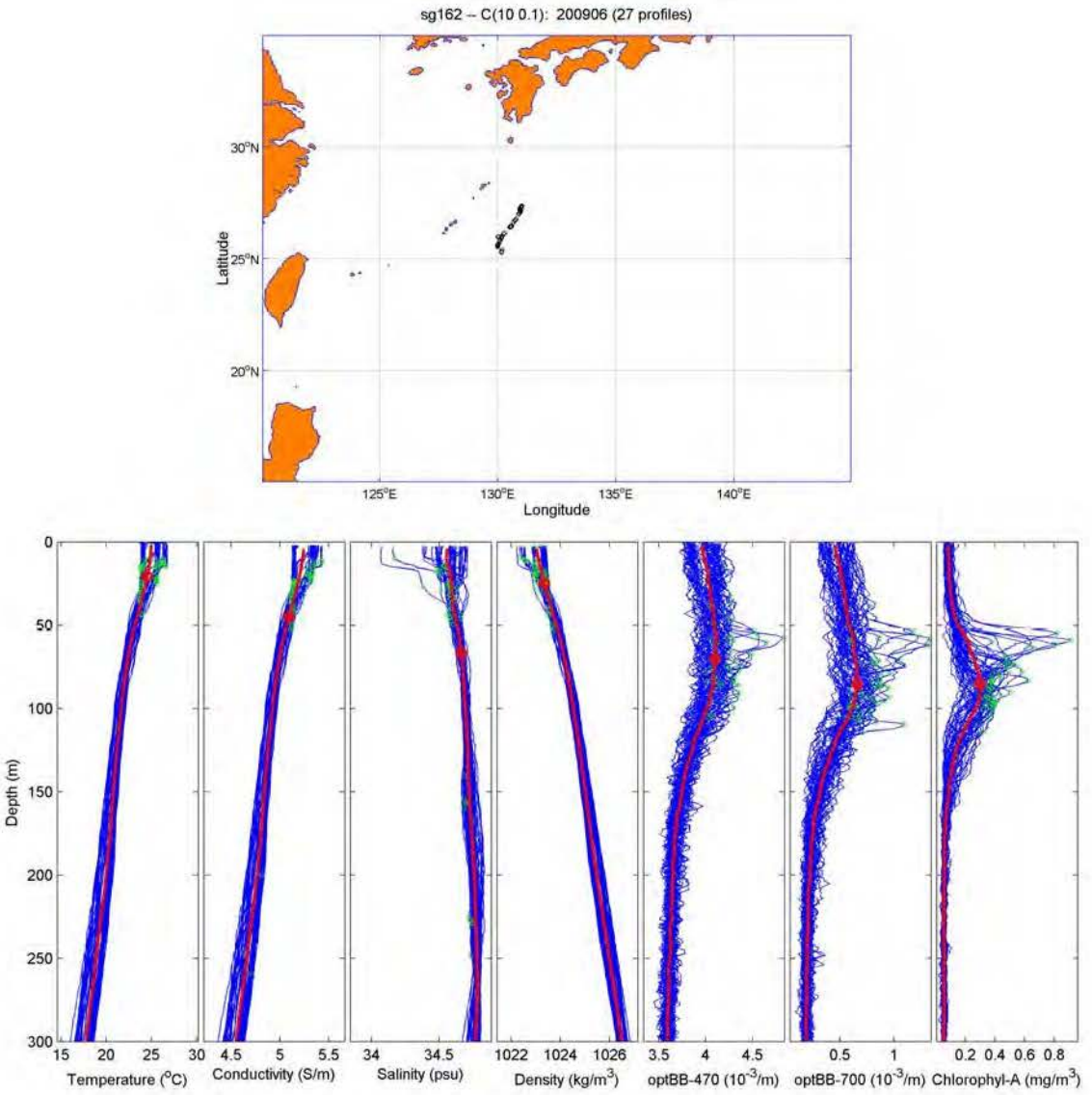
sg162 -- C(10 0.1): 200906 (27 profiles)
30°N
25°N
20°N
Latitude
125°E
130°E
135°E
140°E
Longitude
Depth (m)
0
50
100
150
200
250
300
15 20 25 30
Temperature (°C)
4.5 5 5.5
Conductivity (S/m)
34 34.5
Salinity (psu)
1022 1024 1026
Density (kg/m3)
3.5 4 4.5
optBB-470 (10-3/m)
0.5 1
optBB-700 (10-3/m)
0.2 0.4 0.6 0.8
Chlorophyl-A (mg/m3)

THIS PAGE INTENTIONALLY LEFT BLANK

LIST OF REFERENCES

Australian Government, Department of Defence 2013: Defence White Paper 2013. [Available online at http://www.defence.gov.au/whitepaper2013/docs/WP_2013_web.pdf.]

Bachkosky, J. M, T. Brancati, D.R. Conley, J.W. Douglass, P.A. Gale, D. Held, L.R. Hettche, J.R. Luyten, I.C. Peden, R.L. Rumpf, A. Salkind, J.M. Sinnett, and G.E. Whistler, Jr., 2000: "Naval Research Advisory Committee Report *Unmanned Vehicles (UV) In Mine Countermeasures(U).*" [Available online at http://www.nrac.navy.mil/docs/2000_rpt_unmanned_vehicles_mine_countermeasures.pdf]

Barkley, R.A. 1970: "The Kuroshio Current." *Sci. J.*, **6,** 54–60. [Available online at http://swfsc.noaa.gov/publications/CR/1973/7302.PDF]

Boss, E., D. Stramski, T. Bergmann, W.S. Pegau, and M. Lewis, 2004: Why Should We Measure the Optical Backscattering Coefficient?. *Oceano.*, **17**(2), 44–49.

Campbell, K., Andrews, B., 2013: "Explaining the U.S. 'Pivot' to Asia." Chatham House, August 2013 [Available online at http://www.chathamhouse.org/sites/files/chathamhouse/public/Research/Americas/0813pp_pivottoasia.pdf.]

Chu, P. C., and Fan, C., 2011: Determination of Ocean Mixed Layer Depth from Profile Data. *Prcdgs15th Symp Int Obs Ass Sys Atmos, Ocn Lnd Sfc, AMS.* 1001–1008

Chu, P. C., and Fan, C., 2011: "Maximum angle method for determining mixed layer depth from seaglider data." *J. Oceano.,* **67,** 219–230.

Chu, P. C., and Fan, C., 2011: "Optimal Linear Fitting for Objective Determination of Ocean Mixed Layer Depth." *J. Atmos and Ocean Tech.*, **27**(11), 1893–1898.

Discovery of Sound in the Sea website. University of Rhode Island 2012–2014. [Available online at http://www.dosits.org/people/defense/findsubmarines/?CFID=2854846&CFTOKEN=96881650]

Eriksen, C. C., T. J. Osse, R. D. Light, T. Wen, T. W. Lehman, P. L. Sabin, J. W. Ballard, A. M. Chiodi, 2001: "Seaglider: A Long-Range Autonomous Underwater Vehicle for Oceanographic Research." *IEEE J. of Oceanic Engineering,* **26,** 424–436.

Ingram, J. A., 1974: *Introductory Statistics.* Cummings Publishing Company, 341 pp.

Janzen, C., N. Larson, R. Beed, K. Anson, and Sea-Bird Electronics, 2008: "Accuracy and Stability of ARGO SBE 41 and SBE 41CP CTD Conductivity and Temperature Sensors." Seabird Electronics, Inc. [Available online at http://www.seabird.com/technical_references/LongtermTSstabilityAGUDec08Handout2Pages.pdf]

Journal of Commerce, 2014: Trans-Pacific Trade. [Available online at http://www.joc.com/special-topics/trans-pacific-trade]

Kudo, I., and K. Matsunaga, 1999: "Environmental Factors Affecting the Occurrence and Production of the Spring Phytoplankton Bloom in Funka Bay, Japan." *J. of Oceanography*, **55**, 505–513.

Lin, I. I., G. J. Goni, J. A. Knaff,, C. Forbes, and M. M. Ali, 2012: "Ocean heat content for tropical cyclone forecasting and its impact on storm surge." *Nat Hzrds*., **66**(3), 1481–1500.

MathWorks, 2014. MatLab product description. [Available online at http://www.mathworks.com/products/matlab/]

de Boyer Montegut, C., G. Madec, A. S. Fischer, A. Lazar, and D. Iudicone, 2004: "Mixed layer depth over the global ocean: An examination of profile data and a profile-based climatology." *J. Geophys Rsrch.,* **109**(C12003)**,** 1–20.

Monterey, G., and S. Levitus, 1997: "*Seasonal Variability of the Global Ocean Mixed Layer Depth*." National Oceanographic Data Center/NOAA. 96 pp.

Naval Research Laboratory 2012."Dr. Weilin Hou and Mr. Bob Arnone Selected to Chair SPIE Ocean Sensing and Monitoring IV." [Available online at http://www.nrl.navy.mil/media/news-releases/2012/dr-weilin-hou-and-mr-bob-arnone-selected-to-chair-spie-ocean-sensing-and-monitoring-iv]

Office of U.S. Trade Representative. [Available online at http://www.ustr.gov/countries-regions/southeast-asia-pacific]

OSIL (Ocean Scientific International Ltd) 2012: IAPSO Standard Seawater and the Practical Salinity Scale [Available online at http://www.osil.co.uk/Resources/SeawaterTechNotes/tabid/104/articleType/ArticleView/articleId/219/IAPSO-Standard-Seawater-and-the-Practical-Salinity-Scale.aspx]

McBride, J. L., 1995: "Tropical cyclone formation." Global Perspectives on Tropical Cyclones, R. L. Elsberry (ed.). World Meteorological Organization, Geneva, Switzerland, Report No. TCP -38.[Available online at http://derecho.math.uwm.edu/classes/TropMet/GPTC/tcclimo.pdf]

Plaschke, R. B., 1999. “Shipboard analysis of seawater for salinity, dissolved oxygen and nutrients.” Hobart, Tas.: CSIRO Div. of Marine Research. (Report. CSIRO Marine Laboratories; no. 237). 44 pp.

Qiu, B., 2001: “Kuroshio and Oyashio Currents.” *Ency. Ocn Scncs.*, **1,** 1413–1425.

Russell, L. A., 2012: Naval Oceanographic Office WG/CSAB update. PowerPoint lecture [Available online at www.ofcm.gov/wg-csab/.../NAVO%20WGCSAB%20Apr%202012.ppt.]

Unidata Program Center 2014. “netCDF fact sheet.” [Available online at http://www.unidata.ucar.edu/publications/factsheets/current/netcdf_factsheet.pdf.]

United Nations Development Programme, 2011: Towards Human Resilience: Sustaining MDG Progress in an Age of Economic Uncertainty [Available online at http://www.undp.org/content/dam/undp/library/Poverty%20Reduction/Towards_SustainingMDG_Web1005.pdf.]

Seabird Electronics 2008: “SBE41/41 CP CTD Module for Autonomous Profiling Floats (ARGO).” Data and marketing sheet [Available online at http://www.seabird.com/sbe41-argo-ctd.]

Sprintall, J., and D. Roerich, 1999 “Characterizing the structure of the surface layer in the Pacific Ocean” *J. Geophys Rsrch.*, **104**(C10), 23, 297–23, 311.

YSI Environmental 2013: Tech Note *The basics of Chlorophyll Measurement.* YSI, Inc / Xylem, Inc. [Available online at http://www.ysi.com/media/pdfs/T606-The-Basics-of-Chlorophyll-Measurement.pdf.]

THIS PAGE INTENTIONALLY LEFT BLANK

INITIAL DISTRIBUTION LIST

1. Defense Technical Information Center
   Ft. Belvoir, Virginia

2. Dudley Knox Library
   Naval Postgraduate School
   Monterey, California